The study of the membrane microdomain localization of the prion-family proteins, prion and Shadoo and their interaction with calnexin

Divya Teja Dondapati

Ph.D. Thesis

Szeged
2021

DOCTORAL SCHOOL OF MULTIDISCIPLINARY MEDICAL SCIENCES
UNIVERSITY OF SZEGED

The study of the membrane microdomain localization of the prion-family proteins, prion and Shadoo and their interaction with calnexin

Ph.D. Thesis

Divya Teja Dondapati

Supervisor:
Dr. Elfrieda Fodor

INSTITUTE OF BIOCHEMISTRY
BIOLOGICAL RESEARCH CENTRE
SZEGED
2021

Table of Contents

LIST OF PUBLICATIONS AND CONFERENCE ABSTRACTS

Publications related to the thesis

I. **Divya Teja Dondapati**, Pradeep Reddy Cingaram, Ferhan Ayaydin, Antal Nyeste, Andor Kanyó, Ervin Welker and Elfrieda Fodor. Membrane Domain Localization and Interaction of the Prion-Family Proteins, Prion and Shadoo with Calnexin. (2021) *Membrane* 11(12), 978. IF: 4.106

II. Pradeep Kumar Reddy Cingaram, Antal Nyeste, **Divya Teja Dondapati**, Elfrieda Fodor, Ervin Welker. Prion Protein Does Not Confer Resistance to Hippocampus-Derived Zpl Cells against the Toxic Effects of Cu^{2+}, Mn^{2+}, Zn^{2+} and Co^{2+} Not Supporting a General Protective Role for PrP in Transition Metal Induced Toxicity. (2015) PLoS ONE 10 (10): e0139219. IF: 3.3

Conference abstracts related to the thesis

I. **Divya Teja Dondapati**, Ferhan Ayaydin, Pradeep Kumar Reddy Cingaram, Andor Kanyó, Ervin Welker, Elfrieda Fodor, "Interaction of prion-family proteins prion and shadoo with calnexin in membrane microdomains", in Straub Days Conference, Biological Research Center, Szeged, Hungary, 2019.

II. **Divya Teja Dondapati**, Pradeep Kumar Reddy Cingaram, Ferhan Ayaydin, Ervin Welker, Elfrieda Fodor, "Study of the membrane micro-domain localization of prion protein family members in N2a cells using a detergent free density gradient method" in the International Prion Conference, Edinburgh, Scotland, 2017.

III. **Divya Teja Dondapati,** Pradeep Kumar Reddy Cingaram, Ervin Welker, Elfrieda Fodor, "Study of the membrane micro-domain localization of overexpressed GPI-anchored proteins in mammalian cells", in the Recombinant Protein Technology-2016 ELRIG International Conference, Gothenburg, Sweden, 2016.

ACKNOWLEDGEMENTS

First and foremost, I thank **Almighty God** for being with me in all the circumstances throughout these years. Without Him, I would neither have wisdom nor the physical ability to come thus far.

I am forever grateful to **Dr. Elfrieda Fodor**, my supervisor, for her expertise guidance, significant discussions, efforts and encouragement in my success and failures in addition to being beyond supervisor for her teachings, lessons and experiences, which are valuable not only during doctoral period but throughout my life. Without her help, extraordinary care and orientation this thesis would not have been possible.

I would like to convey my heartfelt gratitude and sincere appreciation to **Dr. Ervin Welker**, Scientific Advisor and Principal Investigator at the Laboratory of Conformational Diseases for giving me the opportunity to do ITC course and Ph.D. studies in his group. I am grateful for his timely critical suggestions, support, help and review.

A debt of gratitude also owed to **Dr. Ferhan Ayaydin**, Head of the Advanced Core Facility, at the Hungarian Centre of Excellence for Molecular Medicine, University of Szeged, Functional Cell Biology and Immunology group (HCEMM-USZ-FCBI), formerly, head at the Cellular Imaging Laboratory, Biological Research Centre, Szeged, for his help, valuable discussions and assessment, which made my work colorful and attractive at the same time.

I would like to thank, many people in several aspects at the Doctoral School of Multidisciplinary Medical Sciences, Faculty of Medicine, University of Szeged notably at the Institute of Biochemistry, Biological Research Centre (BRC), Szeged, for their support and encouragement until the completion of the thesis. I specifically thank the administrative staff at university, Tünde Bodnár and Bódi Renáta and at the BRC, Katalin Bozóné Tóth, Olga Miklós, Timea Varga, Dr. Monika Bali and Katalin Burkovics for their help during my studies. I also would like to thank the Institute of Biophysics, BRC, for providing me the possibility to regularly use their ultra-centrifuge instrument, Sorvall WX 80+ Ultracentrifuge, Thermo Fisher Scientific brand.

I am thankful to all members of our group, the Laboratory of Conformational Diseases: at first to my colleague Dr. Pradeep Reddy Cingaram and my husband and colleague Sudheer Babu Sangeetham for their help, support and valuable scientific discussions. I am especially thankful to

ABBREVIATIONS

AD: Alzheimer's disease

Aβ: amyloid beta

BSA: bovine serum albumin

CNS: central nervous system

CNX: calnexin protein

DAPI: 4′,6-diamidino-2 phenylindole HCl

DMEM: Dulbecco's Modified Eagle's Medium

DRM: detergent-resistant membrane

ECL: enhanced chemiluminescence

EGFP: enhanced green fluorescent protein

ER: endoplasmic reticulum

EYFP: enhanced yellow fluorescent protein

GA: Golgi apparatus

GPI-anchor: glycosylphosphatidylinositol-anchor

HD: Huntington's disease

HRP: horseradish peroxidase

IP: immunoprecipitation

NPC: nuclear pore complex protein

PAGE: polyacrylamide gel electrophoresis

PBS: phosphate buffered saline

PD: Parkinson's disease

PDI: protein disulfide isomerase

PNGase F: Peptide-N-glycosidase F

PRND: prion like protein doppel precursor gene

PRNP: major prion protein precursor gene

PrP: prion protein

PrP^C: cellular prion protein

PrP^{Sc}: scrapie prion protein

RFP: red fluorescent protein

SDS: sodium dodecyl sulfate

Sho: Shadoo protein

SPRN: shadow of prion protein precursor gene

Tris: Tris(hydroxymethyl)aminomethane

TSE: transmissible spongiform encephalopathy

SUMMARY OF THE THESIS

Prion diseases or transmissible spongiform encephalopathies (TSEs) are a group of fatal, infectious neurodegenerative diseases caused by the accumulation of an abnormally folded isoform, called scrapie prion (PrP^{Sc}), of the normal cellular prion protein (PrP^C). PrP^{Sc} possesses infective characteristics and is capable to induce the transition of the healthy PrP^C-s to a similar conformational state. Prion diseases have no available cure at present. Despite decades of intensive research, neither the mechanism of developing the disease nor the exact role of the native cellular prion protein is known at present.

The cellular PrP^C is a glycosylphosphatidylinositol (GPI) -anchored membrane glycoprotein highly conserved among mammalian species. It is expressed mostly in the central nervous system (CNS) and also in a variety of different organs. A large number of binding partners have been reported for PrP^C, indicating that it is involved in many different cellular processes. Among them, it was reported to participate in cell proliferation, adhesion, neurotransmitter metabolism and peripheral myelin maintenance, to exert antioxidant activity and neuroprotection and to play role in copper homeostasis and homeostasis of trace elements. These latter roles had been attributed to PrP$^{C'}$s ability to bind copper (Cu^{2+}) and other divalent cationic transition metals such as Zn^{2+} and Mn^{2+}, mainly by its highly conserved octapeptide repeat region (OR). Metal binding was also reported to affect PrP$^{C'}$s folding and trafficking, such as copper induced its clathrin-dependent internalization, and it was proposed to be linked to disease as well. Although PrP$^{C'}$s metal binding is well-documented and characterised, there is no consensus on its exact role in either the normal physiology of the cellular PrP^C or in the development of TSEs.

Recently, two other proteins had been identified as paralogs of the prion protein and are members of the prion-family: Doppel (Dpl) and the more recent Shadoo (Sho) protein. While Dpl is testis specific and toxic if ectopically expressed in the CNS, Sho is mostly expressed in the CNS and present also in the other organs, like PrP^C. Its function is the least understood at present among the prion-family members. Interestingly, Sho has been reported to share some neuroprotective actions with the wild type prion protein (PrP) (against the toxic effects of Dpl or of Shmerling-mutant Δ[32–121]PrP in primary cerebellar granule neuronal cultures from *Prnp*$^{0/0}$ mouse or of the hydrophobic domain deletion mutant, Δ[113–133], PrPΔHD in human SH-SY5Y cells and against the excitotoxic stress of glutamate, but opposing roles had also been observed in

other experimental settings (contrary to wild type PrP, Sho sensitized cells against some drugs and provoked large inward ionic currents, similarly to toxic PrP mutants). Intriguingly also, while both proteins are abundantly expressed in the brain, they display both overlapping and complementary localizations in certain areas. Sho is a natively unstructured protein, similar to the N-terminal half of PrP^C, although with little sequence similarity. Both proteins (and Dpl) are GPI-anchored and are known to reside in the outer leaflet of the plasma membrane in the so called membrane "lipid-rafts". Cellular membrane rafts are known as specialized microdomains enriched in cholesterol, gangliosides, sphingomyelin and acylated proteins related to a variety of signalling processes, and had typically been isolated and characterized using the detergent-based isolation protocols. $PrP^{C'}$s association with the membrane rafts is reported to be required for its proper folding as well as for its conversion to the TSE-related isoform. However, how exclusively are these largely and fully unstructured proteins, PrP and Sho, respectively, confined to rafts and/or how they maintain their proper fold through their normal biology remains to be uncovered.

The major aims of the studies presented in this Thesis are the following. First, we set forward to test the membrane microdomain preference of Sho and PrP in N2a stable transgenic mouse neuroblastoma cells expressing the proteins, using a non-detergent based OptiPrep density gradient fractionation method, which avoids eventual artefacts encounterable during the classical, detergent-based raft isolation methods. Secondly, our aim is to test whether calnexin (CNX), a reported binding partner of PrP would be shared by Sho as well, and whether these proteins interact with CNX preferentially in rafts or non-rafts. Thirdly, after studying $PrP^{C'}$s protective role against transition metal induced toxicity in hippocampus-derived mouse ZW and Zpl cells (not presented in the Thesis) and using similar copper-treatment on the transgenic N2a cells, we set forward to study if $PrP^{C'}$s microdomain localization changes in response to copper treatment. The most important results and findings of the presented work are the following. By constructing plasmids to encode for a fluorescent protein tagged mouse mPrP (PrP-EGFP-GPI$_{(mPrP)}$) or mSho (Sho-EYFP-GPI$_{(mSho)}$) or their corresponding control proteins EGFP- GPI$_{(mPrP)}$ or EYFP-GPI$_{(mSho)}$, respectively, and by transfecting these separately into N2a cells, four stable transgenic N2a cell populations had been developed, named as: PrP-EGFP cells, Sho-EYFP cells, EGFP-cells and EYFP-cells, respectively. The adequate expression levels of the transgenes in the developed cells, as well as the correct localization and glycosylation, i.e., as expected for GPI-

anchored proteins and for the natively complex glycosylated PrP and Sho, was confirmed by microscopy and Western blotting combined with PNGase-F treatment. By using these cells and a non-detergent based continuous OptiPrep density gradient fractionation method, we report that while prion and Shadoo proteins occupy raft-type membrane fractions, a significant proportion of them are present in the transferrin receptor-marked, non-raft membrane domains. Further, additional two stable transgenic cell populations, expressing Sho with an additional FLAG-tag (Sho-EYFP-FLAG cells) and a corresponding control (EYFP-FLAG cells) were developed by constructing and transfecting N2a cells with plasmids encoding for Sho-EYFP-FLAG-STREP-GPI$_{(Sho)}$ and EYFP-FLAG-STREP-GPI$_{(Sho)}$ fusion proteins, respectively, in order to permit co-immunoprecipitation studies in case of Sho. Using these and the PrP-EGFP cells and transfecting them transiently to also express a red fluorescent protein tagged CNX, colocalization of both Sho and PrP with CNX could be detected by live cell confocal imaging. Next, using co-immunoprecipitation by FLAG for Sho-expressing cells, in parallel with pull- down assay by Ni-NTA beads in case of the PrP-EGFP cells employing the Ni-binding of the OR region of the PrP, co-immunoprecipitation and the pull-down of the chaperone CNX could be demonstrated for both Sho and PrP in the total cell lysates. This indicates their binding to CNX. Interestingly, this interaction could be detected also in both type of membrane domains, rafts and non-rafts, for both Sho and PrP. Furthermore, we could not observe relocation of PrP from rafts to non-rafts upon copper-treatment of these N2a cells, in line with a lack of the rescue effect of PrP observed upon the copper- and other transition metal treatments of Zpl (*Prnp*$^{0/0}$) cells when PrP was reintroduced into the cells.

Overall, our results demonstrate that the GPI-anchored Sho and PrP have similar preference for membrane microdomain fractions and interestingly, they display a dual raft/ non-raft distribution. This possibly reflects a loose raft confinement and may serve their multifunctional roles. We report that calnexin is a binding partner of both Sho and PrP irrespective of their localization to raft- or non-raft type membrane domains. We speculate that the unfolded structure of these proteins necessitates chaperone assistance, among which CNX is one of the chaperones, for at least a proportion of them at a given time, independent of their localization. We also propose that the involvement of PrP in rescuing cells of the toxic effects of copper (or the other metals studied) and its relocation to non-rafts as a response to copper-

treatment may be more complex than its metal-binding and also dependent on the cellular models used.

ÖSSZEFOGLALÁS

A prionbetegségek vagy fertőző szivacsos agysorvadás (TSE) betegségei, a neurodegeneratív betegségek egy végzetes csoportja, amelyeket a sejtekben fellelhető normál prionfehérje (PrP^C) egy abnormális konformációjú izoformája, az úgynevezett scrapie-prion (PrP^{Sc}) és annak felhalmozódása okoz. A PrP^{Sc} fertőző tulajdonságokkal rendelkezik, és képes az egészséges PrP^C-k hasonló konformációs állapotba való átmenetét indukálni. A prionbetegségeknek jelenleg nincs gyógymódja. A több évtizedes intenzív kutatás ellenére sem a betegség kialakulásának mechanizmusa, sem a natív egészséges celluláris prion fehérje pontos szerepe jelenleg nem ismert.

A celluláris PrP^C egy glikozilfoszfatidilinozitol (GPI) által membránba horgonyzott glikoprotein, amely erősen konzervált az emlősfajok között. Leginkább a központi idegrendszerben (CNS) de számos különböző szervben is kifejeződik. Eddigi kutatások a PrP^C számára nagyszámú kötőpartnert jelentettek, ami azt jelzi, hogy számos különböző sejtfolyamatban vesz részt. Többek között leírták, hogy részt vesz a sejtproliferációban, adhézióban, a neurotranszmitter anyagcserében és a perifériás mielin fenntartásában; antioxidáns aktivitást és neuroprotektív hatást fejt ki, valamint szerepet játszik a réz és egyéb nyomelemek homeosztázisában. Ez utóbbi szerepeket a PrP^C réz- (Cu^{2+}) és más divalens kationos átmenetifémek, például Zn^{2+} és Mn^{2+} megkötő képességének tulajdonították, amit főként az erősen konzervált oktapeptid ismétlődő régiója (OR) által fejt ki. Beszámoltak arról is, hogy a fémkötés befolyásolja a PrP^C hajtogatódását és sejtbeni mozgását (mint például réz-hatására kiváltódó klatrin-függő internalizációja), és azt feltételezték, hogy a betegségekkel is összefüggésbe hozható. Bár a PrP^C fémkötése jól dokumentált és jellemzett, nincs konszenzus a pontos szerepét illetően sem a PrP^C sejten belüli normál fiziológiájában, sem a TSE-k kialakulásában.

A közelmúltban két fehérjét is azonosítottak a prionfehérje paralógjaként, és ezek a prion fehérje mellett, a prionfehérje-család tagjait alkotják: a Doppel (Dpl) és az újabban felfedezett

Shadoo (Sho) fehérje. Míg a Dpl herespecifikus és toxikus, ha ektopikusan expresszálódik a központi idegrendszerben, a Sho leginkább a központi idegrendszerben expresszálódik, és más szervekben is jelen van, úgy mint a PrP^C. Funkciója jelenleg a legkevésbé ismert a prioncsalád tagjai közül. Érdekes módon, arról számoltak be, hogy a Sho a vad típusú prionfehérjével (PrP) megegyezően, bizonyos neuroprotektív hatásokat fejt ki (mint a Dpl vagy a Shmerling-mutáns Δ[32–121]PrP toxikus hatásai ellen $Prnp^{0/0}$ egérből származó primer kisagy granulátum neuronkultúrákban, vagy a hidrofób domén deléciós mutánssal Δ[113–133], PrPΔHD szemben humán SH-SY5Y sejtekben, vagy a glutamát okozta excitotoxikus stresszel szemben). Viszont, ellentétes szerepeket is megfigyeltek más kísérleti körülmények között (a vad típusú PrP-vel, ellentétben, Sho expressziója érzékennyé tette a sejteket egyes gyógyszerekkel szemben, és magas befelé irányuló ionáramot váltott ki, hasonlóan a toxikus PrP mutánsokhoz). Érdekes az is, hogy bár mindkét fehérje bőségesen expresszált az agyban, bizonyos területeken mind átfedő, mind komplementer lokalizációt mutatnak ki a kettőre. A Sho, hasonlóan a PrP^C N-terminális feléhez, egy natívan rendezetlen fehérje, bár csekély szekvenciahasonlósággal bírnak. Mindkét fehérje (és a Dpl) GPI-horgony által membránhoz kötött, és mint ilyen fehérjékről általában tudott, a plazmamembrán külső féltekében találhatóak, az úgynevezett membrán „lipid-raftokban" vagy tutajokban. A sejtmembrán tutajok koleszterinben, gangliozidokban, szfingomielinben és acilezett fehérjékben dúsúlt speciális mikrodoménekként ismertek, amelyek különféle jelátviteli folyamatokhoz kapcsolódnak, és melyeket jellemzően detergens-alapú izolációs protokollokkal izoláltak/-nak és jellemezték őket. A jelentések szerint a PrP^C membrán tutajokban való jelenléte szükséges a megfelelő hajtogatódásához, valamint a TSE-hez kapcsolt izoformává való átalakulásához. Azonban, hogy a nagyrészt- vagy teljesen strukturálatlan PrP és Sho, fehérjék lokalizációja mennyire korlátozódik a membrán tutajokra, és/vagy hogyan tartják meg a megfelelő konformációjukat a normál biológiájuk során, még nem tisztázott.

A dolgozatban bemutatott vizsgálatok fő céljai a következők. Először, a Sho és PrP membrán mikrodomén preferenciájának tesztelését tűzzük ki célul, a fehérjéket expresszáló N2a stabil transzgenikus egér neuroblasztóma sejtekben, egy nem-detergens alapú OptiPrep sűrűséggradiens frakcionálási módszerrel, amely elkerüli a klasszikus, detergens-alapú raft-izolálási módszereknél esetlegesen előforduló artefaktumok létrejöttét. Másodszor, célunk annak tesztelése, hogy a calnexint (CNX), a PrP egyik jelentett kötőpartnere, a Sho is köti-e? Valamint, hogy a PrP és Sho, a CNX-szel vajon prefernciálisan, a raftokban vagy a nem-raft típusú

membránokban, kötődik-e? Harmadszor, miután megvizsgáltuk a PrP^C átmenetifém-indukált toxicitással szembeni védő szerepét hippokampuszból származó egér ZW és Zpl sejtekben (a tézisben nem bemutatott), és hasonló réz-kezelést alkalmazunk a transzgenikus N2a sejteken, tanulmányozzuk, hogy megváltozik-e a PrP^C mikrodomain lokalizációja, válaszul a rézkezelésre?

A munka legfontosabb eredményei és megállapításai a következők. Fuoreszcens fehérje-tag-elt PrP-t, Sho-t és ezek kontroll fehérjéit kódoló plazmidokat létrehozva és N2a sejtek transzfekciójával négy stabil transzgenikus N2a sejtpopulációt hoztunk létre. Ezek rendre az EGFP-vel jelölt prion fehérjét (PrP-EGFP sejtek), annak kontroll, EGFP-GPI$_{(PrP),}$ fehérjéjét (EGFP-sejtek), az EYFP-vel jelölt Sho-t (Sho-EYFP sejtek), vagy annak kontroll EYFP-GPI$_{(Sho)}$ fehérjéjét expresszálják (EYFP-sejtek). A kifejlesztett sejtek megfelelő expressziós szinten és megfelelően, azaz, a GPI-horgonyzott fehérjéktől valamint a komplex-glikolizált natív PrP és Sho-tól elvárt módon lokalizált és glikozilált fehérjéket expresszálnak, melyeket konfokális mikroszkópia, valamint, Western blot és PNGase-F enzimemésztéssel igazoltunk.. E sejteket használva és egy nem-detergens alapú OptiPrep folytonos-sűrűséggradiens frakcionálási módszer alkalmazásával kimutatjuk, hogy míg a PrP és a Sho fehérjék raft-típusú membránfrakciókat foglalnak el, jelentős részük jelen van a transzferrin receptorral jelölt, nem-raft típusú membrán doménekben. Továbbá, két másik stabil N2a transzgenikus sejtpopulációt is létrehoztunk: egy a Sho-t további FLAG-taggel expresszáló- (Sho-EYFP-FLAG sejtek) és az ennek megfelelő kontroll (EYFP-FLAG sejtek) sejtpopulációt, hogy lehetővé tegyük koimmunprecipitációs vizsgálatok végzését Sho esetén. Ezekhez, rendre a következő fúziós fehérjéket kódoló plazmidokat készítettük: Sho-EYFP-FLAG-STREP-GPI$_{(Sho)}$ és EYFP-FLAG-STREP-GPI$_{(Sho)}$. E két sejtpopulációt, valamint, a PrP-EGFP és kontrollja sejteket felhasználva és átmenetileg transzfektálva egy vörös fluoreszcens fehérje-taggelt CNX-t kódoló plazmiddal, élő-sejt konfokális mikroszkópiával kimutattuk, hogy mind a Sho, mind a PrP kolokalizál CNX-szel. Ezt követően, a Sho-t expresszáló sejtek FLAG általi ko-immunoprecipitációjával és párhuzamosan Ni-NTA pull-down esszével PrP-EGFP sejtek esetében (ahol a PrP OR régiójának Ni-kötődését használjuk ki), a CNX chaperon precipitációja mind Sho, mind PrP esetében kimutatható a teljes sejtlizátumban. Ez a PrP és Sho CNX-hez való kötődését jelzi. Érdekes, hogy a kölcsönhatás mindkét fajta membránban, raft- és nem-raftokban kimutatható volt, mind Sho, mind PrP esetében. Végezetül, a PrP mentőhatásának hiányát észleltük réz- és egyéb átmenetifém-kezelés során Zpl (*Prnp*$^{0/0}$) sejtekben, a PrP visszajuttatása mellett, valamint, a PrP-t kifejező

transzgenikus N2a sejtekben rézkezelés hatására nem volt megfigyelhető a PrP raft- és nem-raft disztribúciója között különbség.

Összefoglalva, eredményeink azt mutatják, hogy a GPI-vel horgonyzott Sho és PrP ugyan jelen van a raftokban, de érdekes módon kettős, raft- és nem-raft eloszlást mutat. Ez valószínűleg a gyenge kötődést tükrözi a raftokhoz, és a két fehérje sok-funkciós szerepét támogatja. Jelentjük, továbbá, hogy a calnexin mind a Sho, mind a PrP kötőpartnere, függetlenül attól, hogy a tutaj- vagy nem tutaj típusú membrándoménekben lokalizálódnak. Feltételezéseink szerint ezeknek a fehérjéknek (adott időben legalább egy hányadnak) a rendezetlen szerkezete szükségessé tesz dajka-fehérjekötődést, domén-lokalizációjuktól függetlenül, amelyek között a CNX az egyik. Azt javasoljuk, továbbá, hogy a PrP mentő szerepe réz vagy a vizsgált többi fém toxikus hatásaival szemben, vagy rézkezelésre adott válaszként való átrendeződése raft és nem-raft között, komplexebb folyamat az egyszerű fémkötés képességétől, és a használt modellrendszertől is függhet.

1. INTRODUCTION

Transmissible spongiform encephalopathies (TSEs), also called prion diseases, are signature members of conformational diseases or protein misfolding diseases, a category of diseases characterized by protein misfolding and aggregation. Apart of TSEs other major neurodegenerative diseases that fall into this category, such as Huntington diseases, Alzheimer's disease, amyotrophic lateral sclerosis, Parkinson's disease and motor neuron disease[1]. These diseases are commonly associated to specific intrinsically disordered proteins ,with remarkably flexible structures, able to adopt many intermediate states of conformations, and usually form amyloidal self-assemblies during the evolution of the disease[2,3].

1.1 Transmissible spongiform encephalopathies or prion diseases

Prion diseases or TSEs represent a class of incurable neurodegenerative diseases that are infectious and occur in humans and animals. These diseases are characterised by neurodegeneration, synaptic and dendrite loss and neuronal death and in later stages by the spongiform appearance of the brain tissue or gray matter, ultimately leading to death (**Figure 1**)[4]. Prion diseases are believed to be caused by "prions" a term that was created based on the observation that the infectious material in these diseases is made of nucleic acid-free "proteinaceous infectious particle" which was abbreviated as "prion"[5,6]. It was found that at the core of this material stands one protein only, the protein called prion protein (PrP), which was the only protein identified in the infectious prion particles. Prions are remarkably infectious and cause a group of invariably fatal neurodegenerative diseases. These diseases may originate as genetically inherited or acquired through iatrogenic transmission or consumption of infectious material.
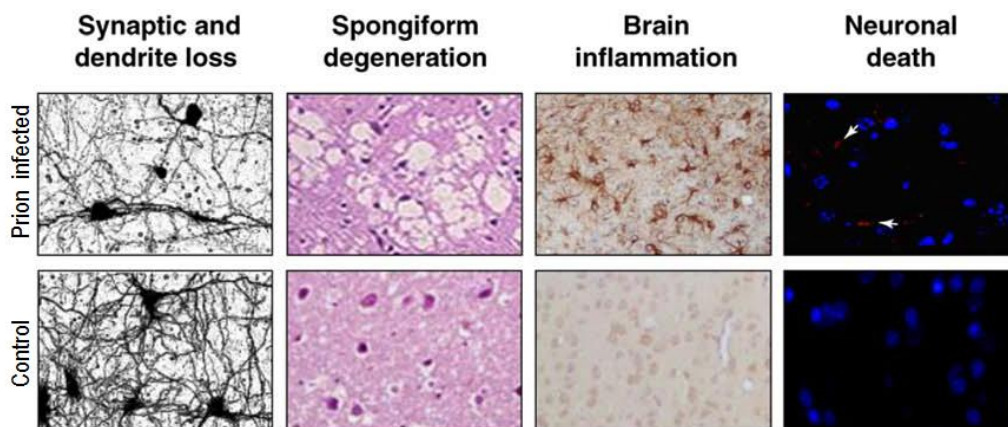
Figure 1. Comparison of mammalian normal and prion infected brain with TSE characterised by synaptic and dendrite loss, spongiform degeneration, brain inflammation and neuronal death. (Adapted from: *Soto C and Satani N, 2011*[4])

Creutzfeldt-Jakob disease (CJD) is the most well-known of the human TSEs, it affects about one in every one million people each year. Other human prion diseases include kuru, Gerstmann-Sträussler-Sheinker disease (GSSD) and fatal familial insomnia (FFI) as summarised in **Table 1**[7]. Prion diseases in animals include scrapie in sheep and goat; bovine spongiform encephalopathy (BSE), also known as "mad cow diseases" in cattle, chronic wasting disease (CWD) in deer and elk[5], or camel spongiform encephalopathy (CSE)[8] in camel, just to name a few among many. The first animal spongiform encephalopathy described was the scrapie of sheep, which was reported to had been transmitted by contact with infectious fluids and/or ingestion of infected material through feed[9]. The symptoms of prion diseases generally include behavioural and movement disturbances, dementia, astrogliosis, degeneration of CNS tissues and absence of immunological responses, where all these symptoms are rapidly progressive and fatal, being incurable at present[5].

PRION DISEASE	MODE	PATHOGENESIS
CJD, Sporadic	Unknown	Spontaneous conversion of PrP^C to PrP^{Sc} or Somatic mutation
CJD, Familial	Inherited	PRNP gene mutation
CJD, Iatrogenic	Transmitted	Infection from prion contaminated growth hormones, duramatter, corneal transplants, surgical procedures etc.
CJD, variant	Transmitted	Infection from BSE prions
KURU	Transmitted	Infection from ritualistic cannibalism
GSSD	Inherited	PRNP gene mutation
FFI	Inherited	PRNP gene mutation

Table 1: Human prion diseases and their aetiology. (Adapted from: *Macalister GO and Buckley RJ, 2002*[7])

Prion diseases are diagnosed only at a late stage, mostly because neither the mechanism of developing disease nor the exact role of native protein is known. There is currently no treatment that can halt progression of any of the prion diseases.

1.2 Protein-only hypothesis of prion propagation

The historical background of TSEs started from description of scrapie in 1732. Initially the TSE agent was thought to be a slow virus and it was assumed that the agent is part of the receptor for virus, under the "Unconventional virus hypothesis"[10,11] Later, after Alper and co-workers (1967) stated that the infectious agent is devoid of nucleic acids and resistant to UV radiation, J.S Griffith and co-workers (1967) proposed the "protein–only" hypothesis for the mechanism of the disease, according to which the infectious agent consists of a modified or self-replicating protein[12,13]. In 1982, Stanley B. Prusiner formulated the currently valid "prion hypothesis" stating that the proteinaceous infectious particle or "prion", resistant to most procedure that modify nucleic acids, stands the basis of the disease[5,6] where the protein ascribed to this particle is none other than a conformationally changed isoform of the normal cellular prion protein[5,14]. During prion disease this normal cellular prion protein (PrP^C) converts to disease-associated conformer, which is called also as scrapie prion (PrP^{Sc}) with different physicochemical

properties, as listed in **Table 2**, and accumulation of this insoluble isoform that are protein aggregates, form intra- and extra-cellular deposits, leading to neurotoxicity and neurodegeneration[15].

PrP^C	PrP^{Sc}
Normal cellular prion protein	Scrapie prion protein (the disease related isoform)
Gene *PRNP* (short arm of chromosome 22)	Reproduced by binding to PrP^C and stimulating conversion of PrP^C to PrP^{Sc}
Rich in alpha helix structures	Rich in beta pleated sheets
Soluble protein	Insoluble protein aggregate
Proteinase K sensitive	Proteinase K resistant
Does not form aggregates	Forms aggregates

Table 2: Biochemical properties of PrP^C and PrP^{Sc}.

According to protein only hypothesis, two mechanisms had been proposed to explain the conformational conversion of PrP^C to PrP^{Sc}: *(a)* The template-assisted model postulates that an interaction between the pathogenic PrP^{Sc} and endogenous PrP^C is sufficient to cause template-driven formation of more PrP^{Sc}[16]; *(b)* The seeding or nucleation-polymerization model postulates that PrP^C and PrP^{Sc} are in a reversible thermodynamic equilibrium and only if several monomeric PrP^{Sc} molecules bind to form a highly ordered seed, then further monomeric PrP^{Sc} are recruited and eventually aggregate to amyloids[17]. Despite many studies, the exact mechanism of conversion of PrP^C to PrP^{Sc} or the disease related isoform is still elusive[5,18,19]. Furthermore, since a prion–like mechanism is common to the other conformational neurodegenerative diseases as well,[20,21] understanding the details of the mechanism and the function of the proteins involved, such as PrP^C along with its family member proteins is of outmost importance.

1.3 The cellular prion protein: structure, biosynthesis and known functions

PrP^C, is a sialoglycoprotein, highly and constitutively expressed mainly in the central nervous system (CNS) and also in other organs, such as liver, heart, lungs, lymphoid system intestinal muscle and testis[22–25]. The three dimensional structure of PrP^C shows two structurally distinct domains **(Figure 2)** for the protein: a flexible, unstructured, intrinsically disordered N-

terminal domain (residues 23-124) comprising about half of the protein, and a structured, globular domain (residues 125-228) called C-terminal globular domain. The globular domain is composed of three α-helices and two short anti-parallel β-strands and possesses also two glycosylation sites (Asn181 and Asn197) and a disulphide bond between Cys179 and Cys214[26,27]. The nascent mouse PrP^C is of 254 amino acids with an N-terminal signal peptide (aa. 1-22), which directs it to the endoplasmic reticulum (ER), and a propeptide (aa. 231-254), which is a signal peptide for a C-terminal GPI-anchor attachment. The mature protein sequence (aa. 23-231) harbours several important regions at its N-terminal half, among them two regulatory positively charged regions, the N-terminal polybasic region and a second basic patch; an octapeptide repeat region (OR) between the two polybasic patches that binds copper and divalent cations; a hydrophobic domain (HD) responsible for many protein-protein interactions, and overlapping with HD, the so called central region (CR) where several disease related mutations occur and deletion of which is lethal to the mice. After several post translational modifications in the ER and Golgi apparatus (GA), PrP^C is routed to the outer leaflet of the plasma membrane (PM), especially to specialised lipid-ordered entities called lipid-rafts[28].

The explicit function of PrP^C is still unknown but studies suggested that it might be a pleiotropic protein with multiple functions and it was shown to participate in various cellular activities, such as signal transduction, copper homeostasis, cell adhesion, protection from apoptotic stimuli and oxidative stress, immunoregulation, neuroprotective signaling and neurotoxic pathways [29–33].

Interestingly, even though PrP is a highly conserved protein among mammals, its deletion is not lethal to mice[34] nor causes developmental abnormalities in cattle and goat[35]. This resulted in the supposition that there might be another protein which in PrP^C's absence it could take over PrP's functions. Despite long-term studies, there are still challenging questions to untangle related to the physiological function of PrP^C and the processes of the disease development: are there any additional factor or factors contributing to the pathophysiological developments? Thus, a better understanding of the details of the normal biology of the cellular prion protein is important, as well as to evaluate the roles of the other members of the prion-family proteins, in normal biology as well as TSE pathogenesis.

1.4 The prion protein as a copper binding protein

One, if not the most obvious, characteristic of PrP^C is linked to the presence of an OR region in its sequence, which confers the ability to the protein to bind divalent cations. Due to this, the most straightforward proposition for the PrP^C's functions is a role as a transition metal-binding protein[36–38]. It is known that metal imbalance occurs in prion disease and metal ions such as copper (Cu$^{2+)}$), manganese (Mn^{2+}) and zinc (Zn^{2+}) play an important role in prion pathogenesis[39,40]. Studies demonstrated that PrP binds Cu^{2+}, Zn^{2+}, Ni^{2+}, Fe^{2+} and Mn^{2+}, among which it has a high affinity specifically for Cu^{2+} ions[41]. Copper binding occurs not only at the OR region, but at two other sites on the protein as well, which are populated by Cu^{2+} in function of its ambient concentration, adding up to six copper molecules that PrP^C can hold at a time, *in vivo* [36,42]. Cu^{2+} binding is also reported to affect the folding and structure of PrP, inducing conformational changes as well as conversion to PK-resistant species and PrP^{Sc}[43–45].

Although PrP^C is able to bind transition metal ions it is much less clear which of these interactions are related to PrP^C's physiological functions. The physiological importance of Cu^{2+} binding to the OR region may be inferred from the studies reporting Cu^{2+} induced internalization and shedding of PrP^C[46–48]. The internalized PrP^C constitutively cycles between the plasma membrane and endocytic compartment via clathrin coated pits-dependent pathway[49–51] and PrP^C had been proposed to be involved in copper sequestration and uptake and maintaining Cu^{2+} and other metals' homeostasis, however, whether it in fact does transport these metals is not clear[33,52,53]. Furthermore, it is plausible that Cu^{2+} or Zn^{2+} binding to PrP^C, which causes endocytosis is a signal for antioxidative defense[33,53]. PrP's antioxidant functions have also been documented in several instances and oxidative stimuli, and a protection against transition metal induced toxicity, exerted by PrP or its fragments had been reported by a few studies[54–56]. However, the mechanisms by which these effects are achieved are not clear at present.

1.5 The members of the prion-family proteins

The human prion gene locus consists of four genes, the *PRNP* encoding for the prion protein, the *PRND* (downstream of prion protein–like gene) encoding for Doppel (Dpl), *PRNT* (prion protein testis specific gene) encoding the Prt protein, and a novel gene *SPRN* (shadow of the prion protein gene), which encodes the Shadoo (Sho) protein[57]. All four genes demonstrate low sequence homology, implying that although they may be evolutionarily related, they may be

functionally distinct[58]. Unlike PrP[C] and Sho, which are mostly expressed in the CNS, Dpl and Prt are testis specific. The least known among them, Prt, is in many cases considered as being a pseudogene, it is not present in all vertebrates, and it is predicted to be a soluble protein with the most distant structure from the other three proteins that are the so far well-recognized members of the prion-family proteins. PrP[C], Sho and Dpl are all GPI-anchored proteins. The structure of Dpl is similar to the C-terminal part of PrP[c]: git is lobular with three alpha helixes and two beta sheets possessing also two glycosylation sites and with two disulphide bonds (compared to one for PrP) (Figure 2) and shows 25% sequence identity to PrP[C59,60]. Several lines of evidence argue against the involvement of Dpl in prion disease[61,62].

1.6 Shadoo protein, the "Shadow of prion protein"

The *SPRN* gene, encoding the PrP[C] paralogue Sho, had been first discovered *in silico* in 2003 and it was termed as the Shadow of prion protein precursor, and the protein as "Shadow of prion protein" or Shadoo (the Japanese word for shadow). The gene is located on the chromosome 7 in mouse (chromosome 10 in humans) and it was found to be highly conserved in all vertebrates from fish to mammals[63]. Sho is mostly expressed in the CNS, especially in the brain, with highest expression in hippocampus and cerebellum[64]. Sho is also expressed in other organs including kidney, lungs, liver, pancreas, prostate, testicle and ovary[65,66]. The secondary structure of Sho is similar to the intrinsically disordered N-terminal part of PrP[C], fully unstructured. The amino acid sequence of Sho possesses characteristic segments, such as starting from the N-terminal, a signal peptide sequence, which directs the protein to the ER, a basic repeat region rich in arginine and glycine, which then is followed by a central hydrophobic domain (HD), a C-terminal region with a single glycosylation site, and finally a terminal signal peptide for a GPI anchor attachment. (Figure 2). Sho appears to lack secondary structures in its C-terminal region, unlike to PrP, possibly due to lack of cysteine residues hence, disulfide bridges in Sho, as well as the region analogous to the α-helical domain present in PrP[C] is too short in Sho to accommodate three α-helical structures[67].
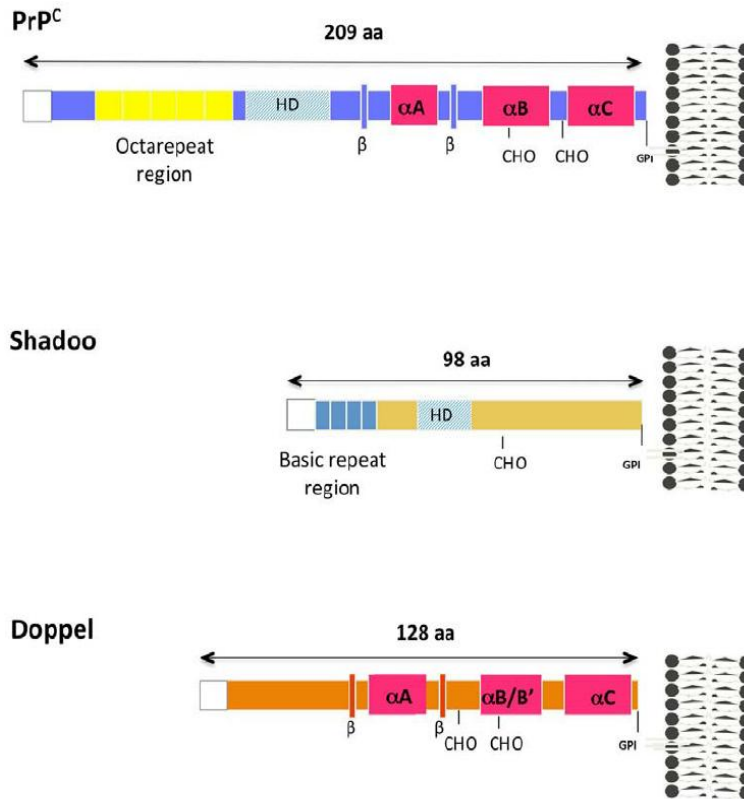
Figure 2: Domain structures of the prion-family member proteins. Schematic representation of PrP^C: in the N-terminal domain the octapeptide repeat region (Octarepeat region), the hydrophobic domain (HD) and in the C-terminal domain, the two beta strands (β) and three alpha helix (α) with the two glycosylation sites (CHO) and at the C-terminal the GPI signal peptide sequence (GPI) anchoring the protein to the membrane. Schematic representation of Shadoo: N-terminal arginine-glycine rich region (Basic repeat region), central hydrophobic region (HD) and one glycosylation site (CHO) with GPI signal peptide sequence (GPI) at the C-terminus anchoring the protein to membrane. Schematic representation of Doppel: three, C-terminal alpha helices (α) and two beta strands (β), two glycosylation sites (CHO) and a GPI signal peptide sequence (GPI) anchoring the protein to membrane, are shown. (Adapted from: *Daude N and Westaway D, 2011*[65])

Sho as a glycoprotein is synthesised in the secretary pathway and is attached to the external leaflet of the plasma membrane via a GPI-anchor[68]. Sho is also present in nucleus besides ER and GA[69,70]. Recently, it was demonstrated that the ER signal peptide of Sho can mediate an alternative targeting of Sho to the mitochondria, a process that is governed by structural features in its intrinsically disorder elements; and that the GPI anchor signal peptide is sufficient to promote efficient ER import of the protein[71]. The physiological functions of newly discovered protein Sho, are less characterized in comparison to PrP^C and Dpl. Howbeit, Sho

proved to be essential for the CNS development in zebrafish in gain and loss of function experiments[63,72].

1.6.1 Structural similarities and differences between Sho and PrP^C

Apart of the similarities in linear domain alignment of Sho and PrP^C, the two proteins have low sequence homology. The most similar domain in the sequence is HD region possessed by the two proteins, and the HD of Sho has a middle stretch of hydrophobic amino acids with 44% sequence similarity with the HD region of PrP^C, this being the only homologous sequence of the two proteins. Similarly to PrP^C, Sho also possesses an endoproteolitic cleavage site near to its GPI anchor. Contrary to PrP^C, Sho has (i) an N-terminal repeat region composed of "RGG" boxes or (RXXX)$_8$ motifs, which does not resemble the histidine-containing octapeptide repeats of PrP^{C69,73}, the octapeptide repeat region of PrP^C binds copper, triggering copper-mediated protein dimerization, however, involvement of Sho's tetra-repeat region in metal binding or induced dimerization is unknown, (ii) the HD region of Sho harbours "GxxxG" motifs, whereas the analogous HD region of PrP harbours palindromic sequence of AGAAAAGA and (iii) Sho's C-terminal region is not known to possess any secondary structure, whereas PrP is familiar for three α-helices[57,63,67,69,73]. Additionally, unlike the C-terminal of PrP^C where two glycosylation sites are present, Sho has only one glycosylation site. In terms of folding and aggregation, however, Sho was also reported to have an ability to refold *in vitro* into an amyloid-like form as well as to be able to form PK-resistant aggregates in cells[67,74–76].

1.6.2 Functional similarities and differences between Sho and PrP^C

The exact biological functions of Sho are not yet uncovered. While both PrP and Sho are expressed at highest levels in the CNS, interestingly, the complementary expression of the two proteins were also observed in certain areas, such as in hippocampus and cerebellum and/or within the same type of neurons: in hippocampal pyramidal cells Sho was intensely detected in the cell bodies, but it was observed to be absent in axonal process, while PrP appeared primarily abundant in axonal projections of the pyramidal cells and presented low expression in cell bodies. Sho was detected in Purkinje cells where PrP is absent[64,77]. Other studies reported that contrary to PrP^C, Sho expression is low in cerebellar granular neurons and high in PrP^C-deficient dendritic processes[64]. Sho had also been found in nuclei of the cells and it was shown to bind DNA and RNA with its N-terminal arginine rich region[69,73,78–80].

26

Sho and PrP[C] are reported to play roles in embryonic development and tissue formation [32,81], and their expression overlaps in the trophoblastic development[82]. It has been suggested that Sho probably participates in the overlapping embryonic pathways with PrP[C] as the *Sprn* mRNA knockdown in the *Prnp*[0/0] mice proved lethal[82]. However, its absence in *Sprn*[0/0] or in double-knockout *Sprn*[0/0]-*Prnp*[0/0] mice proved otherwise, resulting in no dramatic phenotypes[83,84], and rendering Sho's cellular role also puzzling.

Interestingly, during prion infection levels of Sho in the brain decrease in several experimental rodent models and sheep[64,85,86], as well as a study reported the simultaneous occurrence of specific mutations in the *SPRN* gene in CJD-patients[87], suggesting its involvement in the prion disease process. In addition, Sho on its own demonstrated ability to form fibrils in model membranes[88] and amyloid-like aggregates in cell membranes[67] and recombinant Sho increased PrP conversion rate in cell culture setting when administered to the cell media prior infection with scrapie brain homogenate[89]. Moreover, yeast two-hybrid studies and also native crosslinking and immunoprecipitation in mouse neuroblastoma cells, reported that Sho can interact with PrP, indicative also of that they may occupy the same environment *in vivo*[89–91]. However, the significance of this interaction to the evolution of prion pathology remains unknown. On the other hand Sho's its overexpression did not influence prion replication kinetics in transgenic mice[92] and altogether Sho did not prove to have direct involvement in propagating PrP[Sc 86,92,93]. Taking together, the mechanisms governing Sho's involvement in the TSE infected brains remains unclear.

In several experimental settings expression of Sho manifested neuroprotective activities similar to the wild type PrP: its expression prevented neuronal cell death induced by the expression of Dpl or the toxic PrPΔHD or the highly toxic Schmerling mutant PrPΔCR[64,67,94,95]. In addition, ShoΔHD mutant did not acquire neurotoxic potential, but lost the stress-protective activity, contradictory to PrPΔHD mutant, which is toxic[94]. Moreover, like PrP[C], Sho also protects cells against physiological stressors such as excitotoxin glutamate[94]. On the other hand, opposing roles for Sho and wild type PrP had also been reported: expression of Sho caused drug hypersensitivity in certain type of cells, while expression of wild-type PrP rescued cells against the effect of the same drugs[96]. Also, Sho induces large spontaneous ionic currents similarly to the toxic PrP mutant associated with familial human prion diseases, whereas expression of wild type PrP rescues the same cells against these effects[97]. Altogether, these demonstrate that while Sho

and PrP may act similarly then may undertake opposing roles as well depending on the experimental setting and the process studied, and more data are required to understand their exact relation and interplay.

1.7 Role of lipid rafts in the biology of prion and Shadoo proteins and disease

Lipid rafts had been reported to play vital role in various neurodegenerative diseases such as Alzheimer's disease, Parkinson's disease, Huntington's disease, multiple sclerosis and epilepsy[98–101]. The association of GPI anchored proteins, as it is also PrP[C] and Sho, with lipid rafts is well documented and was inferred to be also instrumental in the pathogenesis of PrP[Sc] and prion diseases[102,103]. The segregation of certain lipids into raft-like domains in lipid-membranes, composed of lipid-only mixtures, has long been observed in several experimental settings[104,105]. The existence of similar segregations in the multi component cellular membranes could not directly be observed *in situ* (in lack of appropriate techniques), but had been proven by several indirect methods, based on which a consensus definition for cell membrane lipid rafts was formulated. This defines membrane rafts as being the heterogeneous, dynamic, cholesterol and sphingolipid-enriched membrane nanodomains (10–200 nm) that have potential to form microscopic domains (>300 nm), which dissociate and associate rapidly, and form functional clusters (induced by protein–protein and protein–lipid interactions) by confining specific proteins together to perform specific functions (**Figure 3**), hence, they regulate cellular processes[106,107]. The definition of rafts has been influenced, in large part, by the development of methodologies available for their investigation. Various techniques and tools had been used to study membrane domains and rafts such as the separation and density-gradient flotation of detergent resistant membranes, antibody patching and immunofluorescence microscopy, immunoelectron microscopy, chemical crosslinking, single fluorophore tracking microscopy, photonic force microscopy and fluorescence resonance energy[105,106]. The most widely used methods to gain insights of membrane rafts, specifically of their composition, is their isolation through detergent-based membrane fractionation protocols. In these protocols the membrane rafts are considered as being the detergent-resistant membrane fractions, or DRMs, floating on top of the sucrose gradients[28,108]. The association of PrP[C] to lipid rafts was also studied by this kind of isolation techniques, which revealed that PrP[C]-s raft localization is mediated not only by its GPI-anchor

but also by the N-terminal region of its ectodomain, possibly by the charged polybasic patches, through which PrP can establish various molecular interactions[102,109,110].
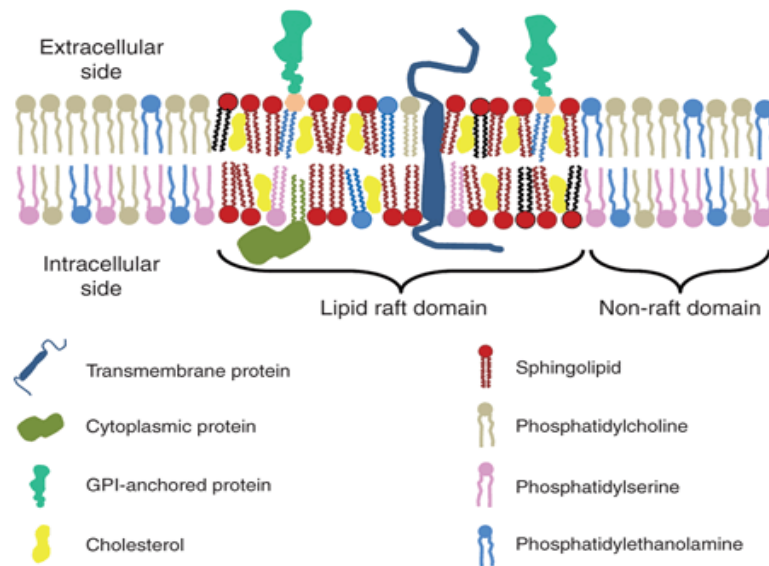
Figure 3: Schematic presentation of cell membrane lipid raft and non-raft domains (Adapted from: *El-Sayed A and Harashima H, 2013*[111]).

Lipid rafts are known as to be involved in various aspects of PrP's metabolism[112]. Not only PrP^C but also PrP^{Sc} is reported to be enriched in the lipid raft fractions that are resistant to detergent extraction and float in the low-density region of the gradients in detergent-based fractionation protocols[28,113]. PrP^C and PrP^{Sc}'s association with lipid rafts is reported to be crucial for PrP's folding and it is a proposed conversion sites of PrP^C to a PrP^{Sc} form, although the exact mechanism of conversion is not known to-date[28,114–118]. In this regard presumed roles of rafts, as depicted by **Figure 4,** are that they could act as trafficking vehicle or meeting place for conversion or contain factors responsible for prion propagation. Internalization of PrP^C was observed to occur also by caveolae, that is in a raft dependent manner, which indicates that the localisation of PrP^C to lipid rafts may be important for maintaining the cellular homeostasis of PrP^C[119–121]. PrP^C's association with lipid rafts in the ER was shown to stabilize its conformation[122]. Furthermore, Taylor and co-workers demonstrated that upon copper exposure a significant proportion of PrP^C present in lipid rafts exits the rafts and relocates to non-rafts in the plasma membrane and proceeds to undergo a clathrin dependent endocytosis, arguing for an effect of copper on PrP's membrane microdomain partitioning[123,124]. Exchanging of PrP^C's GPI-

anchor with a non-raft type transmembrane protein domain prevented its conversion to PrP^{Sc} highlighting that the binding of PrP^{C} to membrane-rafts has importance in prion conversion[102,115,125]. Additionally, disruption of rafts during early stage of PrP^{C} biosynthesis caused the protein to misfold, suggesting a functional role for rafts in maintaining the proper folding of PrP^{C}[122]. These studies support that association of PrP^{C} to membrane rafts is important not only for its conformational conversion, but also for the normal biology of the prion protein[126].
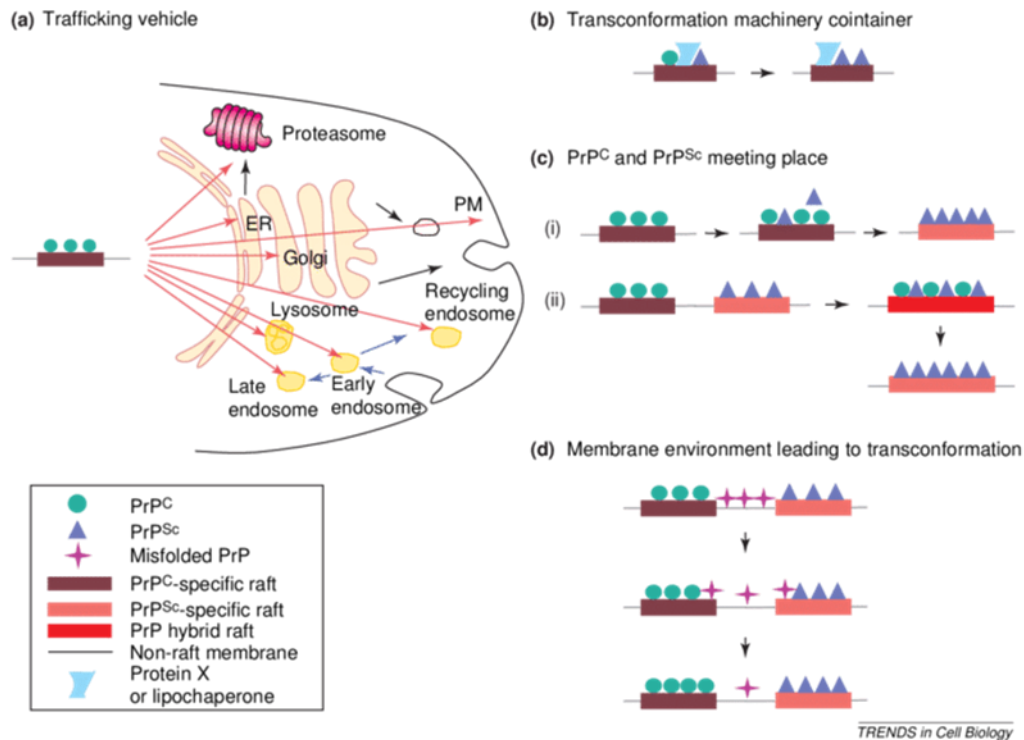
Figure 4: Different possible roles for rafts in prion conversion. (a) Rafts could be the vehicle of prion transport; (b) Rafts could contain the factors (protein X or lipid chaperones); (c) Rafts could be a platform on which PrP^{C} accumulation occurs and lead to prion propagation by promoting encounter between PrP^{C} and PrP^{Sc}(i) or alternatively, coalescence of two specific prion rafts could initiate prion conversion(ii); (d) Specific raft domains could be involved in stabilizing the conformation of PrP^{C} so that, when PrP^{C} exits the rafts, it is misfolded and can interact better with PrP^{Sc} to undergo transconformation (Adapted from: *Campana V and co-workers, 2005*[114]).

On the other hand, the importance of the association of Sho to lipid rafts in the conversion process of PrP^{C} to PrP^{Sc} is not known. Whilst similarly to PrP, Sho in found in lipid rafts (according to isolations using detergent-based methods) and its raft localization proved to be crucial for its folding, as an accumulation of a PK-resistant form and an increase of an

unglycosylated form of Sho in the ER was reported upon lipid raft-disruption[76]. Interestingly, the same authors also found that a percentage of Sho is, contrary to PrP, in a partially PK-resistant and aggregated state already at natural conditions in cells. In addition, studies also demonstrated that Sho binds to anionic lipid vesicles (in model membranes), forms amyloid-aggregates and undergoes fribillization under physiological conditions, but this is not verified yet in *in vivo*[67]. Puig and co-workers showed that the GPI anchor signal sequences play a potential role in the GPI anchor composition, consequently may control the subcellular localisation of proteins *in vivo*[127]. Furthermore, Brügger and co-workers demonstrated that PrP^C and another GPI anchored protein Thy-1 are found in separate microdomains, they traffic very differently and show distinctive differences in their resistance to detergent solubilization and membrane-domain partitioning, emphasizing the significance of GPI anchor in localization of proteins[128]. Bate and co-workers reported that the sailic acid in GPI anchor composition of PrP^C, which is unusual among the mammalian GPIs, regulates the PrP-mediated cell signaling and plays a role in the induction of neurodegeneration[129,130]. A presence of sailic acid in GPI anchor of Sho is not been reported until now. These studies suggest that although the core of GPI anchors is conserved, variable glycan side chains and lipid moieties could localise the proteins to similar or different membrane microdomains. Characterizing exact localization of Sho especially in membrane microdomain in comparison to PrP^C is pivotal to identify the mechanisms if any that underlie prion formation.

1.8 The role of endoplasmic reticulum in prion protein and Shadoo biology and diseases

Endoplasmic reticulum stress associated with protein misfolding, is emerging as being a driving factor in the most common neurodegenerative diseases including Alzheimer's disease, Parkinson's disease and amyotrophic lateral sclerosis[131–133]. In prion diseases, the ER plays a significant role as well[134–136]. One of the proposed routes for conformational conversion of PrP^C is the retrograde transfer of PrP^{Sc} to GA and/or ER, where it binds to the newly synthesized PrP^C precursor protein triggering the formation of PrP^{Sc}[49,137,138]. The cellular factors involved in folding/misfolding of PrP^C, and the initial steps that trigger prion related diseases, are still undefined. Studies showed that different toxic PrP mutants localized principally to the ER. In parallel, in familial forms of CJD, PrP^C-mutants are retained in the ER by chaperones, emphasize the significance of chaperones in prion diseases[138–142]. Furthermore, in CJD patients, misfolded prion aggregation lead to upregulation of the chaperones and folding enzymes caspase-12 and

ERp57. These facilitate the proper folding of proteins in association also with calnexin (CNX) and play a key role in the proper formation of disulfide bonds[143–147]. At the same time, studies demonstrated that the overexpression of quality control proteins (ERp57 and VIP36) reduced prion conversion in prion-infected cells. Native crosslinking studies aimed to delineate an interactome for prion paralogs and using the three prion-family proteins as baits also indicated that PrP^C and its mammalian paralogs pull-down various proteins including ER resident proteins, including CNX and calreticulin (CRT). Although the nature of the method did not permit testing of direct interactions, this endorsed the importance of chaperones, which also play hitherto role in conversion to PrP^{Sc} [90,148,149].

Both ER-chaperones, CNX and CRT, are known to assist in the correct glycosylation and folding, as well as, in the quality control of nascent glycoproteins in the early secretory pathway. They were reported to act together in a concerted manner and together also with ERp57, which in turn forms complexes with both CRT and CNX in the process[150]. While CRT is a soluble chaperone of the ER lumen and known to assist in correct folding of glycoproteins preventing their aggregation, it also has other than chaperoning functions: acts as a calcium-storage protein, affecting many other cellular functions, and correspondingly, it can also be found localized to other cellular compartments, such as cytoplasm and nucleus where primarily serves this latter function[151]. Calreticulin is a paralog of calnexin, which on the other hand is a transmembrane protein, it is reported only to have chaperoning functions, and typically assists the nascent N-glycosylated proteins as soon as they enter the ER lumen[151], involving primarily its luminal domain, which exerts a dual binding activity: its lectin-like globular subdomain binds monovalent glycans on intermediate-glycosylated and unfolded substrate proteins and with an extended arm-like domain can bind to polypeptide chains of substrate and/or other proteins, as for example to the ERp57[150]. Calnexin is proposed to repeatedly bind and releases the same substrate while the nascent protein samples its folding space and undergoes repeated re-glycosylation in presence of CTR and ERp57. Retention of incomplete or incorrectly folded substrate proteins by CNX and CTR protects cells from their toxicity and also a prolonged retention regulates the degradation pathway of misfolded proteins[151,152].

Wang and co-workers reported that PrP interacts with CNX *in vitro* and by this inhibits thermal aggregation of PrP. The same work also showed that and PrP immunoprecipitated CNX *in cellulo* in cultured 293T cells and also in SK-N-SH cells where prevented the cytotoxicity of

PrP expression, draws attention towards the prominence of CNX in reduction of neurotoxicity of PrP[153]. On the other hand, Pepe and co-workers, demonstrated that mature and unglycosylated forms of Sho co-immunoprecipitated with the other ER-chaperone, CRT, in GT1 and human neuroblastoma SH-SY5Y cells[76]. However, the interaction of CNX with PrP in the specialized membrane microdomains, where the conformational conversion of PrP^C proposed to occur, is unknown. Furthermore, whether CNX interacts with Sho, as PrP, and in which membrane microdomains such interaction would be preferred is also not known.

2. AIMS OF THE STUDIES

The main objective of the presented studies is to reveal more information on the properties of the prion-family proteins, prion and Shadoo, with special focus on their localization and distribution to specific membrane microdomains of raft and non-rafts. Beside their distribution, we aim to study their binding with the ER-chaperone protein calnexin within these domains, as well as to test the protective effects of PrP against transition metal toxicity and specifically its membrane domain re-distribution if any, in response to copper treatment. In line with the goals, we proposed the following aims:

1. To compare the membrane microdomain partitioning of prion and Shadoo proteins by using a non-detergent-based fractionation method and N2a transgenic cells expressing the proteins.

Specific aims:

1.1 To establish N2a stable transgenic cells suitable for the studies, which express the Sho or PrP proteins in fusion with a fluorescent protein tag, as well as, corresponding control cells, in order to be able to monitor the proteins by confocal fluorescence microscopy.

1.2 To compare the distribution of PrP and Sho in the isolated membrane microdomain fractions of the developed stable transgenic cells, using a detergent-free, OptiPrep density-gradient fractionation method.

2. To test whether calnexin, is a binding partner of both PrP and Sho and whether the interaction is specific to the type of membrane-domain the proteins reside in.

33

Specific aims:

2.1 To develop transgenic Sho-expressing and corresponding control, transgenic N2a cells, where a FLAG tag is inserted in addition to the fluorescent protein, in fusion with Sho, to allow for performing co-immunoprecipitation assays.

2.2 To compare the partition of FLAG-tagged and non-FLAG-tagged Sho in the membrane microdomains of the cells developed, using the non-detergent, density-gradient fractionation method.

2.3 To study the localizations of Sho and PrP with respect to the localization of calnexin by using live-cell imaging and immunocytochemistry combined with confocal microscopy of the transgenic cells developed.

2.4 To test, whether PrP and Sho interact with calnexin, and furthermore, if such an interaction is observed, whether it is specific to the type of the membrane domain the proteins occupy, using anti-FLAG co-immunoprecipitation and Ni-NTA bead pull-down assay in the transgenic cells developed.

3. To study the effect of copper treatment on the membrane domain localization of PrP.

Specific aims:

3.1. To test the protective effects of PrP against transition metal induced toxicity using mouse hippocampus-derived wild type ZW($Prnp^{+/+}$) and PrP knock-out Zpl($Prnp^{0/0}$) cells without and with reintroduction of PrP gene (part not presented in details in the Thesis).

3.2. Based on the experiments at aim 3.1., to test the effect of the presence of Cu^{2+} on the distribution of PrP in the membrane fractions of the transgenic N2a cells developed above.

<center>3. MATERIALS AND METHODS</center>

3.1 Materials, chemicals and reagents

Cell culture media, supplements and reagents, such as Dulbecco's modified Eagle medium high glucose (4.5 g/l) with glutamine and sodium pyruvate (DMEM, 41966-029), fetal bovine serum (10500-064), GlutaMAX^{TM}(100X) (35050-038), Penicillin-Streptomycin (15070063), TrypLE Express Enzyme (12605-028), G418 Geneticin (10131.019); TurboFect

<center>34</center>

transfection reagent (R0531); Amplex® Red Cholesterol assay kit (A12216) and CellLight™ Golgi-RFP, BacMam 2.0 (C10593) reagent are purchased from Thermo Fisher Scientific. The 100 mm cell culture dishes, Orange Scientific Tissue Culture Dish, surface treated (4450300N) are purchased from Orange Scientific. 8-well covered microscopic glass bottomed plates are obtained from Nunc, Lab-Tek II. Protease inhibitor cocktail (P2714), Calpain inhibitor-I (A6185), Pepstatin (P4265), OptiPrep density gradient medium (D1556), sucrose (S9378), bovine serum albumin (A7906), sodium azide (S2002), Tween®20 (P7949), 4′,6-diamidino-2 phenylindole HCl (DAPI) (D8417), TritonX-100 (T9284), Anti-flag®M2 affinity gel beads (A220) are purchased from Merck/Sigma Aldrich. Paraformaldehyde (16005) purchased from Riedel-dehain. RC-DC protein assay kit is purchased from BioRad (500-0121). ProSieve® QuadColor™ protein marker (00193837) is purchased from Lonza. PNGase F (P0704S) is obtained from New England Biolabs. Immobilon®-P Transfer membrane, pore size: 0.45 μm (IPV00010) and chemiluminiscence HRP substrate (WBKLS0500) are from Merck/Millipore.

3.2 Antibodies

Primary antibodies: the monoclonal anti-Prion antibody SAF-32 (A03202) is purchased from SPIbio; the anti-Shadoo polyclonal SRRN antibody (C-terminal) (AP4754b) is from Abgent; the Living Colors® EGFP monoclonal antibody (632569) is from Clontech; polyclonal anti-Calnexin antibody (ab10286) and anti-Nuclear Pore Complex polyclonal antibody (NPC) (ab73291) are purchased from Abcam; the Flotillin-1 antibody (610820) is from BD Transduction; anti-Transferrin receptor antibody (TfRC) (SAB4200398) and the monoclonal ANTI-FLAG® M2-Peroxidase (HRP) Clone M2 antibody (A8592) are purchased from Merck/Sigma Aldrich.

Secondary antibodies: anti-Rabbit IgG (whole molecule)-Peroxidase (A9169) and the anti-mouse IgG(Fab specific)–Peroxidase (A3682) produced in goat are from Merck/Sigma Aldrich. The polyclonal goat anti-rabbit IgG (H+L) secondary antibody Alexa Fluor® 568 conjugate (A11011) and the polyclonal goat anti-mouse IgG (H+L) secondary antibody Alexa Fluor® 488 conjugate (A10667) are from Thermo Fisher Scientific.

3.3 Cells Neuro-2a (N2a) mouse neuroblastoma cells were purchased from American Type Culture Collection (ATCC) (CCL-131™).

3.4 DNA-plasmids used

To generate cells transiently expressing a red fluorescent protein-tagged calnexin, the plasmid pCMV3-C-OFPSpark (MG53126-ACR) purchased from Sino Biological was used, which encodes for mouse calnexin with C-terminal OFPSpark-tag on a CMV promoter. For generation of N2a stable transgenic cells expressing fluorescent fusion protein tagged prion and Shadoo proteins (named as PrP-EGFP- and Sho-EYFP cells) and their control cells (EGFP- and EYFP cells) expressing only fluorescent protein fusion tag, the following plasmids were used. For mPrP-EGFP fusion protein and its control protein, EGFP-GPI$_{(mPrP)}$, the plasmids labelled as p_mPrP-EGFP-GPI(mPrP) and p_SS(mPrP)-EGFP-GPI(mPrP), respectively (APPENDIX-I, Figure A1 and A2), were engineered in which the enhanced green fluorescent protein's coding DNA sequence (CDS) was used as fusion tag to mPrP, inserted in between the PrP protein's C-terminus and its GPI-signal peptide coding sequence, whereas, for the control protein a similar vector backbone was used in which the EGFP CDS cassette was flanked by the ER-targeting- and the GPI-signal sequences of mPrP. For generation of Shadoo expressing N2a (Sho-EYFP cells) and its control cells (EYFP cells), the plasmids developed by our group in an earlier work[69] were used. These were developed similarly to PrP-plasmids, but an EYFP cassette was used instead of EGFP cassette, flanked by the ER-targeting- and the GPI-signal sequences of Sho. These plasmids were also used further, as parental constructs, to develop two additional plasmids, p_mSho-EYFP-FLAG-GPI(mSho) and p_SS(mSho)-EYFP-FLAG-GPI(mSho) (APPENDIX-I, Figure A3 and A4) where a FLAG-Strep-TagII CDS was additionally inserted in between the EYFP CDS and the GPI-signal sequence of Sho, in the respective parental constructs. These plasmids were used to generate the N2a stable transgenic Sho-EYFP-FLAG and its control, EYFP-FLAG cells. Two other plasmids with the DNA sequences reported earlier[96] were used to develop the stable transgenic N2a/PrP(+EGFP) and its control N2a(+EGFP) cells, which express untagged PrP and soluble EGFP (simultaneously, but not in fusion) and only soluble EGFP, respectively.

3.5 Cell culturing

Cells were cultured in Dulbecco's modified Eagle medium with high glucose (4.5 g/l) (DMEM) supplemented with 10% heat inactivated fetal bovine serum, 1% Penicillin-Streptomycin and 1% GlutaMAX at 37 °C in humidified atmosphere with 5% CO_2. Cells were

passaged regularly at 1:10 ratio after every two days. For storage, cells were frozen in growth media with 10% DMSO.

3.6 Establishment of stable transgenic cell populations

N2a PrP(+EGFP)- and N2a(EGFP) cells: N2a cells overexpressing untagged mouse PrP along with soluble EGFP (N2a/PrP(+EGFP)) and its control cells expressing only soluble EGFP (N2a(EGFP)) established by transfecting N2a cells with EGFP and PrP and only-EGFP encoding pSB transposon vectors with TurboFect transfection reagent using Sleeping Beauty gene delivery system described in Nyeste and co-workers (2016)[96]. After two weeks of post transfection, cells expressing stable transgene were separated from non-transfected cells using fluorescence-activated cell sorting (FACS).

PrP-EGFP-, Sho-EYFP-, Sho-FLAG-EYFP- and their respective EGFP-, EYFP- and EYFP-FLAG- control cells: N2a stable transgenic PrP-EGFP, Sho-EYFP, Sho-FLAG-EYFP and their control cells EGFP-, EYFP- and EYFP-FLAG were made by transfecting N2a cells with plasmids containing respective protein with fluorescent fusion tags. Transfections were carried out using TurboFect transfection reagent as indicated by manufacturer. Briefly, N2a cells plated on 8-well chambered cover glass bottomed plate, a day before the transfection to reach 50-60% confluence. 0.25 µg of plasmid DNA and 0.5 µl TurboFect were mixed in 20 µl DMEM and incubated for 20 min at room temperature (RT), prior to its addition to the cells. Media with transfection mixture was removed from the cells after 6 h and replaced with fresh growth media and cultured for additional 12 h. Growth media with 500 µM geneticin added to the cells maintained for two days followed by transferring cells to 60 mm cell culture dish. Cells were grown under antibiotic selection was exchanged with fresh growth media alternate days for ten days prior to transfer to 100 mm Petri dish to obtain well separated single individual colonies. Individual colonies were hand-picked under fluorescence microscope and cultured until it reached confluence in 100 mm Petri dish. GFP positive cells were additionally sorted using BD FACSJazz fluorescence-activated cell sorter instrument (BD, Franklin Lakes, NJ, USA). Mixed populations were made by mixing individual colonies in equal ratios and maintained in growth media.

3.7 Confocal microscopy

Fluoview FV1000 (Olympus Life Science Europa GmbH, Hamburg, Germany) confocal laser scanning microscope was used to image the live cells (presented on Figure 6, 8, 14). The specific settings used were as follow: UPLSAPO 20x (N.A. 0.75) objective, with applying 4.0 µs/pixel sampling speed and sequential, unidirectional scanning mode. For DAPI, EGFP/EYFP and RFP used excitation lasers of 405 nm, 488 nm and 543 nm with emission filters of 425-475 nm, 500-530 nm, LP560, respectively.

VisiScope CSU-W1 spinning disk confocal microscope (Visitron Systems GmbH, Puchheim, Germany) was used to image live and fixed cells (presented on Figure15 and 16). Specific settings used were as follows: 100x oil immersion objective and excitation lasers of 405 nm for DAPI, 488 nm for EGFP/EYFP or Alexa Fluor 488- and 543 nm for RFP or Alexa Fluor 568- labelled antibodies were used, and the corresponding fluorescence signals were detected by using the emission filters of 425-475 nm, 500-550 nm and 570-640 nm, respectively.

3.8 Transient transfection of cells

For transient overexpression of calnexin, 24 h prior to transfection, 3.5×10^4 cells/well were seeded on 8-well coverslip glass bottom plates in 250 µl of complete DMEM. Mixed the plasmid-DNA (0.38 µg/well) and Turbofect transfection reagent (0.6 µl/well) in serum-free DMEM and incubated for 20 min at RT followed by its addition on top of the cells. After 48 to 72 h after transfection, cells were imaged using VisiScope CSU-W1 spinning disk confocal microscope.

3.9 Golgi apparatus labeling

Respective transgenic- and parental N2a cells were labelled for Golgi apparatus using CellLight™ Golgi-RFP, BacMam 2.0 reagent as according to manufacturer's protocol. Briefly, 24 h prior to addition of the reagent, 0.4×10^5 cells were plated on 8-well chambered cover glass-bottomed plates. Next day, 12 µl of reagent mixed with growth media to give a PPC (particles per cell) value of 30 for the final concentration of reagent, was added to the cells followed by overnight incubation in CO_2 incubator at 37 °C. Labelled cells were imaged using a Fluoview FV1000 confocal laser scanning microscope.

3.10 Immunocytochemistry

At 24 hours prior to the experiment, PrP-EGFP- and Sho-EYFP-FLAG cells along with their controls cells were seeded on an 8-well covered glass bottomed plate, such that they reach 80%-90% confluence at the time of the experiment. Cells were washed with phosphate-buffered saline (PBS) and were fixed using 4% paraformaldehyde (PFA) for 7 min at RT followed by PBS washes and permeabilization with 0.1% Triton X-100 (dissolved in PBS) for 7 min at RT. After permeabilization, the Triton X-100 was removed from the cells by washing the cells with PBS, after which the cells were blocked by adding blocking solution (1% BSA in PBS) for 1 h at RT. Primary antibodies against prion, Shadoo (anti-GFP for PrP-EGFP- and Sho-EYFP-FLAG cells) and calnexin (polyclonal anti-calnexin for cells) at 1:200 dilution in blocking solution was added and the cells were incubated at 4 °C, overnight. Next day, the primary antibodies were removed and cells were washed using blocking solution, which was followed by addition of the corresponding Alexa fluor conjugated secondary antibodies, as follows: for prion protein and Shadoo primary antibodies, anti-mouse Alexa fluor A488 (green emitting) and for calnexin anti-rabbit Alexa fluor A568 (red emitting) secondary antibodies were added, each at 1:300 dilution in blocking solution for 1 h at 37 °C. The unbound secondary antibodies were washed off from the cells by PBS and the cell nuclei were stained by 100 ng/ml of DAPI for 5 min at 37 °C. Cells were washed with PBS to remove the excess DAPI the cells were kept in PBS to record the images of the fluorescent signals using VisiScope CSU-W1 spinning disk confocal microscope.

3.11 Extraction of total cell lysates

Cells grown on one 100 mm Petri dish were washed with ice-cold PBS (137 mM NaCl, 2.7 mM KCl, 6 mM $Na_2HPO_4.2H_2O$, 1.4 mM KH_2PO_4, pH 7.4), scraped in PBS and pelleted at 500 x g for 5 min. To the pellet 1 ml cold lysis buffer (50 mM Tris–HCl pH 7.4, 150 mM NaCl, 1 mM EDTA, 1% Triton X-100, 1 mM phenylmethyl sulfonyl fluoride and protease inhibitor cocktail) was added, resuspended pellet and kept on a rocker for 30 min at 4 ºC to extract the proteins. The concentration of protein determined using the RC-DC protein assay kit according to the manufacturer's instructions.

3.12 Detergent-free separation of membrane-rafts

Prior to membrane-rafts isolation, the population of cells were examined under microscope to ensure that 90% of cells express the fluorescent protein. Cells were seeded at 1x10^6 cells per one 100 mm Petri dish, in total of ten dishes. Membrane-rafts isolation was performed using the detergent-free, OptiPrep density gradient method developed by Macdonald and Pike, 2005[154] as follows. All procedures were performed at 4 °C. The cells grown on Petri dishes for 24-36 h, up to ~80% confluency, were washed with cold PBS, were scraped from the dishes into 2 ml of Buffer A (20 mM Tris-HCl, pH 7.8, 250 mM Sucrose, 1 mM $CaCl_2$ and 1 mM $MgCl_2$) and were centrifuged at 250 x g for 2 min to collect the pellet. Cell pellets were resuspended in 1 ml of ice cold-Buffer A containing protease inhibitors at final concentrations of 0.2 mM aminoethylbenzenesulfonyl fluoride, 1 µg/ml aprotinin, 10 µM bestatin, 3 µM E-64, 10 µg/ml leupeptin, 2 µM pepstatin, and 50 µg/ml calpain inhibitor I, and sheared through 18G × 1.5″ needle 30 times. The lysate was centrifuged 250 x g for 2 min and the first post nuclear supernatant was collected and transferred to fresh tubes. The pellets were lysed again in a similar way and the resultant second post nuclear supernatant was merged with the first. DC protein assay kit was used to assess the total protein concentration of the combined sample. For separation of membrane microdomains, 5 mg of total protein from each cell type was taken and mixed with Base buffer (50% OptiPrep density gradient medium in 20 mM Tris-HCl, pH 7.8, 250 mM sucrose) to give a final concentration of 25% OptiPrep in volume of 4 ml and placed in bottom of 12 ml ultracentrifuge tube. In the ultracentrifuge tubes, an 8 ml continuous gradient of 0–20% OptiPrep in Base buffer was laid on top of 25% OptiPrep-sample solutions. The gradients centrifuged for 90 min at 52000 x g in Sorvall ultracentrifuge (Sorvall WX 80+ Ultracentrifuge, Thermo Fisher Scientific, USA) at 4 °C using a TH641 rotor. From each tube commencing from top to bottom of the gradient 18-fractions of 0.67 ml volume were collected, and subjected to sodium dodecyl sulfate-polyacrylamide gel electrophoresis (SDS-PAGE) followed by Western blot analysis of selected proteins using equal amounts of proteins from each fraction. A blank (only Buffer A without protein sample) density gradient was performed in parallel to measure density of OptiPrep gradient corresponding to each fraction. The density of each gradient fraction was calculated by measuring the absorbance of OptiPrep at 340 nm with a Nanodrop-1000 13 spectrophotometer. Raft-type membrane fractions were identified from non-raft type fractions based on Persaud-Sawin and co-workers (2009)[155] by monitoring the total protein- and

cholesterol contents of fractions and by detection of raft resident protein Flottlin-1 and non-raft resident protein, transferrin receptor protein (TfRC) using Western blot.

3.13 PNGase F treatment

The post nuclear samples of PrP-EGFP-, Sho-EYFP- and parental cells obtained as mentioned under the section Detergent-free separation of membrane-rafts, were used to perform PNGase F treatment. Total protein concentrations of the samples were measured using RC-DC protein assay kit. Samples of 20 µg total proteins were subjected to deglycosylation using PNGase F (Peptide-*N*-Glycosidase F) enzyme as follows. Two parallel aliquots of sample were denatured at 100 ºC for 10 min, after which to one of the samples 1500 units of PNGase F enzyme was added (+ samples), while from the other this was omitted (-, control samples) and samples were incubated at 37 ºC for 2 h. The degree of deglycosylation of the proteins in the processed samples was assessed by performing SDS-PAGE and Western blotting.

3.14 Copper treatment of cells

Stable transgenic PrP-EGFP- and EGFP cells were seeded at $1x10^6$ cells per 100 mm diameter Petri plates using in total ten plates. After ~24 h when cells reached 80-90% confluency, the cells were washed once each with PBS and then by OptiMEM-1 media supplemented by 1% GlutaMAX. $CuSO_4$ at 500 µM concentration was mixed with glycine in OptiMEM-1 media supplemented by 1% GlutaMAX at 1:4 copper to glycine molar ratio and the mixture was incubated for 1 h at RT. Next, this incubated mixture of copper-glycine was added to the cells and cells were incubated for 30 min at 37 °C in CO_2 incubator. In parallel, as negative control, only OptiMEM-1 media supplemented by 1% GlutaMAX, without copper-glycine mixture, was added to another set of cells, which were incubated similarly. After the treatment, membrane-rafts were separated from cells as mentioned in the section Detergent-free separation of membrane-rafts (Materials and methods), and the distribution of various proteins along the gradient fractions were assessed by Western blotting.

3.15 Western blotting

Total cell lysate (4 µg total proteins/sample) or separated membrane fractions were used for Western blotting. In case of the membrane fractions, an aliquot of 10 µl from each gradient fraction (1 through 18) was denatured in 2.5 µl of 5x SDS gel loading buffer and loaded on to

8%, 10% or 12% SDS-polyacrylamide gels (PA), depending on the size of the protein of interest. Gradient samples from fractions #1 to #18 were loaded in parallel on two separate gels with the same percentages (fractions #1 to #12 on one gel and fractions #13 to #18 on the second gel) and SDS-PAGE was run for 60 min at 150V. The two gels with resolved proteins were electro-blotted side by side onto a single methanol-activated Immobilon®–P PVDF transfer membrane (with samples from fractions 1 to 18 aligned on blot) in cold transfer buffer (25 mM Tris, 192 mM glycine and 20% methanol pH 7.4) for 1 h at constant current (400 mA). The blotted membrane was blocked for 1 h at RT in blocking buffer (5% non-fat milk in PBS in presence of 0.05% Tween-20) and was washed by three washes of PBS with 0.05% Tween-20 (PBST) each for 5 min, and was incubated overnight at 4 $^{\circ}$C with the appropriate primary antibodies. The primary antibodies used were as follows: anti-prion SAF-32 (1:3000) for prion protein, anti-shadoo SPRN (1:4000) for Sho, anti-GFP (1:4000) for EGFP and EYFP, anti-Flotillin-1 (1:4000) for Flottilin-1 used to indicate rafts, anti-transferrin TfRC (1:4000) for transferrin receptor protein as non-raft, anti-Calnexin (1:4000) for calnexin which is abundant in the endoplasmic reticulum, anti-nuclear pore complex NPC (1:4000) for the nuclear pore complex protein as nuclear membrane marker. After incubation with primary antibody followed by four washes with PBST (5 min each wash) to remove unbound antibodies, blots were incubated with the corresponding horseradish peroxidase-conjugated secondary antibodies in blocking buffer for 2 h at RT, at a dilution of 1:60000. After secondary antibody incubations, blots were washed for five times (5 min each time) with PBST to remove the unbound secondary antibodies and chemiluminescent HRP substrate was added to detect the protein bands, which were visualised on X-ray films.

3.16 Cholesterol determination

Amplex® Red Cholesterol assay kit was used to measure the total cholesterol in gradient fractions by following the protocol as suggested by the manufacturer. Briefly, 50 μl of even numbered gradient fraction samples (fraction number: 2, 6, 8, 10, 12, 14, 16), cholesterol reference standards, positive controls (hydrogen peroxide) and negative control (only buffer) were placed separately in each well of 96-well flat-bottomed plate. Next, 50 μl of Amplex Red reagent/HRP/cholesterol oxidase/cholesterol esterase working solution [300 μM Amplex Red reagent, 2 U/ml HRP and cholesterol oxidase, 0.2 U/ml cholesterol esterase] was mixed with each sample in the 96-well plate and incubated for 30 min at 37 ºC protected from light. After 30 min, fluorescence was measured using 565 nm excitation and 580 nm emission wavelengths in a

Fluoroskan Ascent FL Microplate Fluorometer and Luminometer (Thermo Fisher Scientific) microplate reader.

3.17 Ni-NTA bead pull-down assay

Either total cell lysates of stable transgenic PrP-EGFP-, EGFP- and parental cells or each gradient fraction of PrP-EGFP cells were used in pull-down experiments, where the prion protein was pulled with Ni-NTA beads in the assay. Samples of 1 mg of protein from total cell lysates or 50 µl of each gradient sample were incubated with 30 µl of pre-equilibrated Ni-NTA beads in 1 ml Tris-Sucrose buffer (20 mM Tris-HCl, pH7.8 and 250 mM sucrose) at 4 °C for overnight with end-over-end rotation. Next, centrifuged the beads at 14000 rpm for 1 min and washed with Tris-sucrose buffer containing 0.25% Triton X-100 for 5-times. The beads were boiled with SDS-sample loading buffer for 5 min, and were subjected to SDS-PAGE followed by Western blotting for prion protein (SAF-32 and anti-GFP) and calnexin (anti-CNX antibody) protein.

3.18 Co-immunoprecipitation

Either total cell lysates or fractionated samples of Sho-EYFP-FLAG- and EYFP-FLAG cells were pooled separately as raft- and non-raft fractions based on the distribution of raft resident protein Flotillin-1 and non-raft resident protein, transferrin receptor, along the density gradient as detected by Western blotting. 1 mg of total cell lysate or separately pooled raft or non-raft fractions were subjected to co-immunoprecipitation with anti-FLAG beads. 30 µl anti-flag affinity beads were incubated with or without sample (negative control) in 5 ml incubation buffer (50 mM Tris-HCl, pH 7.4, 150 mM NaCl and 1% Triton X-100) at 4 ºC for overnight with end-over-end rotation in order to pull FLAG tagged proteins along with their binding partners. Pelleted beads were washed 5-times with wash buffer (50 mM Tris-HCl, pH 7.4, 150 mM NaCl and 0.25% Triton X-100) and were boiled in SDS-sample loading buffer for performing SDS-PAGE followed by Western blotting for Sho (α-Sho and α-GFP) and calnexin (α-CNX).

4. RESULTS

4.1 The study of the membrane-domain localization of prion and Shadoo proteins

4.1.1 N2a stable transgenic cells developed for the studies and their characterization.

To study the membrane microdomain localization of the two prion-family proteins, Shadoo and prion, we chose mouse neuroblastoma Neuro-2a (N2a) cells. These cells are well characterized and broadly used as a cellular model system in the study of physiology of cellular and the pathological prion protein[90,156]. N2a cells possess detectable amounts of endogenous PrP but not Sho; at least the endogenous Shadoo expression cannot be detected in these cells with the currently available shadoo antibodies[70,86,96,97,157]. To compare Sho and PrP, we generated N2a cells stably expressing either Sho or PrP in fusion with a fluorescent protein (EYFP for Sho and EGFP for PrP) tag by using the plasmid constructs described in the Materials and methods section for PrP (for the plasmid Map see Appendix-I, Figure A1) and earlier by our group for Sho[69]. We named these generated cells populations as Sho-EYFP- and PrP-EGFP cells, respectively. We similarly generated also control cells, by using corresponding control plasmids for the PrP construct (Appendix-I, Figure A2) and for Sho[69]. These plasmids were developed similarly, but by using this time –only the coding sequence (CDS) of the respective protein's fluorescent protein tag, flanked by the ER-targeting and the GPI-signal sequences of Sho or PrP. The schematic of DNA constructs used are represented in **Figure 5**.

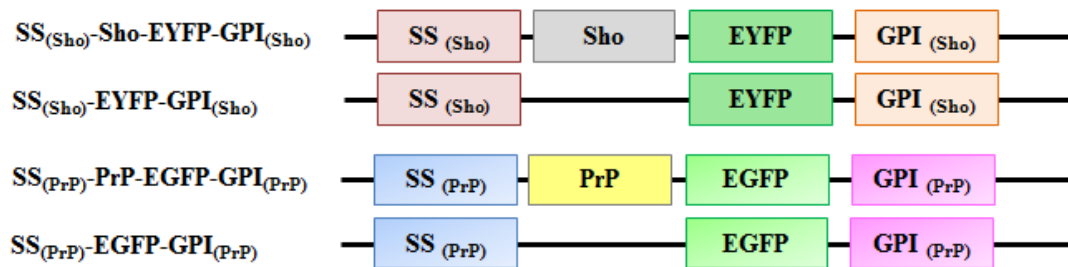**Figure 5: Shadoo and prion protein DNA-constructs used in the studies.** Schematics of the DNA constructs used with the major sequence elements are depicted that code for as follows. SS(Sho)/SS(PrP): N-terminal signal peptide of Sho or PrP; EYFP/EGFP: yellow fluorescent protein or green fluorescent protein, GPI(Sho)/GPI(PrP): propeptide of Sho or PrP leading to glycosylphosphatidylinositol anchor attachment.

Thus, the N2a cell populations stably expressing fluorescent proteins only (EYFP-GPI$_{(Sho)}$ and EGFP-GPI$_{(PrP)}$) were developed and termed as EYFP- and EGFP cells, respectively.

4.1.2 Subcellular localization and expression of the transgenes, fluorescent protein-tagged prion protein and Shadoo and of their control proteins, in the stable transgenic cells developed.

To test whether Sho and PrP fluorescent fusion protein constructs expressed and localized as expected in Sho-EYFP- and PrP-EGFP cells, the proteins were visualized in live-cells using confocal microscopy **(Figure 6)**. We found that both proteins with fluorescent tags, Sho-EYFP-GPI$_{(Sho)}$ (Figure 6A, a-d) and PrP-EGFP-GPI$_{(PrP)}$ (Figure 6A, e-h) are predominantly localized to the plasma membrane and also to the perinuclear region where they appear as intense fluorescent patches on one side of nuclei in the cytoplasm in Sho-EYFP- or in PrP-EGFP cells. Treating the cells with the Golgi apparatus fluorescent marker CellLight™ Golgi-RFP (Figure 6A, c,g,k), the characteristic patches of the Sho or PrP could be identified as GA, demonstrating the localization of Sho (merged picture, Figure 6A, d) or PrP proteins (merged pictures, Figure 6A, h) to the GA. FACS analysis of the N2a cells expressing Sho and PrP proteins tagged with fluorescent proteins, indicate that more than 97% of the cell populations used for the experiments were expressing the respective proteins (Figure 6B).
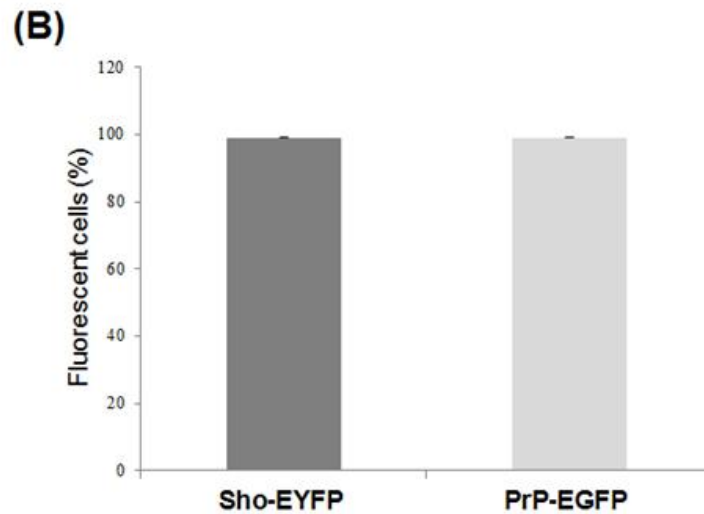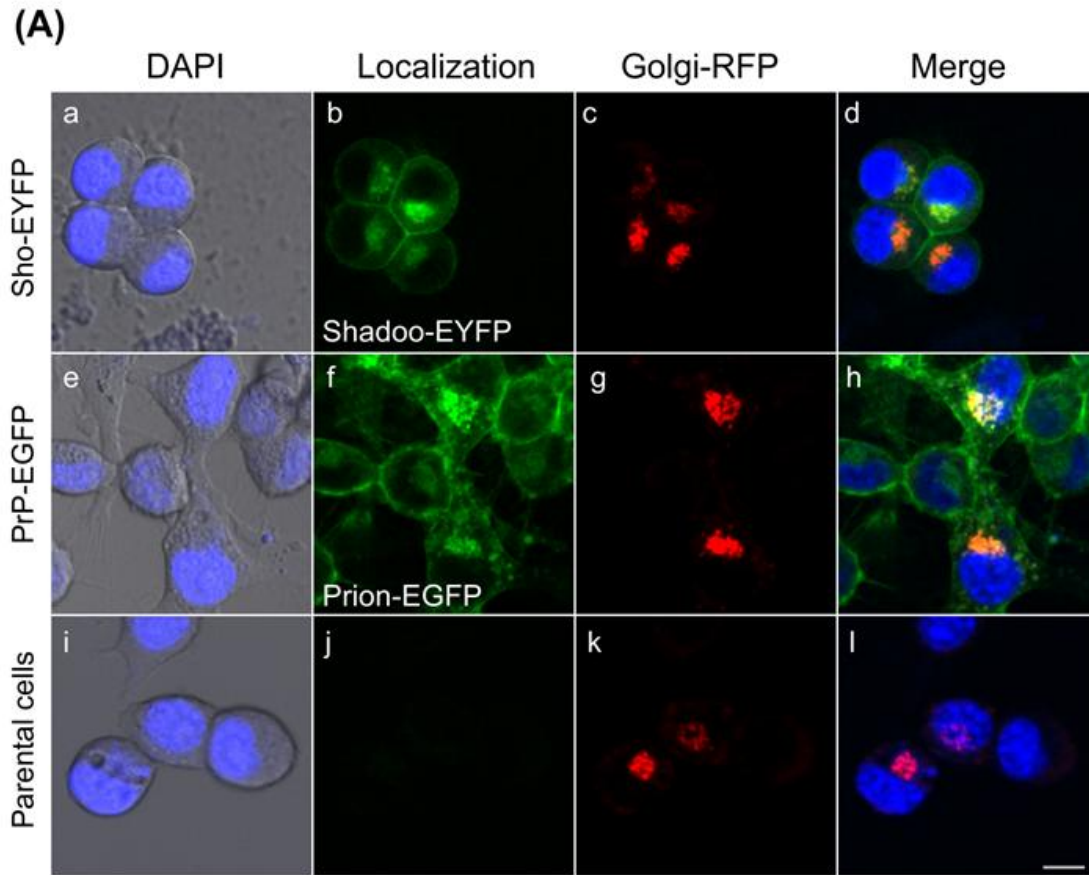
Figure 6: Subcellular localization of fluorescent fusion protein tagged Shadoo and prion protein in N2a Sho-EYFP- and PrP-EGFP cells. (A) Representative confocal microscopy images of the stable transgenic N2a Sho-EYFP- and PrP-EGFP cells overexpressing Sho-EYFP-GPI$_{(Sho)}$ labeled as Shadoo-EYFP (a-d), PrP-EGFP-GPI$_{(PrP)}$ (e-h) proteins labeled as Prion-EGFP and of the parental N2a cells (i-l). Fluorescent signals of overexpressed proteins are shown in

green. The Golgi apparatus labeled by CellLight™ Golgi-RFP is shown in red. Cells nuclei labeled by DAPI are shown in blue. Transmitted light- and DAPI images of the respective cells were merged and are shown in the first column. All fluorescent channels merged are shown in the last column. Scale bar: 10 µm. (B) Percentage of N2a cells overexpressing Sho-EYFP-GPI$_{(Sho)}$ and PrP-EGFP-GPI$_{(PrP)}$ in stable transgenic Sho-EYFP- and PrP-EGFP cell populations.

Total cell lysates of Sho-EYFP- and PrP-EGFP cells were analysed for expression of overexpressed Sho and PrP by Western blotting and using the antibodies α-Sho and α-GFP for Sho- and α-PrP and α-GFP for PrP to detect the protein constructs. Western blot analysis confirmed that both Sho and PrP are appearing at their expected molecular weights corresponding to their sizes as fusion proteins, ~45-49 kDa for Sho and ~60-70 kDa for PrP, detected with respective antibodies (**Figure 7**). In Sho-EYFP cells, two bands within the expected molecular weight range of Sho-EYFP-GPI$_{(Sho)}$ (~45-49 kDa) are detected by α-Sho or α-GFP antibodies (Figure 7A, lane 4-5), which are not present in parental cells (Figure 7A, lane 1-2). This indicates that two forms of Sho are present, since these two bands are visualized by α-GFP as well. Since there are no unambiguously excellent α-Sho antibodies available, cross reactive bands were commonly produced on the blots of various other cells by anti-Sho antibodies[64,70,96,97,157]. Since Sho and PrP possess one and two N-glycosylation sites, respectively, they may exist as a mixture of proteins with different states of glycosylation, hence, with different molecular weights. Therefore, on an SDS gel these populations will appear as different proteins bands. When Sho-EYFP- and PrP-EGFP samples are treated with PNGase F (an enzyme that removes complex N-glycans) to test if the overexpressed proteins had complex N-glycosylations; a small shift in both forms of Sho bands can be been observed by α-Sho or α-GFP demonstrating their identity as Sho-bands as well as evidence that both forms are glycosylated forms of Sho (Figure 7A, lane 6). This result is in line with earlier findings, and the two bands observed for Sho in our N2a cells may correspond to the two glycosylated forms of Sho identified by Pepe and co-workers in GT1 cells[76]. In PrP-EGFP cells, the different glycosylated forms of PrP, expected at molecular weight range of ~60-70 kDa for the overexpressed EGFP tagged PrP, are not well separated in the untreated sample (Figure 7B, lane 6). However, in response to enzyme treatment, similarly to Sho, a small shift is observed for the PrP-band, as detected by both α-PrP and α-GFP, indicating that PrP-EGFP fusion protein is also glycosylated. Contrary, in parental N2a cells, multiple forms of the glycosylated endogenous PrP^C are well detected and are appearing at apparent molecular

weights in the range of 26-42 kDa (Figure 7C, lanes 1-2). These bands, upon deglycosylation by PNGase F shifted to form a single band (Figure 7C, lanes 3) as also commonly observed[122,158]
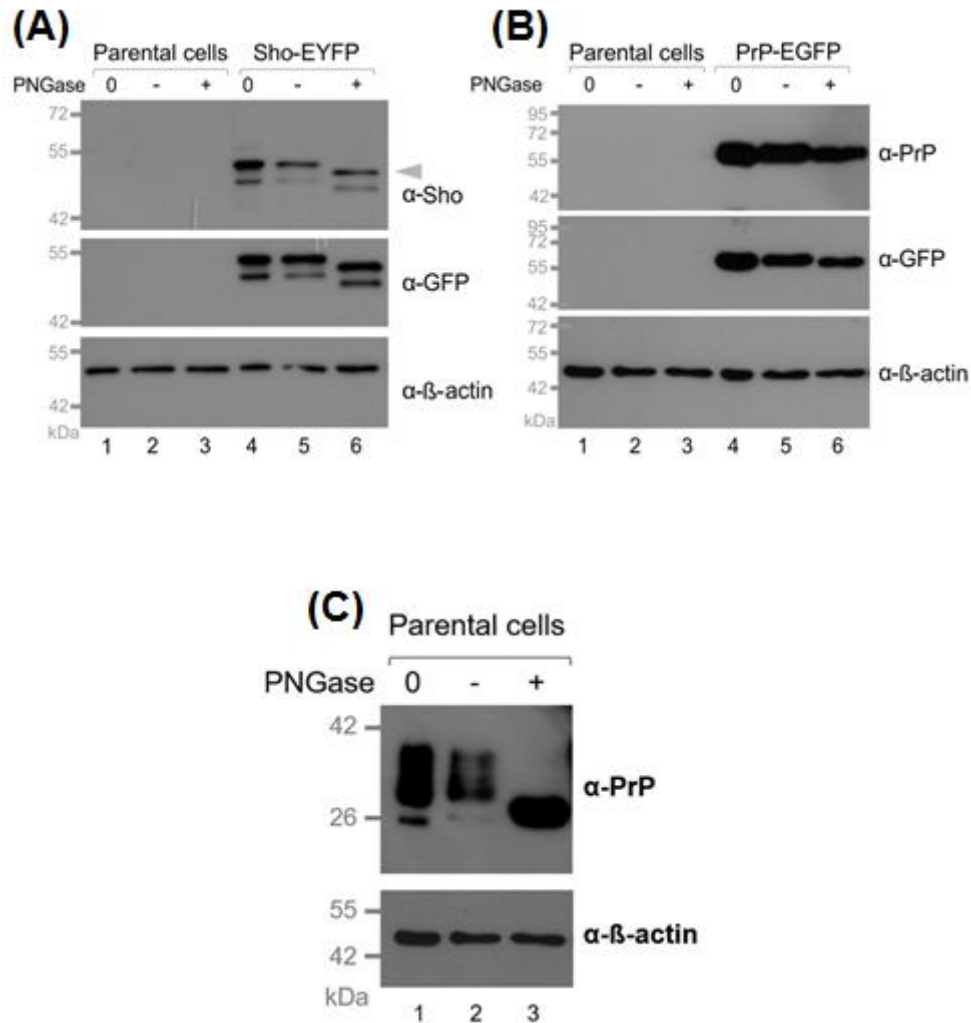
Figure 7: Expression of overexpressed Shadoo, Sho-EYFP-GPI$_{(Sho)}$, PrP-EGFP-GPI$_{(PrP)}$ and endogenous prion proteins in N2a cells. Western blots of the total cell lysates of control (0), PNGase F treated (+) and untreated (-) samples of Sho-EYFP (A) and PrP-EGFP (B) cells, both side-by-side to parental N2a cells, and of parental N2a (C) cells. The expression of Sho is tested by α-Sho and α-GFP and of PrP by α-PrP and α-GFP antibodies. "Arrow-head symbol" on panel-A indicates the corresponding band for Shadoo. β-actin is used as loading control.

In parallel to PrP-EGFP- and Sho-EYFP cells, we also examined the localisation of the control proteins (EGFP-GPI$_{(PrP)}$ and EYFP-GPI$_{(Sho)}$) in the control cells (EGFP- and EYFP cells)

which were established as controls for PrP-EGFP- and Sho-EYFP cells, respectively, by using confocal microscopy **(Figure 8)**.
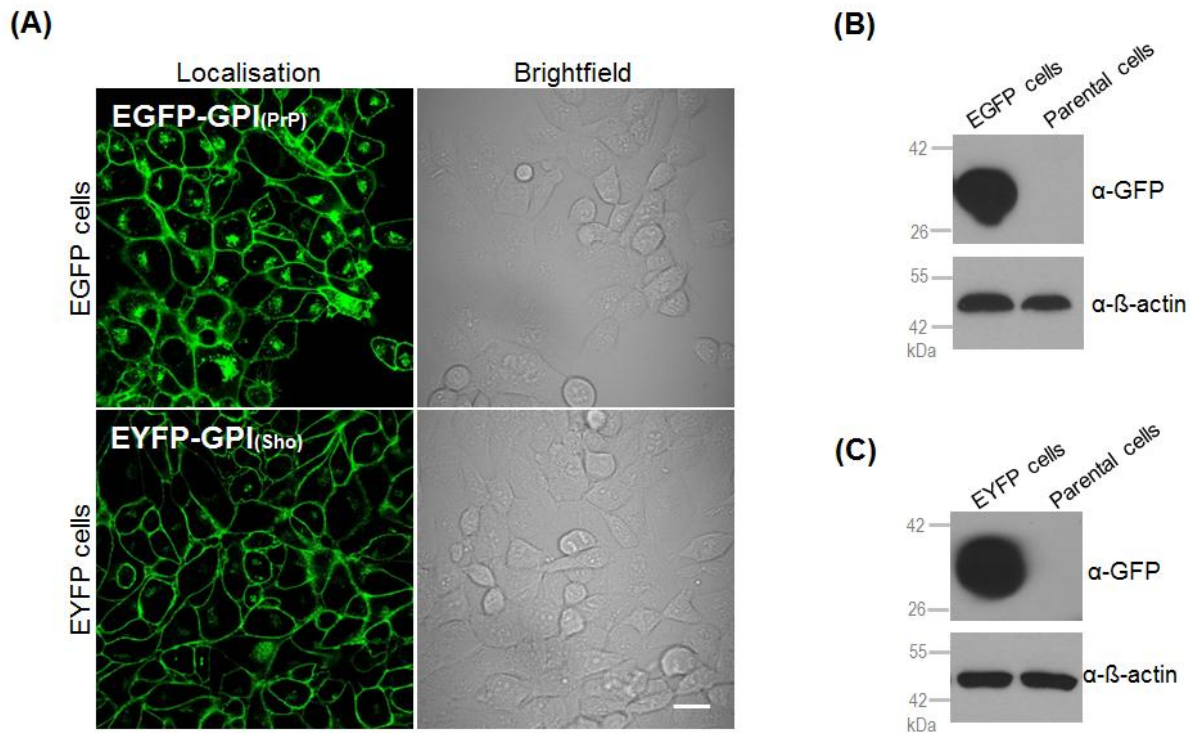
Figure 8: Subcellular localization and expression of the control proteins in the control, EGFP- and EYFP cells. (A) EGFP-(upper panel) and EYFP(lower panel) cells expressing only fluorescent proteins tags with GPI anchor signal sequences of Sho and PrP, respectively, but without the protein of interest. Fluorescent images of cells are acquired with 60X oil immersion objective of Fluoview FV1000 laser scanning confocal microscope. Scale bars: 10 μm. Western blots of the total cell lysates isolated from EGFP- (B) and EYFP (C) cells detected by α-GFP to confirm the expression of fluorescent proteins tags. Total cell lysate of parental N2a cells are used as control. β-actin is used as loading control.

As can be seen, both control proteins, localize to PM and ER (Figure 8A), similar to Sho and PrP in Sho-EYFP- and PrP-EGFP cells. Western blots of total cell lysates of EGFP- and EYFP cells (Figure 8B, C) demonstrated the expression of control proteins at expected molecular weight approximately 30 kDa with α-GFP which is not present in the parental cell.

4.1.3 Characterization of the membrane density-gradient fractions of N2a cells, obtained by using a non-detergent-based cell-fractionation method.

Most of GPI anchored proteins, similar to PrP and Sho, tend to reside in the specialized portions of PM called lipid-rafts or membrane microdomains. Knowing that functionally different GPI anchored proteins are reported to be organized in different domains in neuronal cells[159] and also since PrP and Sho are reported to participate in both identical and divergent processes, we set forward to investigate the two proteins membrane microdomain partitioning in the established stable transgenic N2a cells.

For this purpose N2a stable transgenic PrP-EGFP and Sho-EYFP cells along with their respective controls, EGFP-and EYFP cells were used, and membrane rafts were isolated from total post-nuclear fractions of cell lysates. To examine the distribution of PrP and Sho and to avoid any artefacts caused by detergents into protein partitioning, we chose the non-detergent based OptiPrep continuous density gradient method described by Macdonald and Pike[154]. In this method, detergent-free membrane rafts were separated from non-rafts based on their buoyancy along density gradient and shown to yield pure rafts. To confirm the characteristic densities of gradient fractions within our experimental setup, density of each fraction measured using their corresponding blank (Buffer A without protein sample) OptiPrep continuous density gradient fractions centrifuged in parallel with the samples and calculated their absorbance values **(Figure 9)**. The density values of collected fractions increased from 0.944 g/ml (top of the gradient) to 1.356 g/ml (bottom of the gradient). The mean densities and standard errors of fractions separated on different times (three independent blank density gradients) show the consistency between the gradients and fraction densities.
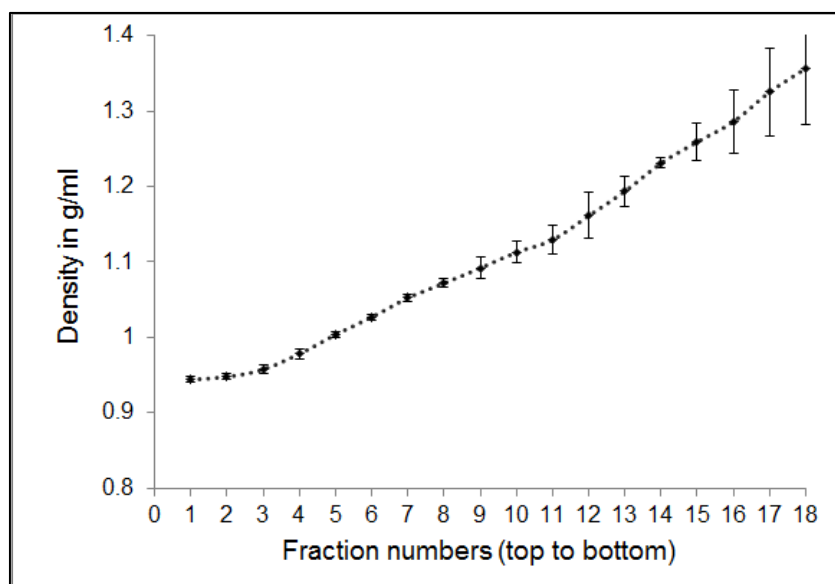
Figure 9: Mean densities of OptiPrep-Sucrose gradient fractions. Buffer-A along with the enzymes, but without any cell-sample, was loaded at the bottom of the centrifuge tube, and a continuous OptiPrep density-gradient was layered on top (in a similar manner as for the membrane-containing samples) of the samples. After centrifugation, fractions are collected in the same way as for membrane-samples. Densities of the fractions are presented in function of the fraction numbers, and are calculated as described in Materials and Methods. Error bars represent the standard deviation of three separate gradients processed on different days.

We used the criteria proposed by Persaud-Sawin and co-workers,[155] to determine which gradient fractions best reflected "true-rafts", i.e fractions that possess (a) low protein content, (b) high cholesterol content, (c) show presence of raft resident protein Flotillin-1 and (d) absence of non-raft resident protein, transferrin receptor, are considered as raft fractions. We divided the gradient fractions into three density groups to analysis of protein distribution easier: low-dense (fraction number 1 through 7), mid-dense (fraction number 8 through 12) and high-dense (fraction number 13 through 18) fractions. The total protein profiles **(Figure 10, green lines)** across gradient fractions of N2a stable transgenic Sho-EYFP-, PrP-EGFP (Figure 10A) and controls, EYFP- and EGFP (Figure 10B) cells show relatively very-less protein quantities in low-dense fractions (fraction number 2 through 6) and low protein quantities in mid-dense fractions (fraction number 8 through 10) while bulk of proteins is being found at the high-dense fractions (fraction number 12 through 16).
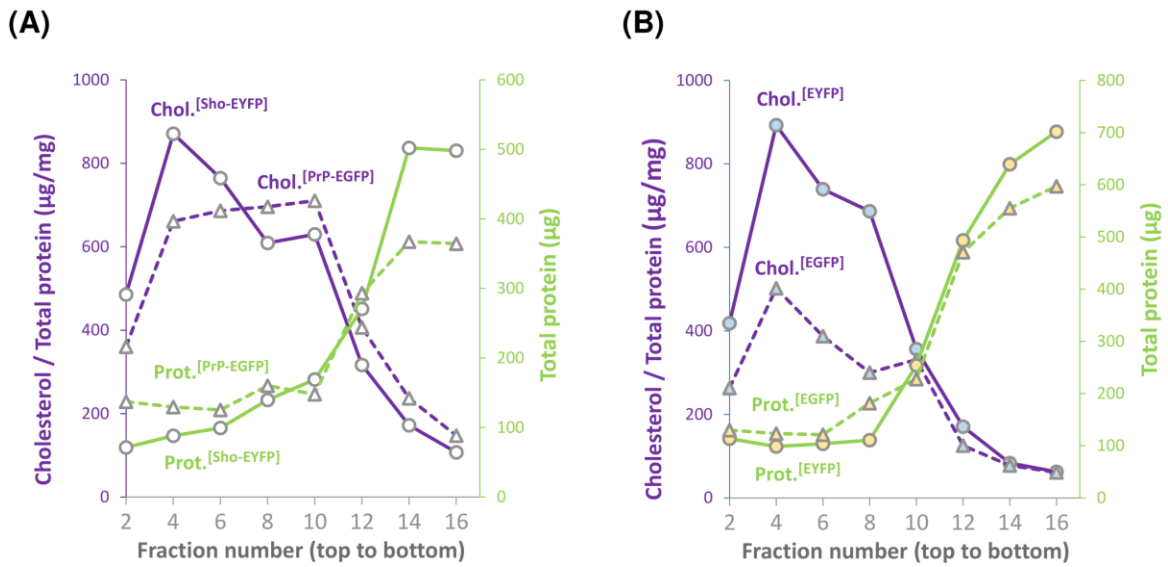
Figure 10: Total protein and cholesterol distribution in various OptiPrep density gradient fractions of the different cell types. Distribution of total protein (green lines) and cholesterol (purple lines) in the fractions collected from top to bottom across the OptiPrep continuous density gradient of N2a stable transgenic Sho-EYFP-,PrP-EGFP- (A) and in controls, EYFP- and EGFP (B) cells.

When total cholesterol levels (Figure 10, purple lines) are measured in same gradient fractions of the four cell populations, the highest levels of cholesterol are observed in the low-dense fraction (fraction number 4), where the protein level is relatively low, compared to mid-dense fractions (fraction numbers 8 through 10) and then declined in high-dense fractions. In order to distinguish the distribution of membrane rafts and non-rafts along gradient fractions we tested the distributions of Flottilin-1 (raft-resident) and transferrin receptor (TfRC) (non-raft marker) by Western blot with corresponding antibodies. In general, Flotillin-1 distributed in all low- to high-dense fractions from fraction numbers 1 through 18 and non-raft marker, TfRC is shown in high-dense fractions from fraction numbers 12 through 18. Taking altogether, in our experimental setup, in general, the criteria proposed by Persaud-Sawin and co-workers[155] for "true rafts" are followed by low- and mid-dense fractions from fraction numbers 1 through 11.

4.1.4 Membrane microdomain localization of the fluorescent protein tagged, untagged and endogenous PrP.

To visualize the distribution of PrP in the OptiPrep density gradient fractionated samples of fluorescent protein tagged prion protein (PrP-EGFP) and its control (EGFP) cells, we performed Western blot analysis, using various antibodies for specific marker proteins. We found that, in PrP-EGFP and EGFP cells, Flotillin-1, raft resident protein distributed over all types of dense-fractions from fraction numbers 1 to 18 (**Figure 11**). This indicates its varied intracellular distribution in the cellular compartments being present in various rafts with different buoyant properties[124,154,160,161]. In PrP-EGFP cells, overexpressed fluorescent tagged prion protein distributed across all types of dense-fractions from fraction number 1 through 18 detected by anti-prion SAF-32 and anti-GFP antibodies (Figure 11A) following similar pattern of distribution to Flotillin-1. Distribution of overexpressed control protein, EGFP-GPI$_{(PrP)}$ in EGFP cells show similar distribution as in PrP-EGFP cells across gradient fractions as monitored by α-GFP (Figure 11B). The typical non-raft plasma membrane marker protein, TfRC, which was excluded from lipid rafts[162] is seen only in high-dense fractions from fraction number 12 through 18 in both PrP-EGFP and its EGFP cells indicating that these fractions are being non-raft fractions. Probing the fractions for calnexin (CNX), show its distribution from low- through high-dense fractions, being more abundant in the high-dense fractions in both cell types. The nuclear pore complex protein (NPC), chosen as nuclear membrane marker protein distribute in the high-dense fractions across fractions 12 through 18, well separated from the major lipid-raft fraction number 1 through 10 in samples corresponding to both cell types: PrP-EGFP and EGFP cells, indicate the low density fractions as free from nuclear envelope contamination.
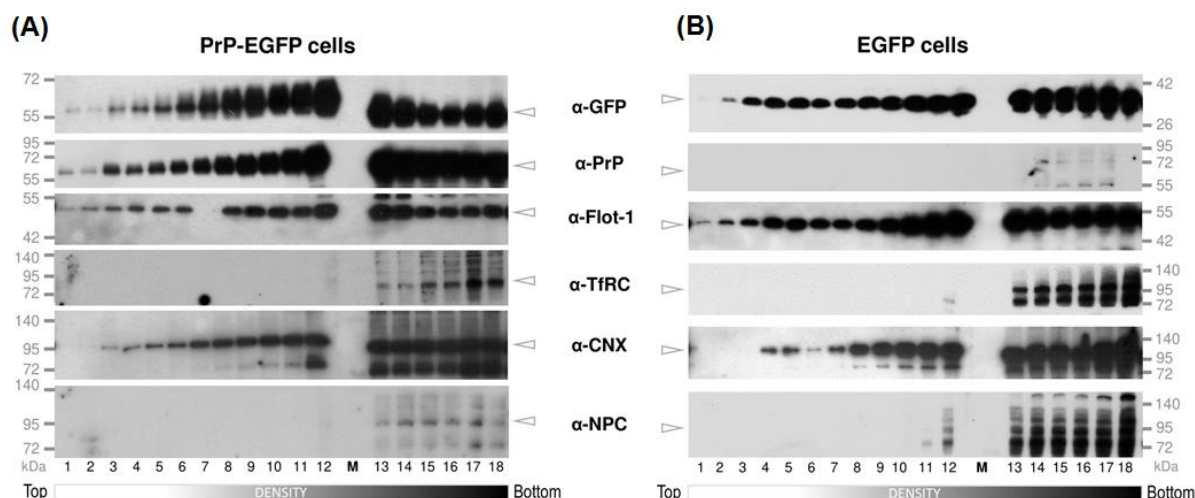
Figure 11: Distribution of various proteins across the gradient fractions of N2a stable transgenic PrP-EGFP and its control, EGFP cells. A, B) Representative Western blots of selected proteins along the gradient fractions obtained from PrP-EGFP (A), EGFP (B) cells. Fractionated samples collected from top to bottom of the centrifuge tubes are numbered 1 through 18. Samples are immunoblotted for the proteins by using the antibodies as indicated: for PrP by α-GFP and α-PrP; for Flotillin-1 by α-Flot-1; for transferrin receptor protein by α- TfRC; for calnexin by α-CNX; for nuclear fore complex protein by α-NPC. Protein molecular weight ladder is marked on the side of the blots.

To test whether the addition of the fluorescent protein tag had any influence on the distribution/behaviour of the prion protein along the OptiPrep density gradient fractions we also examined N2a stable transgenic cells expressing untagged PrP (and simultaneously a soluble EGFP, for transfection monitoring purposes), notated as Na2/PrP(+EGFP) cells, as well as, parental, non-transfected N2a cells, and monitored the distribution of PrP the same set of selected proteins along the density gradient fractions **(Figure 12)**.
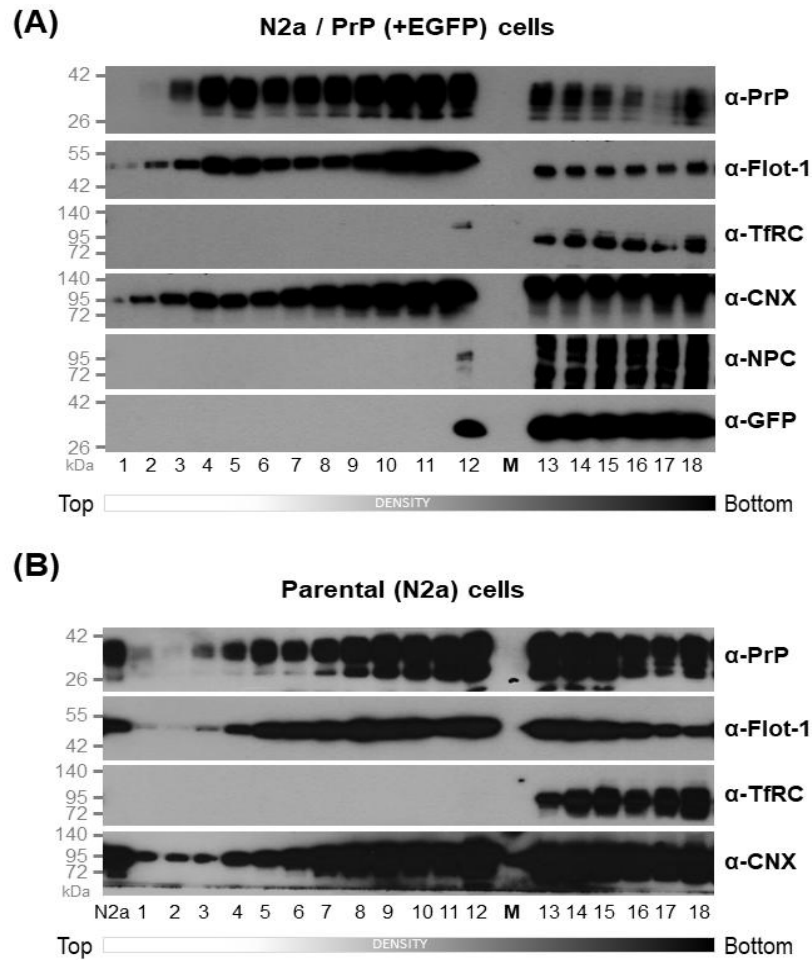
Figure 12: Distribution of selected proteins across the gradient fractions of untagged-prion protein overexpressing- and parental N2a cells. A, B) Transgenic N2a cells overexpressing prion protein without any fluorescent fusion tag and at the same time a soluble EGFP, N2a/PrP (+EGFP) cells (A) and parental N2a cells (B) fractionated on OptiPrep density gradient and the Western blots of the fractions are shown. The distribution of selected proteins along gradient fractions is tested as shown. α-PrP is used to detect the prion protein, α-Flot-1, α-TfRC, α-CNX, α-NPC used to detect Flotillin-1, transferrin receptor protein (TfRC), calnexin (CNX) and the nuclear pore complex protein (NPC), respectively. M: protein molecular weight ladder.

Separating membrane microdomains from post nuclear supernatants of N2a/PrP(+EGFP)-(Figure 12A) and parental N2a (Figure 12B) cells similarly as in case of the tagged-PrP and immunoblotting the gradient fractions for the same selected marker proteins we found that in all three cells, PrP and the selected proteins distribute similarly between membrane raft and non-raft

fractions. Importantly, PrP shows similar distribution pattern irrespective of whether it is expressed as tagged by the fluorescent fusion protein in the PrP-EGFP cells, or expressed as untagged in PrP(+EGFP) cells- or when it is endogenous and tested in parental N2a cells. PrP detected by α-PrP is present from fraction number 1 through 18 in parallel with raft the resident protein Flottilin-1 shown by α-Flot-1. Non-raft protein, transferrin receptor shown by α-TfRC is seen typically only from fraction numbers 12 to 18 in repeated experiments, leaving by this a wide range where it is absent (fraction 1 through 11), which may be qualifying as a true rafts based on the raft criteria of Persaud-Sawin and co-workers[155]. Calnexin and NPC proteins are detected from fraction numbers- 1 through 18 and 12 through 18, respectively, by their respective antibodies. All the marker proteins along with PrP distribution pattern indicate that neither fluorescent protein (EGFP) tag nor the overexpression of proteins affect the natural distribution of PrP in membrane microdomains.

4.1.5 Shadoo exhibits a similar preference for membrane microdomain localization like PrP.

Next, we examined the distribution of Sho by fractionating N2a stable transgenic shadoo-overexpressing- (Sho-EYFP) and its control (EYFP) cells in similar manner (and also tested in parallel) as to PrP-EGFP and its control cells, probing for Sho along with the same other selected proteins by Western blotting **(Figure 13)**. As expected, Flotillin-1 distribution is observed from fraction number 1 throughout the low-dense to highly dense fractions in both Sho-EYFP and its control cells, as before in PrP expressing cells. The transferrin receptor in case of Sho-EYFP- and EYFP cells is detected from somewhat lower densities, from about the mid-dense fraction number 10-11, while populating as expected the high-dense fractions down to 18th. Shadoo, by α-Sho and α-GFP, shows distribution from the low dense fractions #2 through 7, although relatively lower amounts, and it is mostly seen in the mid- and high dense fractions (from 7-8 through 18) of Sho-EYFP cells (Figure 13A). In both Sho-EYFP- and EYFP cells, CNX is detected from fraction numbers 3 through 18 by α-CNX; and low- to mid-dense fractions are free from NPC protein, which is detected only in high-dense fractions from fraction numbers 13-18 by α-NPC. The distribution of the control protein EYFP-GPI$_{(Sho)}$ across gradient fractions of EYFP cells, is detected from fraction number 3 by α-GFP (Figure 13B), similar to the fluorescent protein tagged PrP (PrP-EGFP-GPI$_{(PrP)}$) and its control protein (EGFP-GPI$_{(PrP)}$) in their respective cells (Figure 11).
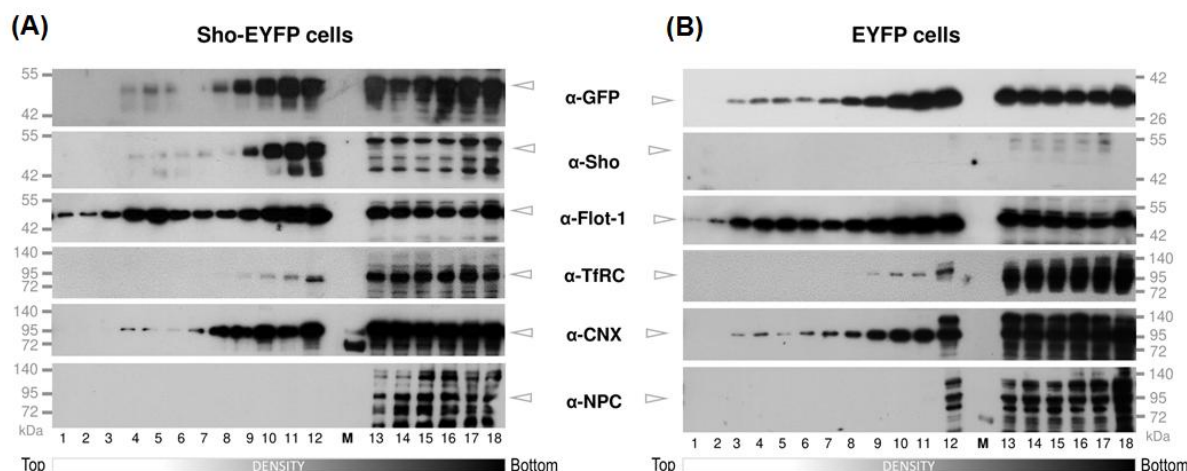
Figure 13: Distribution of various proteins across the gradient fractions of transgenic cells Sho-EYFP- and its control, EYFP cells. A, B) Representative Western blots of the selected proteins along gradient fractions of fluorescent protein tagged Shadoo-and its control fluorescent protein overexpressing transgenic cells. Fractions collected from top to bottom of the centrifuge tubes corresponding to Sho-EYFP (A) and EYFP (B) cells are numbered and loaded on SDS-PAGE as indicated on the bottom of the figures. Samples are immunoblotted for the following proteins with the respective antibodies as indicated: for Shadoo by α-Sho, and α-YFP; for Flotillin-1 by α-Flot-1; for transferrin receptor protein by α-TfRC; for calnexin by α-CNX; for nuclear pore complex protein by α-NPC. Protein molecular weight ladder is marked on the side of the blots.

Altogether, the results indicate that both PrP and Sho, like their GPI-anchored fluorescent protein tags anchors, partition to the raft type membrane domains. Importantly, the results also demonstrate that these proteins are present also as along the non-raft-type membrane fractions.

4.2 The study of the possible interaction of prion and Shadoo proteins with the ER-chaperone calnexin

4.2.1 Stable transgenic N2a cells developed for the studies and their characterisation.

Since both PrP and Sho either possesses a large part or are fully unstructured proteins, it is intriguing how these structures are maintained during their biology and lifecycle. Next we found intriguing to study whether these proteins similarly bind, and if yes in which of these different type of membrane domains, calnexin, an ER-chaperone, which was observed earlier by a single

study to bind PrP in when examining total cell lysates of another type of cells such as 293T and SK-N-SH cells[153]. Calnexin is being monitored here by us, in parallel to the two prion-family proteins, as it is also used as endoplasmic reticulum marker protein. Our results show that calnexin appears detectable in both raft and non-raft membrane microdomain fractions of all type of N2a cells used here (Figures: 11-13).

To approach this goal, we aimed to apply pull-down assay and co-immunoprecipitation (Co-IP) assay to examine interaction of CNX with the two proteins PrP and Sho, respectively, after exploring first the subcellular localisations of CNX, PrP and Sho in our N2a stable transgenic cells by microscopy. Specifically for Co-IP assay, we needed to insert a FLAG tag into the Sho-EYFP protein construct which would allow performing immunoprecipitation of Sho. Therefore, two additional N2a stable transgenic cells had to be generated: one overexpressing Sho-EYFP-FLAG fusion protein and the other is its control, expressing only the fluorescent protein in fusion with the FLAG-tag, and equipped with the ER targeting- and the GPI-signal peptides of Shadoo. We notated these cells as Sho-EYFP-FLAG- and its control, as EYFP-FLAG cells. The schematic representation of DNA constructs are shown in **Figure 14A**.
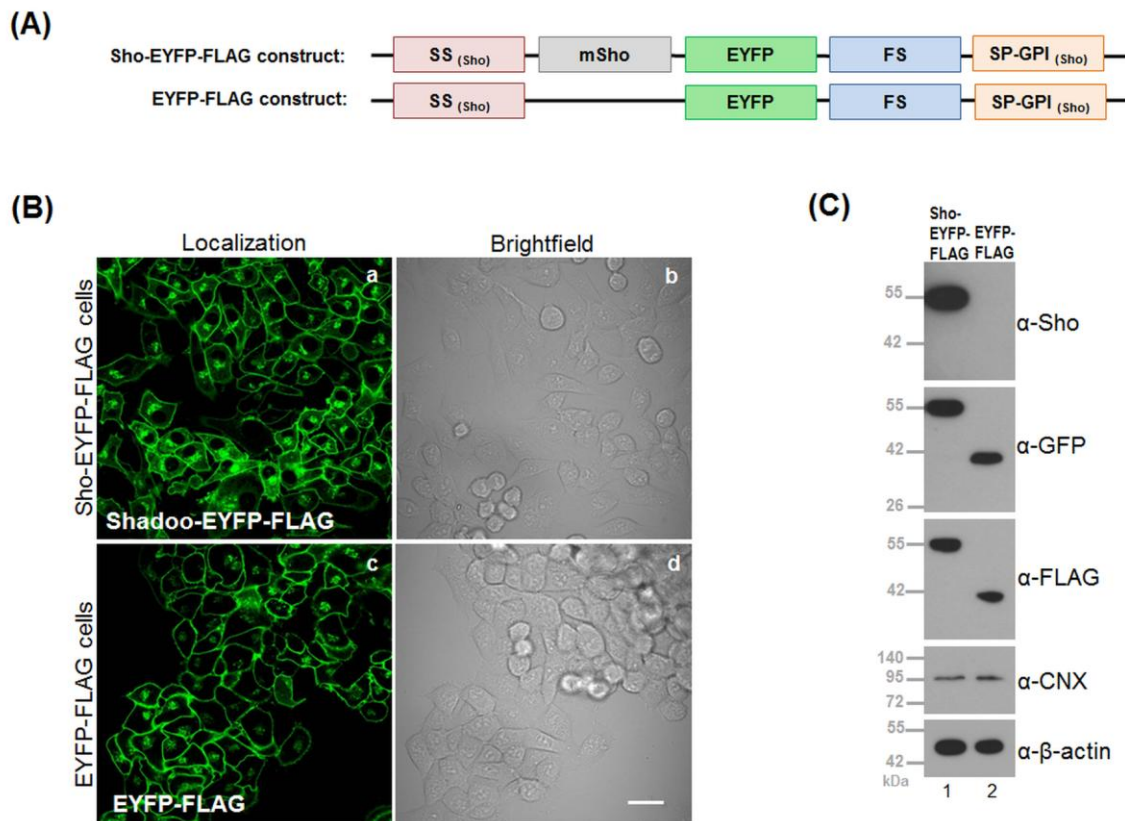
Figure 14: Characterization of the N2a stable transgenic Sho-EYFP-FLAG- and EYFP-FLAG cells developed. (A) Schematics of the DNA constructs used for developing the transgenic cells, encoding the FLAG-tagged Sho protein construct Sho-EYFP-FLAG-GPI$_{(Sho)}$ and its corresponding control protein EYFP-FLAG-GPI$_{(Sho)}$. The major sequence elements are depicted, coding for as follows. SS$_{(Sho)}$: N-terminal signal peptide of Sho; mSho: mouse Shadoo protein; EYFP: enhanced yellow fluorescent protein, FS: FLAG-STREPTAVIDIN-tag sequence; GPI$_{(Sho)}$: GPI-anchor attachment signal sequence of Sho. Note: only FLAG-tag is used in the experiments presented, therefore, in the naming of cells and proteins only FLAG-tag is mentioned. (B) Representative live-cell confocal fluorescence and brightfield images of the stable transgenic Sho-EYFP-FLAG- (top panels) and its control, EYFP-FLAG (bottom panels) cells, made by transfecting N2a cells with plasmids encoding for the protein constructs on (A). Images are taken using 60x oil immersion objective of the Fluoview FV1000 confocal laser scanning microscope. Signals from EYFP are shown in green. Scale bar: 10 μm. (C) Expression of transgenes analyzed by Western blotting of total cell lysates of Sho-EYFP-FLAG and the EYFP-FLAG cells, antibodies used are as indicated on the figure, probing for Shadoo (α-Sho), EYFP (α-GFP), FLAG (α-FLAG) and calnexin (α-CNX). β-actin is used as loading control and probed by α-β-actin.

The subcellular localization and expressions of FLAG-tagged Sho and its control protein in Sho-EFYP-FLAG and EFYP-FLAG cells, respectively, are shown in Figure 14B,C. Confocal microscopy confirmed that, similar to non-FLAG-tagged Sho (Sho-EYFP) and its control (EYFP) cells in Sho-EFYP-FLAG and EFYP-FLAG cells, the overexpressed FLAG tagged Sho proteins predominantly localise to PM and GA (Figure 14B). Western blot analysis confirmed the presence of the overexpressed proteins, which are being detected at their expected molecular weights (Figure 14C).

4.2.2 Immunocytochemical analysis of the localisation of Shadoo, prion protein and calnexin in the transgenic N2a cells.

The subcellular localizations of PrP, Sho and CNX proteins were analysed in the established N2a stable transgenic Sho-EYFP-FLAG-, PrP-EGFP- and in their respective controls, EYFP-FLAG- and EGFP cells by immunocytochemistry combined with confocal microscopy **(Figure 15)**.
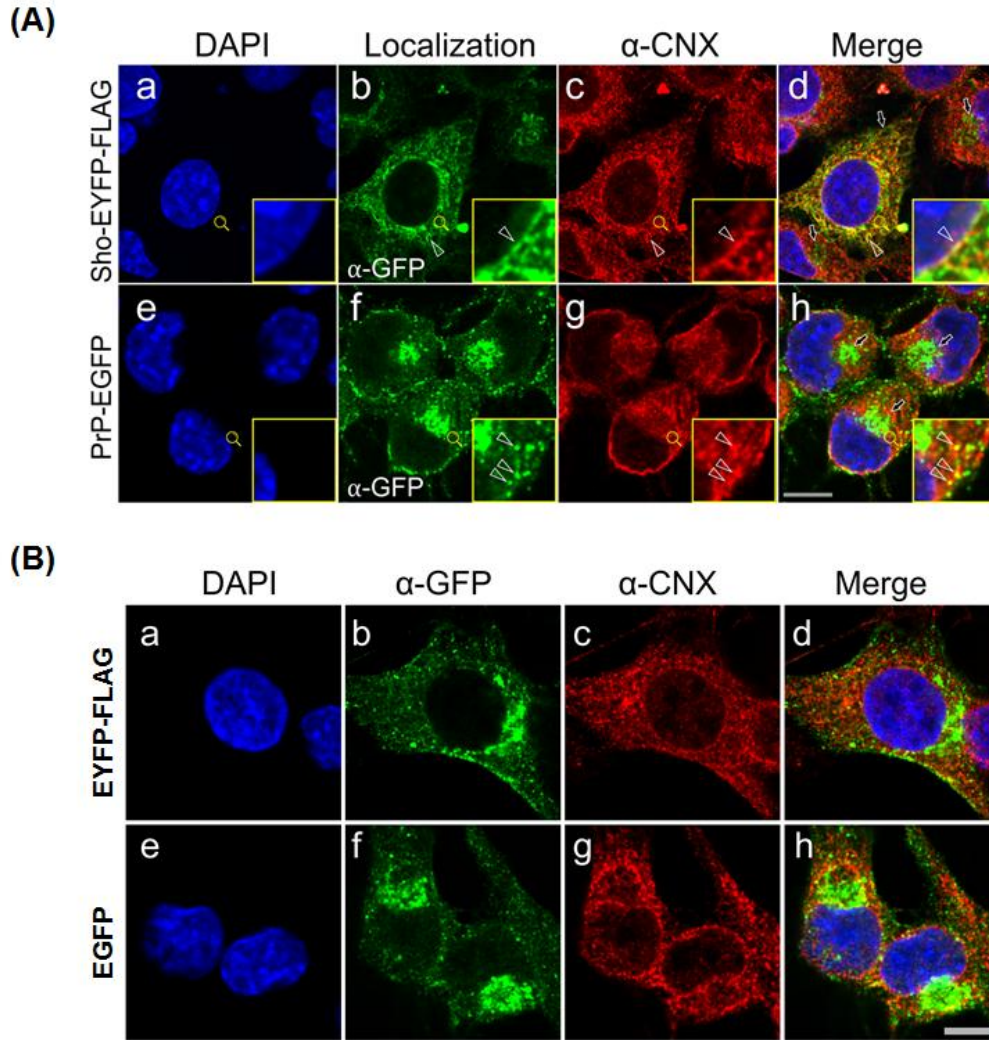
Figure 15: Subcellular localization of the Shadoo, prion and calnexin proteins detected by immunocytochemistry in transgenic Shadoo- and prion protein overexpressing and their respective control cells. Immunocytochemistry and confocal microscopy images of N2a stable transgenic fluorescent protein-FLAG tagged Shadoo, Sho-EYFP-FLAG (a-d) and fluorescent protein tagged prion protein, PrP-EGFP (e-h) cells (A) and their respective control cells noted as EYFP-FLAG (a-d) and EGFP (e-h) (B). Cells are fixed, permeabilised and immunoprobed with α-GFP (b, f) and α-CNX (c, g) prior staining with secondary antibodies anti-mouse-Alexa 488 (green) for α-GFP (b, f) and anti-rabbit-Alexa 568 (red) for α-CNX (c, g). Nuclei (a, e) are counter labeled with DAPI (blue). Merged images (d, h) of the blue, green and red channels are shown in the last column, colocalization of Sho or PrP with CNX is indicated by yellow color pixels. Insets correspond to the areas marked by the magnifying glass symbols; arrows indicate Golgi apparatus and arrowheads mark the examples of colocalization regions. Scale bar: 10 μm.

After fixing and permeabilising the cells, same antibodies were used for detection of Sho and PrP (α-GFP combined with Alexa 488 secondary antibody, green), Sho (b) and PrP (f) are

60

seen to be localize to the same compartments as the plasma membrane and Golgi apparatus - where they form intense fluorescent patches and to endoplasmic reticulum membranes (Figure 15A). The endogenous calnexin detected by α-CNX combined with Alexa 568 secondary antibody (red) localised to the ER membrane network, being absent from the PM and GA in all cells used (Figure 15, c, g). Importantly, calnexin colocalized with Sho and PrP in ER membranes in Sho-EYFP-FLAG and PrP-EGFP cells, specifically their co-localization with CNX indicated by yellow pixels is observed in the nuclear membrane, ER tubular structures and also in ER membrane sheets (Figure 15A, merged images d, h). However, non-colocalized fluorescence with CNX is also observed. In control cells, CNX show partial colocalization with EYFP-FLAG-GPI$_{(Sho)}$ or EGFP-GPI$_{(Sho)}$ proteins, this being confined to the ER membranes, leaving out GA and PM (Figure 15B, merged pictures d, h). Similar images with the same settings were recorded also without primary antibody and with secondary antibody staining to check for background and there was negligible signal from the nonspecific binding of secondary antibodies to the cells, which would mask the evaluation of the images (data not shown).

4.2.3 Shadoo and prion protein co-localize with calnexin in the endoplasmic reticulum compartments of the live transgenic N2a cells.

We opted for a more in-depth analysis using live-cell imaging of the cells to look for prion, Shadoo and calnexin protein localizations, because the immunocytochemistry procedure may not preserve fine features of the cellular structures due to the nature of the experimental procedure. To accomplish this, we transiently transfected Sho-EFYP-FLAG, PrP-EGFP along with their controls EYFP-FLAG and EGFP cells with a plasmid coding for mouse calnexin tagged by a red-fluorescent protein (CNX-RFP) **(Figure 16)**.
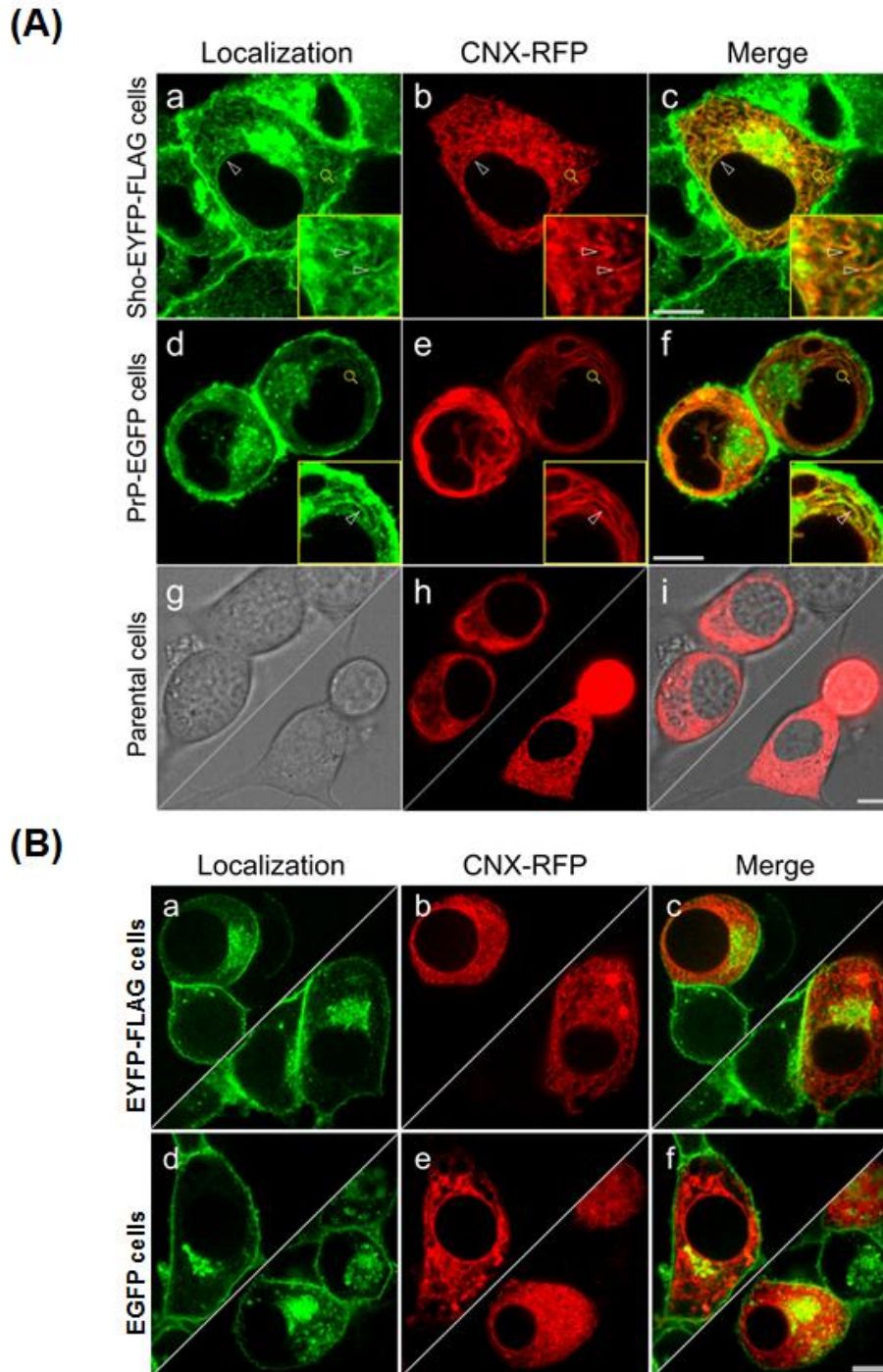
Figure 16: Live cell analysis of co-localization of Shadoo, prion protein and calnexin in the ER membranes. Live cell analysis of subcellular localization of Shadoo (green), prion protein (green) and calnexin (red) (A) in N2a stable transgenic Sho-EYFP-FLAG (A, a-c), or PrP-EGFP (A, d-f) and in parental N2a (A, g-i) cells transiently transfected to expressed calnexin-RFP and also of their respective control proteins (B) in the control EYFP-FLAG (B, a-c) and EGFP (B, d-f) cells transiently transfected to expressed calnexin-RFP (B, b,e). Images are acquired with 100x oil immersion objective on a VisiScope CSU-W1 spinning disk confocal microscope. Yellow

color in the merged images represents co-localization of PrP and Sho with CNX (arrow heads). Split images show two different fields of view. Insets correspond to the regions of magnifying glass symbol. Scale bars: 10 µm.

When visualising the cells under VisiScope CSU-W1 spinning disk confocal microscope using 100x oil immersion objective, similar overall localizations of Sho, PrP and CNX to the specific cellular organelles are found as in the case of immunostaining (Figure 16A). The fine ER localisation of the fluorescent tagged proteins Sho and PrP to both perinuclear and peripheral ER networks, including both tubular and sheet-like ER cisternae, can now be well seen with this technique, given that the ER fine-structures are much better resolved. The localization of CNX appears to be overlapping with both Shadoo (a-c) and prion protein (d-f) in all ER membrane structures, pronouncedly being colocalized with these proteins in the tubular type ER structures (Figure 12A). Sho, in Sho-EYFP-FLAG cells, localizes abundantly to the nuclear membrane and is present in the tubular- and the smooth-ER-sheets, and colocalizes with CNX in these compartments. PrP's localization to nuclear membrane is less intense compared to Sho, but also shows co-localization here with the CNX. The control proteins, EYFP-FLAG-GPI$_{(Sho)}$ and EGFP-GPI$_{(PrP)}$ in the control EGFP and EYFP-FLAG cells, respectively, show intense localisation to PM, GA and a homogeneous intracellular pattern, without pronounced appearance in the tubular ER-structures. When EYFP-FLAG- and EGFP cells are transfected by CNX-RFP, CNX shows a similar pattern as in the other cells marking the fine, tubular ER-structures partially overlapping with control proteins and excluded from PM and GA (Figure 16B).

These results indicate that the two prion-family proteins, Shadoo and prion protein behave in a similar way in respect to their localisation with CNX, both proteins being co-localised specifically in the endoplasmic reticulum with calnexin.

4.2.4 Prion protein pulls down calnexin both in raft- and non-raft-type membrane fractions.

Finding high degree of colocalization between PrP and Sho with CNX in our N2a stable transgenic cells, we set forward to investigate their possible interactions.

Initially, using total cell lysates of prion protein overexpressing PrP-EGFP, its control EGFP- and parental N2a cells, a Ni-NTA bead pull-down experiment was performed (taking advantage of the integral histidines in PrP, which bind nickel) to check for any interaction of PrP

with CNX (**Figure 17**). The bead pulled samples (Bead eluates) along with their respective total cell lysates (cell lysates) were subjected to Western blotting against PrP and CNX proteins using α-PrP and α-GFP for prion protein and α-CNX for calnexin. The results demonstrate the presence of CNX in the bead eluates of both PrP overexpressing and parental N2a cell samples as detected by α-CNX (lanes 2-3), although a very faint band in the control sample from EGFP cells corresponding to CNX is also observed (lane 4), which is in line with the prion protein being endogenously expressed in N2a cells, from which the transgenic cells were generated (seen on the blots with anti-prion antibody), and that they may also pull CNX beside overexpressed prion protein construct. Overall, these results indicate that prion protein, either endogenous or overexpressed with EGFP-tag, does interact with calnexin.
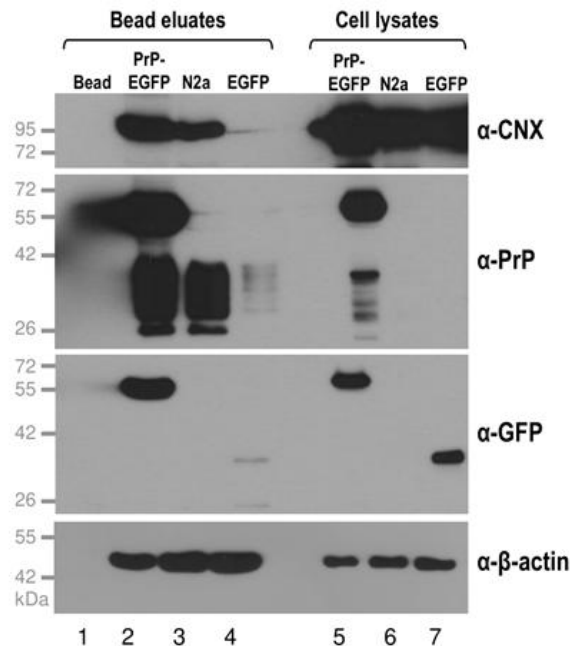
Figure 17: Interaction of prion and calnexin proteins tested in the total cell lysates of prion protein overexpressing and its control cells. Representative Western blots of total cell lysates of PrP-EGFP, EGFP and parental N2a cells pulled by Ni-NTA beads (Bead eluates) and probed in parallel with the input cell lysates (Cell lysates) for prion and calnexin, using the antibodies α-PrP and α-GFP for prion and α-CNX for calnexin. β-actin is used as loading control. Empty beads treated similarly but without sample are used as negative controls (bead); the positions of the molecular weight markers are indicated on the left side of the blots.

As a next goal we set forward to examine, if there is any specificity in the interaction of PrP and CNX depending on the type of membrane microdomains the proteins reside in. Therefore, we proceeded for non-detergent based isolation of membrane microdomains from the PrP-EGFP cells to look for the interaction within the individual fractions. Performing Western blot to characterize the fractions, we found that Flotillin-1 distributes in low- to high dense fractions, while transferrin receptor appears from only mid (fraction number 11) to high dense fractions with their respective antibodies. PrP and CNX are present along the same gradient fractions, from low- to high dense fractions (numbers 4 through 18) as detected by α-PrP and α-CNX (**Figure 18A**). This distribution pattern is also similar to as we found earlier for these cells (Figure 11A).
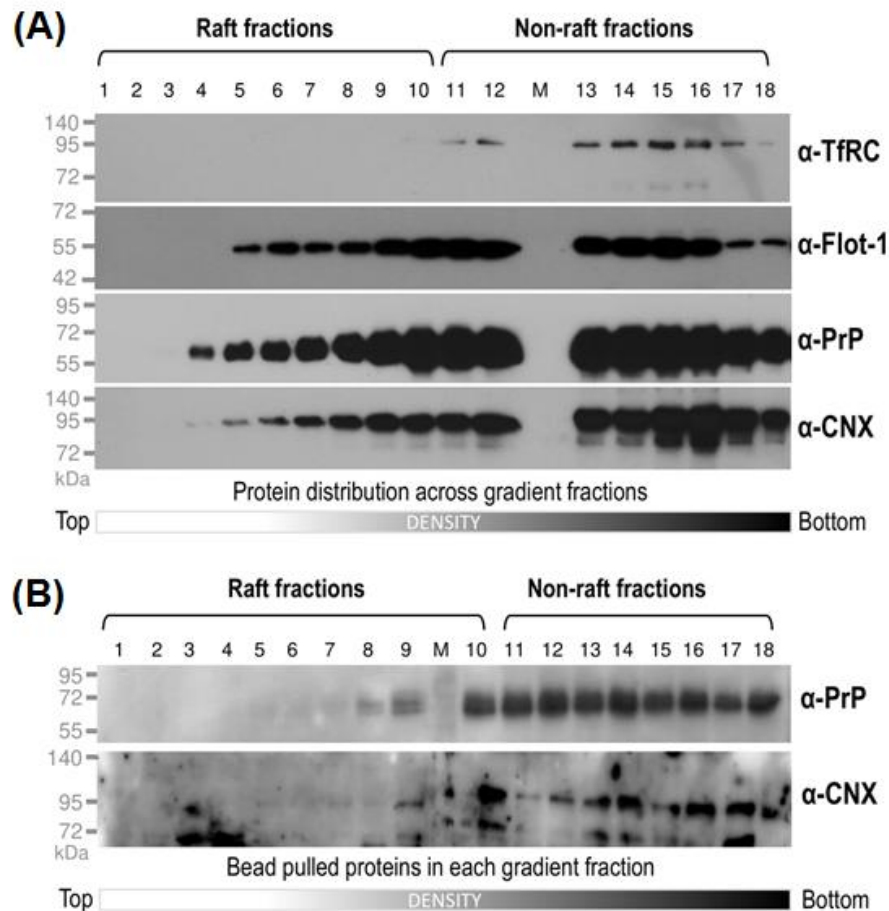

Figure 18: Prion protein interacts with calnexin in the membrane rafts and non-rafts as assessed by Ni-NTA pull-down assay. (A) Fractionated samples of PrP-EGFP cells are probed for the transferrin receptor (non-raft protein), Flottilin-1 (raft protein), prion and calnexin proteins

using the antibodies α-TfRC, α-Flot-1, α-PrP and α-CNX, respectively. (B) The corresponding fractionated samples are pulled by Ni-NTA beads and probed for prion and calnexin proteins with respective antibodies. Molecular weight markers are represented on left side of the blots. Raft and non-raft regions are marked on top of the blots.

To assess the interaction of PrP and CNX along the gradient fractions, we set forward to separately subject each collected fraction to Ni-NTA bead pull-down assay (to pull PrP) after which to test the bead-eluates (Bead eluates) for the presence of CNX, by α-CNX, in the same manner as followed with the total cell lysates (Figure 17). Western blot analysis of Ni-NTA pull-down eluates revealed that CNX is pulled by PrP in low- to high dense fractions, from fraction number 5 through 18, as identified by α-PrP and α-CNX (Figure 18B). Gradient fractions from fraction number 5 to 11 are considered as membrane rafts based on the presence of Flotillin-1 and fraction numbers 12 through 18 are considered as non-raft membranes based on the presence of transferrin receptor protein.

This result shows that PrP bind with CNX in both membrane rafts (fractions number 5 through 11) and non-rafts (fractions number 12 through 18).

4.2.5 Calnexin co-immunoprecipitates with Shadoo in total cell lysates

As a next goal we set forward to analyse whether Shadoo could also interact with calnexin or not, similarly as PrP, which proved to bind with CNX. First, the total cell lysates of FLAG-tagged Shadoo overexpressing Sho-EYFP-FLAG cells, in parallel to its control, EYFP-FLAG- and parental N2a cells, were tested. These cells were subjected to co-immunoprecipitation assay using anti-FLAG beads to precipitate Sho and to look for the presence and CNX in the precipitates by Western blotting **(Figure 19)**.
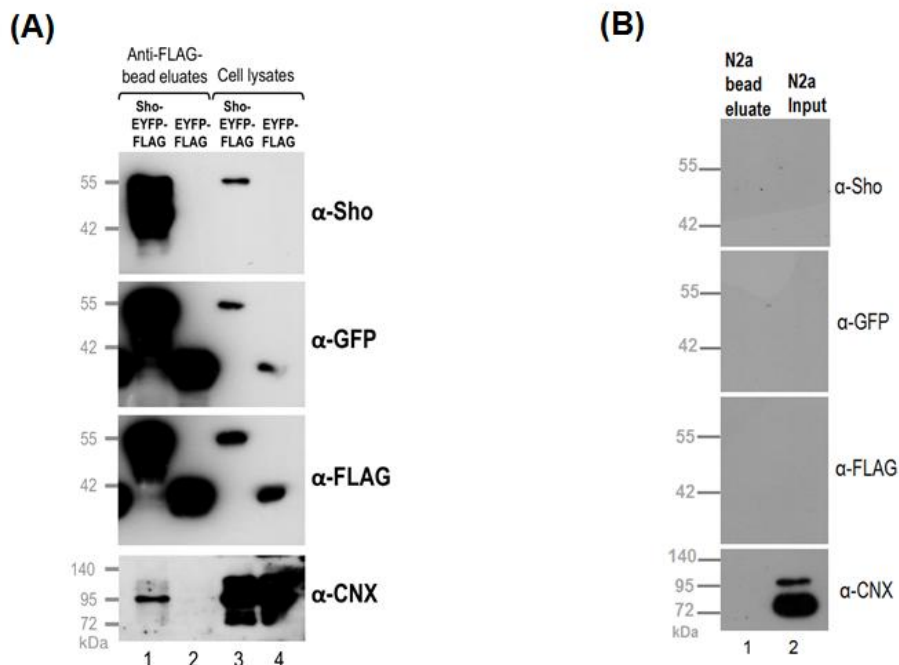
Figure 19: Calnexin is a binding partner of Shadoo. Co-immunoprecipitation of Shadoo and calnexin from the total cell lysates of Sho-EYFP-FLAG- and its control, EYFP-FLAG cells (A) and parental N2a cells (B) using anti-FLAG beads. The bead eluates (labeled as anti-FLAG bead eluates) in parallel to cell lysate samples (cell lysate) are tested by Western blot using three antibodies for the Shadoo-fusion protein construct: α-Sho, α-GFP and α-FLAG, and α-CNX for calnexin as marked on the figures. Molecular weight markers are indicated on the left side of the blots.

As seen on the blots, the presence and absence of Shadoo in bead-eluate of Sho-EYFP-FLAG-, EYFP-FLAG- and parental N2a cells is confirmed by α-Sho, α-GFP, α-FLAG. In the anti-FLAG bead eluates of Sho-EYFP-FLAG samples, calnexin is detected by α-CNX but not in its control, EYFP-FLAG cells (Figure 19A, lanes1-2) or parental N2a cells (Figure 19B). The input total cell lysates are also loaded to the gels as controls and are positive for α-Sho, α-GFP, α-FLAG and α-CNX, as expected, showing that the proteins are present in the input samples. It is of note that endogenous level of Sho expression, contrary to prion protein, was undetectable in these cells. These results indicate that the overexpressed FLAG-tagged Shadoo protein interacts with calnexin, which is well detectable in the total cell lysates of the cells.

4.2.6 Calnexin co-immunoprecipitates with Shadoo both in the raft- and non-raft-type membrane fractions

After finding that CNX co-immunoprecipitated with Sho in the total cell lysates of the transgenic Sho-EYFP-FLAG cells, indicating that they are the binding partners, it was straightforward and also intriguing to look for their possible binding in the isolated membrane fractions as well, similarly as in the case of PrP.

First, using the same procedure of non-detergent based OptiPrep density gradient method as earlier for Sho-EYFP, PrP-EGFP and their respective control cells, the raft- and non-raft membranes were separated from the post nuclear supernatants of Sho-EYFP-FLAG and EYFP-FLAG cells. The collected fractions from the two cells were Western blotted **(Figure 20A)** in a manner that for each protein to be monitored, the corresponding SDS-gels from the two cells were cut, and placed one below the other to be able to transfer them to the same PVDF membrane that would undergo the same antibody treatments. To indicate this, the separation between the SDS-gels are marked on the blots as dashed lines and to each half the corresponding cell is labelled on the side as "Sho-Y-F" for the Sho-EYFP-FLAG cells and as "Y-F" for the EYFP-FLAG cells. The membranes are blotted for the presence of Flottilin-1 (α-Flot-1), TfRC (α-TfRC), to discern raft and non-raft fractions and for calnexin (α-CNX), the Sho-YFP-FLAG fusion protein (α-Sho, α-FLAG and α-GFP) and the control EYFP-FLAG-GPI$_{(Sho)}$ fusion protein (α-FLAG and α-GFP).
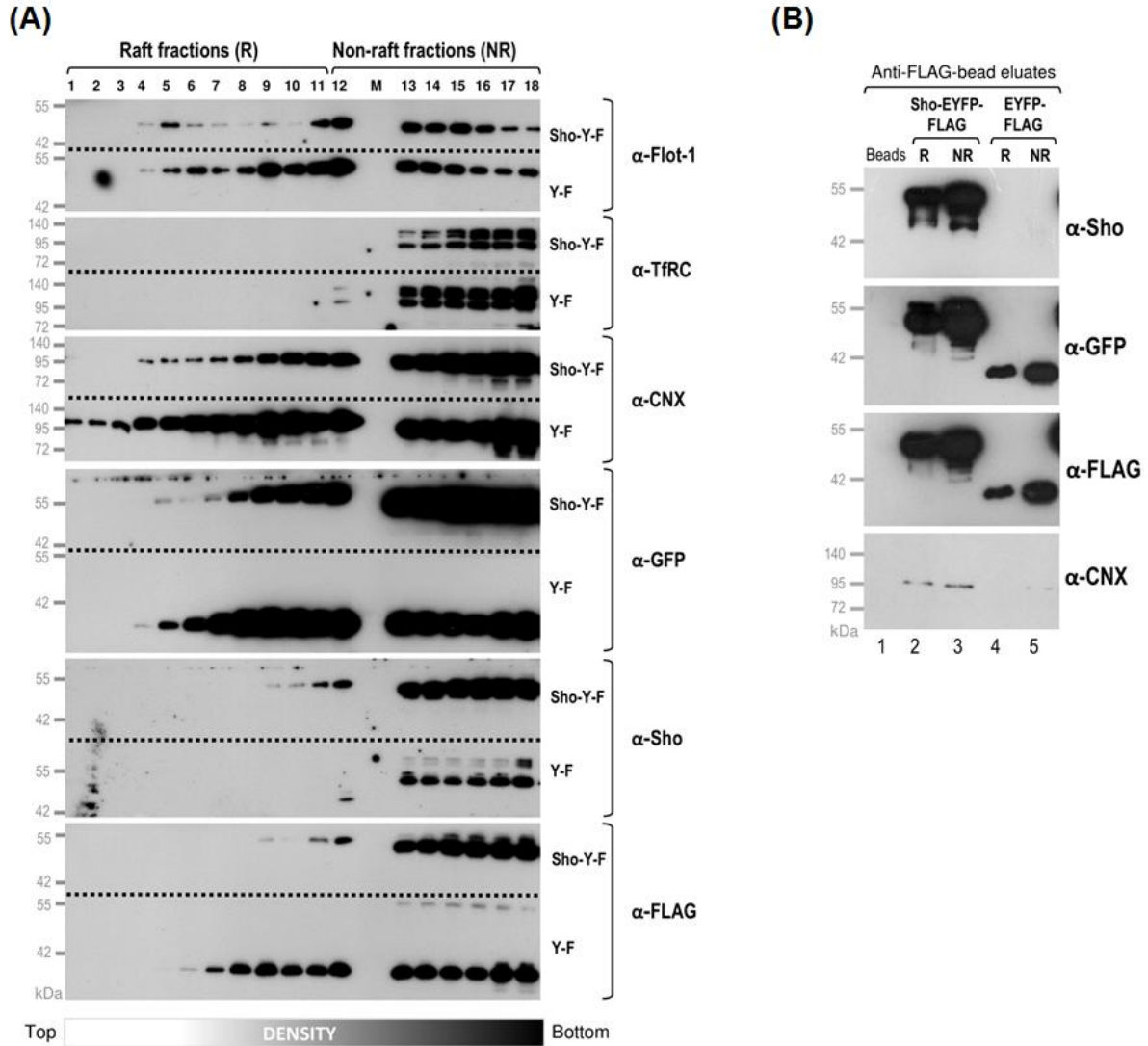
Figure 20: Shadoo interacted with the calnexin in both raft and non-raft type membrane fractions. (A) The fractions collected from the OptiPrep density-gradient-fractionation of Sho-EYFP-FLAG-(labeled as Sho-Y-F) and its control EYFP-FLAG (labeled as Y-F) cells are transferred on to same blot one above the other and are probed by Western blotting for presence of the proteins as marked: for Shadoo by using antibodies α-Sho, α-FLAG, α-GFP; for calnexin, α-CNX and for raft- and non-raft proteins Flotillin-1 and transferrin receptor protein by α-Flot-1 and α-TfRC. (B) Shadoo and calnexin proteins co-immunoprecipitated in fractionated samples of Sho-EYFP-FLAG and EYFP-FLAG cells. Equal quantities of pooled fractions belonging to either raft- (labeled as R) or non-raft (labeled as NR) regions (as on panel A) are loaded to anti-FLAG beads from both Sho-EYFP-FLAG- and EYFP-FLAG cells. The bead-pulled proteins (anti-FLAG bead eluates) tested by Western blot for the presence of Shadoo (Shadoo, FLAG and GFP, using α-Sho, α-FLAG, α-GFP respectively) and for calnexin protein using α-CNX. Empty beads treated similarly but without sample (Only bead) used as negative control, molecular weight ladder is on the left side.

The raft resident protein, Flotillin-1 can be observed from fraction number 4 through 18, whereas the non-raft resident protein, transferrin receptor protein from fraction number 12 through 18. These patterns of distribution are similar in case of Sho-EYFP-FLAG and its control, EYFP-FLAG cells. Therefore, the fractions 1 through 11 were considered as "raft fractions" and from the fraction numbers 12 through 18 as "non-raft" fractions for both types of the cells. Noteworthy that such distribution of raft and non-raft proteins along the gradient fractions is analogous to the non-FLAG tagged Sho expressing and its control (Sho-EYFP and EYFP, respectively) cells as well, indicating that the new newly developed cells with the FLAG-tagged proteins have the same characteristics in terms of the separation patterns of raft- and non-raft domains using this separation protocol. Sho is detected from fraction #5 by α-GFP and from #9 by α-Sho and by α-FLAG throughout fraction 18, indicating its presence in both raft and non-raft type membrane fractions, similarly as found in case of Sho-EYFP cells. Calnexin is detected from fraction number #4 through 18 by α-CNX. In order to look for interaction of Sho and CNX in the two types of membrane microdomains, because the detection of Sho by α-Sho and α-FLAG in the raft-fractions specifically in the upper #1 through 9 fractions is harder due to the fainter signals, we considered it to be feasible to pool all raft-fractions, as well as, separately all non-raft fractions, before performing co-immunoprecipitation. Therefore, based on the distribution of the Flottilin-1 (#4 through 18) and of the non-raft resident protein transferrin receptor from fraction number 12 to 18, we pooled the fractions # 1 to 10 as being the sample corresponding to raft-fractions, and fractions #11 to 18 as corresponding to non-raft fractions. Next, equal total protein amounts from the pooled rafts and non-rafts of Sho-EYFP-FLAG, as well as from EYFP-FLAG cells, were subjected to anti-FLAG beads to immunoprecipitate the FLAG-tagged proteins. The bead-eluates were analysed for the presence of CNX and the FLAG-tagged proteins by Western blotting with corresponding antibodies (Figure 20B). To look for the proteins of interest, after transferring of the protein from the gel to the PVDF membrane, the membrane was cut into two halves at about the level 60-72 kDa, and one part was probed of Shadoo (by α-Sho, α-FLAG, α-GFP) and the other half for calnexin (by α-CNX). We found that both Shadoo and calnexin are present in both raft and non-raft membrane fractions of Sho-EYFP-FLAG cells (lanes2-3). More calnexin can be seen in the non-raft sample, which can be due to distribution of this protein being more in the mid- and high-density fractions as compared to low dense fractions. In control EYFP-FLAG cells, the control proteins are immunoprecipitated by α-FLAG and α-GFP where CNX is

absent indicating the presence of the control protein and absence of co-precipitated calnexin (lanes 4-5). The experiments were repeated at-least for four times and it was found that in case of these raft fractionated samples the detectable calnexin signal with Sho overexpressing cells was generally not strong (as on Figure-20B), hence, considered careful evaluation against control cell and over different exposures. Taking together, both total cell lysates and fractionated samples indicate an interaction between Shadoo and calnexin, similarly as in the case of the prion protein and this binding can be detected in both the lipid- raft and non-lipid raft membrane environments.

4.3 The study of the effect of copper treatment on the PrP membrane domain localization in N2a cells.

Studies suggest that upon exposure of cells to certain metal ions and/or due to metal induced stress, proteins may shed and/or change their localization across cellular organelles and can traffic between different types of membrane microdomains of the cells, phenomena that had also been reported for PrP in certain experimental settings and also in the context its protective abilities against metal-ion induced cytotoxicity[46–48,124,163,164].

During our studies, first we set forward to test PrP-s ability to rescue cells against the cytotoxic effects of transition metals, using mouse hippocampal cells derived from wild type and PrP KO mice, ZW($Prnp^{+/+}$) and Zpl($Prnp^{0/0}$) respectively, as model system. In these experiments, we applied treatments by various concentrations of four transition metals known to bind PrP, testing toxicities of Cu^{2+}, Zn^{2+}, Mo^{2+} and Co^{2+} and assessed general parameters of cellular toxicity, such as morphological changes and overall viability changes measured by two assays: alamarBlue-assay and propidium iodide-based dye exclusion assay. Interestingly, our results reveal that while the PrP expressing cells are more resistant to the toxic effects of these metals, reintroduction of PrP into the PrP-null cells does not protect the cells against the toxicity of any of these metals. This allowed us to conclude that even if PrP^C has an effect on the complex pathways of metal toxicity, it is likely not a robust, general effect, that is discernible in all type of cells. We published these results[165], but do not intend to present them in more detail in the present thesis. However, after these studies on mouse hippocampal ZW and Zpl cells, we also found that when exposed to different doses of metals, specifically with copper, N2a cells show similar morphological changes as the prion expressing ZW cells, at the same concentrations, typically of 500 μM which is the concentration where majority of the cells show morphological changes but

are still alive. Next, applying the same method of copper-treatment used for ZW and Zpl cells, we set forward to analyse PrP's localisation in the membrane microdomains of the N2a stable transgenic prion overexpressing PrP-EGFP cells characterized above, upon exposure to 500 μM $CuSO_4$. We treated PrP-EGFP cells in parallel to its control EGFP cells, with the standardised protocol of Cu^{+2}-glycine mix as in the case of ZW and Zpl cells (see Materials and Methods) and separated the membrane-rafts and non-rafts by using the non-detergent based OptiPrep density gradient fractionation method outlined here in the above presented studies and tested the selected target and marker proteins along the gradient fractions by Western blot analysis (**Figure 21**).
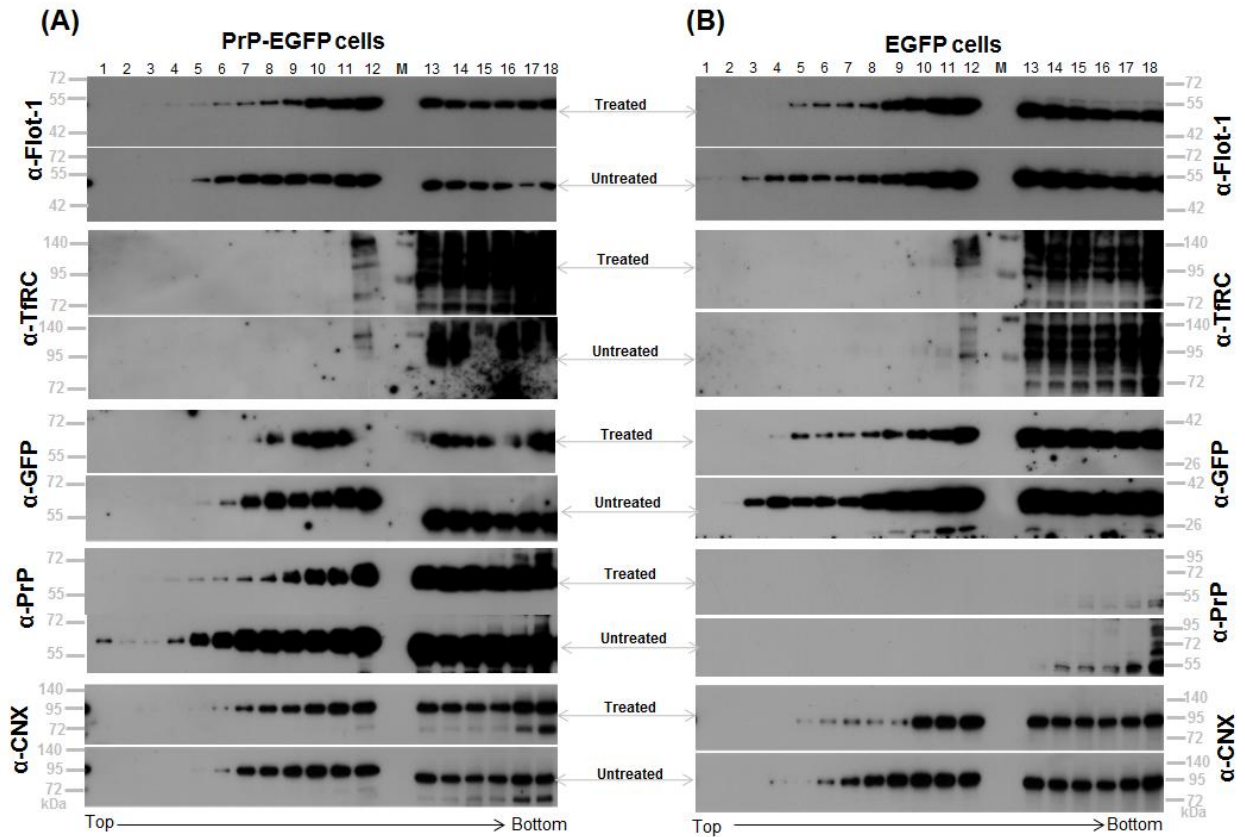
Figure 21: Distribution of various proteins across the raft and non-raft type membranes of copper treated and untreated PrP-EGFP and its control, EGFP cells. A, B) Representative Western blots of selected proteins along the gradient fractions of copper treated and untreated PrP-EGFP (A) and EGFP (B) cells. Both types of cells, in parallel, are treated with 500 μM copper mixed with glycine in OptiMEM media supplemented with GlutaMAX (labeled as "treated") and another set of cells are supplied with only OptiMEM media supplemented with GlutaMAX to serve as controls (labeled as "untreated"), for 30 min at 37 °C in the CO_2 incubator. Fractionated samples are collected from top to bottom of centrifuge tubes and are loaded on SDS-PAGE in order of fraction numbers and are immunoblotted for selected proteins by their corresponding primary antibodies, as indicated: for Flotillin-1 by α-Flot-1; for transferrin receptor

protein by α-TfRC; for PrP by α-GFP and α-PrP; for calnexin by α-CNX. Protein molecular weight ladder is marked on the sides of the blots.

In both PrP-EGFP- and EGFP cells and in both copper-treated and untreated conditions, raft protein, Flotillin-1 is identified from the low density top fractions, here from number 4 through 18, the high dense fractions, whereas the non-raft marker transferrin receptor protein is detected from fraction numbers 12 through 18, high dense fractions. This is also similar to as we found earlier for these cells (Figure 11A and B). This indicates that raft-membranes are present in the copper treated cells similarly as in the untreated and the original transgenic cells. In PrP-EGFP cells, in copper-treated condition PrP is seen from fraction number 3, prominently from fraction number 7 through 18 by both α-PrP and α-GFP antibodies (Figure 21A) that is also qualitatively similar to its untreated counterpart. In the control, EGFP cells, treated by copper a similar distribution is seen for EGFP-GPI$_{(PrP)}$ protein as for PrP-EGFP shown by α-GFP from fraction numbers 3 through 18, low- to high dense fractions, in both treated and untreated conditions (Figure 21B). In both type of cells, CNX distribution along the gradient fractions is seen from fraction numbers 5 through 18 as detected by α-CNX in both copper treated and untreated conditions. Overall, after exposure of prion overexpressing cells to copper, we still see the presence of PrP in the raft fractions, and did not observe an overall re-localisation of fluorescent protein tagged PrP from the raft and non-raft type membrane fractions obtained by the non-detergent based continuous OptiPrep density gradient fractionation method. Since the concentration of copper in these experiments (500 μM) was the highest at which morphological changes well detectable in the population, but we could still collect enough viable cells to perform the raft-fractionation experiments, we deemed unreasonable to try higher concentrations of copper treatment, as well as we did not consider feasible to do more in-depth analysis of copper-response at the membrane-domain level.

5. DISCUSSION

Following its in silico discovery in 2003[63], the third prion-family protein, Shadoo, had been eagerly researched for its possible functional links to the cellular PrP[C], for which a compensatory prion-like protein, coined "pi" (and a hypothetical ligand coined "Lprp") was anticipated at the time[166]. A protein, which would be capable of overtaking key roles of PrP[C] (such as binding to Lprp), specifically in the absence of PrP[C], hence, explaining for the lack of any clear phenotypes detectable in case of *Prnp*[0/0] mice. Although the validity of such a "PrP-Lrp-pi" model had not been resolved and validated experimentally[83], it initiated a comparative framework for the Sho research, which in the past decade indeed uncovered several intriguing similarities between Sho and PrP, including common functions, but importantly also, differences as well, which together may carry important clues to a better understanding of the prion-biology and also indirectly of disease development.

Interestingly, during prion infection, the levels of Sho in brain decrease in several experimental rodent models and sheep[64,85,86] suggesting an involvement of Sho in prion disease process. In addition, Sho on its own demonstrated ability to form fibrils in model membranes[88] and amyloid-like aggregates in cell membranes[67] and recombinant Sho increased PrP conversion rate in cell culture setting when administered to cell media prior infection with scrapie brain homogenate[89]. Moreover, native crosslinking and immunoprecipitation, studies presented Sho as PrP's interactor, indicative that they may occupy same environment *in vivo*[90]. However, its overexpression did not influence prion replication kinetics in transgenic mice[92] and altogether Sho did not prove to have direct involvement in propagating PrP[Sc 86,92,93].

While both PrP and Sho are expressed at highest levels in CNS, the localization of Sho had been found to be partially overlapping with PrP- as demonstrated by *in-situ* hybridization and immunohistological studies in the adult wild-type mice brain[64]. Interestingly, complementary expression of the two proteins is also observed in certain areas, such as in hippocampus and cerebellum and/or within the same type of neurons: in hippocampal pyramidal cells, Sho was detected as being intensely expressed in cell bodies, was absent in the axonal processes and again intensely present in the apical dendritic processes in stratum radiatum of the hippocampus. PrP on the other hand, was found to be primarily abundant in the axonal projections of the pyramidal cells with low expression levels in the cell bodies and yielded a specific complementary

"negative-staining" image within the molecular layer of the neutrophil for the apical dendritic processes stained by Sho. In cerebellar Purkinje cells, Sho was detected in all areas, cell bodies, axonal processes and dendritic arborizations within the molecular layer of the cerebellum. While PrP is absent in Purkinje cells[64,77], it is intensely expressed in the granular layer and the neutrophil molecular layer, yielding similar "negative staining-effect" for dendritic aborizations highly stained by Sho. Contrary to these, a complete colocalization was found for the two proteins in the cerebellar cortex neurons[64]. All together these observations also suggest that the two wild type proteins are capable to support different and/or similar cellular functions *in vivo* depending on the specific cellular environment and/or condition they are in.

In the work presented in this thesis, we studied Sho and PrP in the context of their localization to membrane micro-domains. As one of the results we demonstrate that while Sho and PrP^C, both being GPI-anchored proteins, reside in membrane microdomains called lipid-rafts they similarly display presence in non-raft type membrane fractions as well, when assessed by a non-detergent based fractionation method and using transgenic N2a cells expressing these proteins.

Membrane lipid-rafts are currently defined as a small (10–200 nm), heterogeneous, highly dynamic, cholesterol- and sphingolipid-enriched domains that compartmentalize the cellular processes and can transiently disband or become stabilized to form larger platforms through protein-protein and protein-lipid interactions[107]. Their existence had long been controversial, owing to the inability to prove their existence directly with the methods currently available, mostly due to their transient, dynamic nature and their small size. It has to be mentioned that ongoing technological and scientific advances, continue to shape our understanding of rafts and of the molecules (for example the actin filaments) that actively participate in regulating the formation of cellular membrane-rafts. Nevertheless, several indirect methods in the last decades pointed unequivocally to their existence, making them generally accepted as valid[167,168]. Among the indirect biochemical approaches, the classical, most frequently used techniques to study rafts are the detergent-based (e.g., 1% TritonX-100; CHAPS; Brij 58, 96 and 98; Lubrol; Nonidet P40; octylglucoside and others) cell fractionation methods followed by the sucrose density-gradient separation to isolate raft and non-raft membrane fractions. These methods led first to isolation of the "detergent-resistant membrane fractions" (DRMs), the low-density floating fractions on the density-gradient, as raft-type membrane fractions. The compositional characterization of these

75

had largely contributed to our current understanding of membrane rafts in mammalian cells[169,170]. This approach had widely been used, including also for the study of prion proteins[64,76,124]. Several observations, however, raised concerns over this method, pointing to the ability of detergents to cluster lipids and proteins originally not associated with each other into a raft fraction. The high variation in the reproducibility of data obtained through this method is also argued to be the reason for this experimentally induced clustering effect of detergents[171–173]. Hence, non-detergent-based methods have been developed[155,174]. Considering these, we opted for using a non-detergent-based raft-isolation method, the one improved by Macdonald and Pike in 2005[154]. The approach is known to yield high-purity raft separations based on a detergent-free shearing of cells in an iso-osmotic environment and divalent cations to maintain stability of rafts and using OptiPrep as a continuous density-gradient to fractionate the post-nuclear supernatant in order to separate the rafts and non-rafts based on the density flotation. The low-density fractions occupied by rafts on this gradient correspond to the densities of rafts obtained by the detergent-based sucrose gradient methods[154].

The N2a cells generated in this study, stably expressing PrP or Sho in fusion with either a fluorescent protein alone or in addition with FLAG tag, at C-terminals preceding their GPI-signal peptides, or the untagged protein in case of PrP in one of our cells developed, are correctly processed: they are complex glycosylated and GPI-anchored with subcellular localization that are similar to each other (Figures 6 and7) and is as expected for secretory proteins, being present at the PM, GA and ER, and as reported for PrP and Sho in other studies in various cells[64]. Using the non-detergent based OptiPrep density gradient fractionation method to separate raft- and non-rafts type membrane microdomains and following the criteria of "true-rafts" of Persaud-Sawin and co-workers[155] confirmed that both proteins, PrP and Sho are present in low-dense fractions (Figures11-13) that correspond to raft-type membranes, which is in accordance to earlier studies using detergent-based[64,76,124]. Interestingly, beside their localization to raft type membranes, we show that PrP and Sho is also abundantly detected in denser fractions, where typically the non-raft marker, transferrin receptor is present and are considered non-raft type fractions (Figures 11-13 and 20). This is consistent over repeated experiments on different passage number and cultures of the cells. For PrP, its presence in non-raft type membranes had been observed in previous studies on brain- and N2a cells[159,175]; and this is also in line with raft and caveolae dependent- versus independent- clathrin-mediated endocytosis of PrP following its relocation

from rafts to non-rafts by its N-terminal polybasic region and/or binding with transferrin receptor, non-raft marker protein[124,175]. However, trafficking of Sho between the raft and non-raft type membrane microdomains and an underlying process for this is not yet demonstrated. A similar possibility to PrP for Sho may be envisaged. Such a proposition may be backed up also by the interactome analysis data of the prion-family proteins by Watts and co-workers, showing that proteins with oligomannosidic N-glycans such as the transferrin receptor[90,176], the non-raft marker protein used here specifically co-purified with PrP and Sho in N2a neuroblastoma cells as well as in wild type mice brain[90]. This indicates that these proteins occupy similar environments at leaset at a point in time during their biological activity. Additionally, a temporary residency of proteins in rafts as a regulatory mechanism of their biological activity also had been observed for other proteins (reviewed in[177]).

The most striking similarity between PrP and Sho is in their inherently unstructured nature, PrP's N-terminal half, while Sho being fully unstructured. How these proteins maintain their proper folds during their lifecycle is not fully understood and it is intriguing in itself. Pepe and co-workers[76] using primary neuronal GT1 and human neuroblastoma SH-SY5Ycells, observed that some percentage of Sho, contrary to PrP, was partially in PK-resistant, aggregated state already in natural conditions in cells and this amount increased upon disrupting membrane rafts by cholesterol depletion, a condition where the partially PK-resistant, partly glycosylated, ER-retained forms of PrP also appeared. These authors[76] also demonstrate that the mature form and the unglycosylated form of Sho co-immunoprecipitates with the ER-chaperone calreticulin (CRT). CRT's binding to Sho was also enhanced upon disrupting the membrane rafts. Furthermore, one earlier study on PrP, found that another ER-chaperone, calnexin (CNX), could bind full length PrP both *in vitro*, preventing its thermal aggregation, and in vivo, as it Co-IPed with PrP^C both as endogenous proteins and when co-transfected into either 293T or the human neuroblastoma SK-N-SH cells, where its binding also prevented the cytotoxicity of PrP[153]. Based on these, we set forward to examine binding of both PrP and Sho to calnexin, using the developed transgenic N2a cells expressing the proteins. Our results using immunocytochemistry and live-cell analysis to visualize the localizations of these proteins in the transgenic cells expressing PrP and Sho, demonstrate that PrP and Sho partially colocalize with CNX, being all present in the ER but not in the PM and GA (Figure 15 and 16). The ER is a cellular organelle composed of the structures nuclear membrane, the tubular ER- and the sheet like cisternae[178–182]. Therefore, we

applied live-cell analysis and high magnification spinning-disc confocal microscopy to visualize these structures that were not detectable by immunocytochemistry approach (Figure 15). Imaging the live cells stably expressing PrP or Sho and transiently expressing a fluorescent-protein-tagged calnexin, revealed that in all three ER compartments, Sho and PrP can be found colocalized with CNX. When testing the possible interaction between PrP or Sho with CNX in these cell populations, first we tested total cell lysates.

Ni-NTA bead pull-down experiments on the total cell lysates of PrP-EGFP cells confirmed presence of CNX (Figure 17), indicating that in these N2a cells CNX is also a binding partner of PrP, in line with the earlier observation of Wang and co-workers in 293T and human neuroblastoma SK-N-SH cells[153]. Further, we analyzed this interaction in the separated membrane raft and non-rafts applying the non-detergent based OptiPrep density gradient method for separation and report here that PrP pulled CNX in each type of fraction, raft type (fractions 4 through 11, Figure 4B) and non-raft type (fractions 12 through 18, Figure 18B). These results indicate that at-least a proportion of PrP is found as bound to CNX in both raft and non-raft environments. To analyze whether Shadoo would similarly have an interaction with calnexin or not, we first developed cells stably expressing FLAG-tagged Sho-EYFP (Sho-EYFP-FLAG cells) and its control cells (EYFP-FLAG) and performed immunoprecipitation using anti-FLAG-beads. Here we show that Sho co-immunoprecipitated CNX in the total cell lysates of Sho-EYFP-FLAG cells (Figure 19A). To see if Sho's interaction with CNX is preferred in one of the types of membrane domains or not, applying the non-detergent based fractionation method similarly as for PrP, first we separated the different membrane fractions. Pooling the raft type fractions and separately the non-raft type fractions and subjecting the samples to co-immunoprecipitation assay using anti-FLAG beads, we reveal that, CNX co-immunoprecipitates with Sho in both types of separately pooled rafts and non-raft samples (Figure 20B).

These results are in line with Sarnataro and co-workers[122] findings that PrP enriched in ER-cholesterol rich, membrane domains in early secretary pathway for correct folding of PrP but since sample used for the non-detergent based Optiprep density gradient fractionation is not specifically from ER, we assume PrP from both PM and ER compartments of the cells. Furthermore, similar to PrP, Sho also present in not only ER but PM cholesterol rich membrane domains for correct folding of it.

Based on these results, we can say that at least a proportion of both Sho and PrP interacts with CNX in these cells and irrespective of their localization to raft or non-raft type membrane domains. We propose that the inherently unfolded structures or the domains of these two prion-family proteins need chaperone assistance in both raft and non-raft type membranes during their lifecycle, and that CNX is being at least one of these chaperones.

One of the major characteristics of PrP is its ability of binding copper and other divalent cations. This is mainly exerted by its octapeptide repeat region, OR, but also of other sites on its surface. In line with this, one of the major functions of PrP is refereed to be the regulation of transition metal-, specifically copper, homeostasis and diminishing the toxic effects of these metals[33,36,38,41,54]. It had also been reported that PrP upon Cu^{2+} binding undergoes clathrin-dependent endocytosis, which implies that it should leave the rafts[124]. Using mouse hippocampal cells derived from wild type and PrP KO mice, ZW($Prnp^{+/+}$) and Zpl($Prnp^{0/0}$), respectively, and treatment by various divalent transition metals, we revealed that while the PrP expressing cells are more resistant to the toxic effect of these metals, reintroduction of PrP into the PrP-null cells, did not lead to restoration of their resistance (results not presented in the thesis)[165]. In the work presented here, we tested whether by using our set-up of N2a transgenic cells and the non-detergent based fractionation method, and applying the method of copper-treatment used for ZW and Zpl cells, we could observe the relocation of PrP from rafts to non-rafts. We treated PrP-EGFP in parallel to its control, EGFP cells with standardised concentration of 500 μM Cu^{+2} and separated membrane raft and non-rafts. After performing Western blots for the target and the marker proteins, however, we could not detect a significant shift in the distribution of PrP along the raft-type density fractions. The study reported by Taylor and co-workers,[124] where re-localisation of PrP was observed upon Cu^{2+} treatment, contrary to our study, employed a detergent-based fractionation of cell membranes, and observed the relocation of PrP from the detergent resistant membranes (DRM) to non-DRM fractions. These fractions were isolated using 1% Triton X-100 detergent-based discontinuous sucrose density gradient (of 40%-5%) method, which is differed from ours. Therefore, it may be plausible to argue that the different cellular system and/or the use of detergents and a discontinuous gradient-method of isolation could be the reason of obtaining different results in our case. Together, these results indicate that the process of the rescuing effect of PrP against transition metal toxicity may be more complex than just its ability to bind these metals, as well as that either this role and/or its observed trafficking in

relation to Cu^{2+} treatment may depend on the experimental system and the isolation procedure used, drawing attention to the need of a more careful interpretation of these type of results.

6. CONCLUSIONS

The presented work focuses on the study of PrP and Sho in membrane raft- and non-raft type fractions isolated from transgenic N2a cells expressing the two proteins. The major findings of the studies are the following. We report that beside both prion protein and Shadoo occupying raft-type membrane fractions, a significant proportion of them are present in transferrin receptor-marked non-raft membrane domains. We suggest that their dual raft/non-raft distribution reflects their loose confinement to rafts and may support their multifunctional capacities. The presented results also reveal that both Sho and PrP^C bind with calnexin, an ER chaperone, and that this interaction is present in both type of membrane domains. This allows to propose that calnexin is a binding partner of both Sho and PrP, and that at least a fraction of these proteins is bound to CNX at any given time and independent of their localization to raft-or non-rafts. It may be suggested that the unfolded structure of these proteins may necessitate chaperone assistance, among them of CNX's, in certain instances and independent of their presence in rafts or non-raft type membrane domains. Furthermore, we could not observe the relocation of PrP from rafts to non-rafts upon copper-treatment of these N2a cells, in line with a lack of the rescue effect of PrP observed upon the copper- and other transition metal treatments of Zpl ($Prnp^{0/0}$) cells when PrP was reintroduced into the cells. Based on these, we propose that the involvement of PrP in diminishing the toxic effects of copper (or of the other metals studied) as well as its copper-induced trafficking, may be more complex processes than merely binding these metals, and/or may also be dependent on the cellular models used.

These results add to our understanding of PrP and Sho's biology in terms of their membrane domain localization characteristics; confirm a new binding partner, CNX, for Sho; reveal that the binding with is present for both PrP and Sho in both raft- and non-rafts; and also, report that the rescue effect of PrP against transition metal toxicity, as well as its trafficking influenced by copper binding is not generally observable, indicating the existence of more complex process at place, and/or a possible dependence on the model system used.

REFERENCES

1. Chiti F, Dobson CM. Protein misfolding, functional amyloid, and human disease. *Annu Rev Biochem*. 2006;75:333-366. doi:10.1146/annurev.biochem.75.101304.123901

2. Korsak M, Kozyreva T. Beta amyloid hallmarks: From intrinsically disordered proteins to alzheimer's disease. In: *Advances in Experimental Medicine and Biology*. ; 2015. doi:10.1007/978-3-319-20164-1_14

3. Coskuner-Weber O, Uversky V. Insights into the Molecular Mechanisms of Alzheimer's and Parkinson's Diseases with Molecular Simulations: Understanding the Roles of Artificial and Pathological Missense Mutations in Intrinsically Disordered Proteins Related to Pathology. *Int J Mol Sci*. 2018;19(2):336. doi:10.3390/ijms19020336

4. Soto C, Satani N. The intricate mechanisms of neurodegeneration in prion diseases. *Trends Mol Med*. 2011;17(1):14-24. doi:10.1016/j.molmed.2010.09.001

5. Prusiner SB. Prions. *Proc Natl Acad Sci*. 1998;95(23):13363-13383. doi:10.1073/pnas.95.23.13363

6. Prusiner SB. Novel Proteinaceous Infectious Particles Cause Scrapie. *Source Sci New Ser*. 1982;216(9):136-144. http://www.jstor.org/stable/1687927.

7. Macalister GO, Buckley RJ. The risk of transmission of variant Creutzfeldt-Jakob disease via contact lenses and ophthalmic devices. *Contact Lens Anterior Eye*. 2002;25(3):104-136. doi:10.1016/S1367-0484(02)00008-5

8. Babelhadj B, Di Bari MA, Pirisinu L, et al. Prion Disease in Dromedary Camels, Algeria. *Emerg Infect Dis*. 2018;24(6):1029-1036. doi:10.3201/eid2406.172007

9. Asante EA, Linehan JM, Desbruslais M, et al. BSE prions propagate as either variant CJD-like or sporadic CJD-like prion strains in transgenic mice expressing human prion protein. *EMBO J*. 2002;21(23):6358-6366. doi:10.1093/emboj/cdf653

10. Sigurdsson B. RIDA, A Chronic Encephalitis of Sheep. *Br Vet J*. 1954;110(9):341-354. doi:10.1016/S0007-1935(17)50172-4

11. Liberski PP. Kuru and D . Carleton Gajdusek : a close encounter. *Folia Neuropathol*. 2009;47(2):114-137.

12. Alper T, Cramp W a, Haig D a, Clarke MC. Does the agent of scrapie replicate without nucleic acid? *Nature*. 1967;214(5090):764-766. doi:10.1038/214764a0

13. Griffith JS. Nature of the Scrapie Agent: Self-replication and Scrapie. *Nature*. 1967;215(5105):1043-1044. doi:10.1038/2151043a0

14. Aguzzi a, Heppner FL. Pathogenesis of prion diseases: a progress report. *Cell Death Differ*. 2000;7(10):889-902. doi:10.1038/sj.cdd.4400737

15.   Thellung S, Corsaro A, Villa V, et al. Human PrP90-231-induced cell death is associated with intracellular accumulation of insoluble and protease-resistant macroaggregates and lysosomal dysfunction. *Cell Death Dis*. 2011;2(3):e138-10. doi:10.1038/cddis.2011.21

16.   Aguzzi A, Calella AM. Prions : Protein Aggregation and Infectious Diseases. *Physiol Rev*. 2009;89:1105-1152. doi:10.1152/physrev.00006.2009.

17.   Jarrett JT, Lansbury PT. Seeding "one-dimensional crystallization" of amyloid: A pathogenic mechanism in Alzheimer's disease and scrapie? *Cell*. 1993;73(6):1055-1058. doi:10.1016/0092-8674(93)90635-4

18.   Aguzzi A, Weissmann C. Prion research: the next frontiers. *Nature*. 1997;389(6653):795-798. doi:10.1038/39758

19.   Brown P, Cervenakova L. A prion lexicon (out of control) [4]. *Lancet*. 2005;365(9454):122. doi:10.1016/S0140-6736(05)17700-9

20.   Jaunmuktane Z, Brandner S. Invited Review: The role of prion-like mechanisms in neurodegenerative diseases. *Neuropathol Appl Neurobiol*. 2020;46(6):522-545. doi:10.1111/nan.12592

21.   Goedert M. Alzheimer's and Parkinson's diseases: The prion concept in relation to assembled Aβ, tau, and α-synuclein. *Science (80-)*. 2015. doi:10.1126/science.1255555

22.   Kretzschmar HA, Prusiner SB, Stowring LE, DeArmond SJ. Scrapie prion proteins are synthesized in neurons. *Am J Pathol*. 1986;122(1):1-5.

23.   Kretzschmar HA, Stowring LE, Westaway D, Stubblebine WH, Prusiner SB, Dearmond SJ. Molecular Cloning of a Human Prion Protein cDNA. *DNA*. 1986;5(4):315-324. doi:10.1089/dna.1986.5.315

24.   Moudjou M, Frobert Y, Grassi J, Bonnardiere C La. Cellular prion protein status in sheep: tissue-speci c biochemical signatures. *J Gen Virol*. 2001;82(2001):2017-2024. doi:10.1099/0022-1317-82-8-2017

25.   Aguzzi A. Mammalian Prion BiologyOne Century of Evolving Concepts. *Cell*. 2004;116(2):313-327. doi:10.1016/S0092-8674(03)01031-6

26.   Riek R, Hornemann S, Wider G, Glockshuber R, Wuthrich K. NMR characterization of the full-length recombinant murine prion protein, mPrP(23-231). *FEBS Lett*. 1997;413(2):282-288. doi:10.1016/S0014-5793(97)00920-4

27.   Zahn R, Liu A, Lührs T, et al. NMR solution structure of the human prion protein. *Proc Natl Acad Sci U S A*. 2000;97(1):145-150. doi:10.1073/pnas.97.1.145

28.   Naslavsky N, Stein R, Yanai A, Friedlander G, Taraboulos A. Characterization of detergent-insoluble complexes containing the cellular prion protein and its scrapie isoform. *J Biol Chem*. 1997;272(10):6324-6331. doi:10.1074/jbc.272.10.6324

29.   Andriano Aguzzi CS and MH. Molecular mechanisms of Prion Pathogenisis. *Annu Rev*

Pathol Dis. 2008;3:67-97. doi:10.1146/annurev.path

30.   Westergard L, Christensen HM, Harris DA. PrPc: Function and Role in Disease. *(Review)*. 2007;1772(6):629-644.

31.   Klamt F, Dal-Pizzol F, Conte Da Frota ML, et al. Imbalance of antioxidant defense in mice lacking cellular prion protein. *Free Radic Biol Med*. 2001;30(10):1137-1144. doi:10.1016/S0891-5849(01)00512-3

32.   Passet B, Young R, Makhzami S, et al. Prion protein and shadoo are involved in overlapping embryonic pathways and trophoblastic development. *PLoS One*. 2012;7(7):1-8. doi:10.1371/journal.pone.0041959

33.   Vassallo N, Herms J. Cellular prion protein function in copper homeostasis and redox signalling at the synapse. *J Neurochem*. 2003;86(3):538-544. doi:10.1046/j.1471-4159.2003.01882.x

34.   Büeler H, Fischer M, Lang Y, Bluethmann H, Lipp HP, DeArmond SJ, Prusiner SB, Aguet M WC. Normal development and behaviour of mice lacking the neuronal cell surface PrP protein. *Nature*. 1992;356:577-582. https://doi.org/10.1038/356577a0.

35.   Jeffrey M, González L. Classical sheep transmissible spongiform encephalopathies: Pathogenesis, pathological phenotypes and clinical disease. *Neuropathol Appl Neurobiol*. 2007;33(4):373-394. doi:10.1111/j.1365-2990.2007.00868.x

36.   Brown DR, Qin K, Herms JW, et al. The cellular prion protein binds copper in vivo. *Nature*. 1997;390(6661):684-687. doi:10.1038/37783

37.   Marino T, Russo N, Toscano M. Interaction of the Mn 2+ , Co 2+ , Ni 2+ , and Zn 2+ with prion protein HGGGW pentapeptide model. *Int J Quantum Chem*. 2011;111(6):1152-1162. doi:10.1002/qua.22682

38.   Stöckel J, Safar J, Wallace AC, Cohen FE, Prusiner SB. Prion Protein Selectively Binds Copper(II) Ions. *Biochemistry*. 1998;37(20):7185-7193. doi:10.1021/bi972827k

39.   Wong BS, Chen SG, Colucci M, et al. Aberrant metal binding by prion protein in human prion disease. *J Neurochem*. 2001;78(6):1400-1408. doi:10.1046/j.1471-4159.2001.00522.x

40.   Singh N, Das D, Singh A, Mohan ML. Prion Protein and Metal Interaction: Physiological and Pathological Implications. In: *The Prion Protein*. Vol 12. Caister Academic Press; 2010. doi:10.21775/9781912530076.04

41.   La Mendola D, Rizzarelli E. Evolutionary implications of metal binding features in different species' prion protein: An inorganic point of view. *Biomolecules*. 2014;4(2):546-565. doi:10.3390/biom4020546

42.   Jackson GS, Murray I, Hosszu LLP, et al. Location and properties of metal-binding sites on the human prion protein. *Proc Natl Acad Sci U S A*. 2001;98(15):8531-8535. doi:10.1073/pnas.151038498

43. Qin K, Yang DS, Yang Y, et al. Copper(II)-induced conformational changes and protease resistance in recombinant and cellular PrP: Effect of protein age and deamidation. *J Biol Chem*. 2000;275(25):19121-19131. doi:10.1074/jbc.275.25.19121

44. Quaglio E, Chiesa R, Harris DA. Copper Converts the Cellular Prion Protein into a Protease-resistant Species That Is Distinct from the Scrapie Isoform. *J Biol Chem*. 2001;276(14):11432-11438. doi:10.1074/jbc.M009666200

45. McKenzie D, Bartz J, Mirwald J, Olander D, Marsh R, Aiken J. Reversibility of Scrapie Inactivation Is Enhanced by Copper. *J Biol Chem*. 1998;273(40):25545-25547. doi:10.1074/jbc.273.40.25545

46. Pauly PC, Harris DA. Copper stimulates endocytosis of the prion protein. *J Biol Chem*. 1998;273(50):33107-33110. doi:10.1074/jbc.273.50.33107

47. Brown LR, Harris DA. Copper and zinc cause delivery of the prion protein from the plasma membrane to a subset of early endosomes and the Golgi. *J Neurochem*. 2003;87(2):353-363. doi:10.1046/j.1471-4159.2003.01996.x

48. Parkin ET, Watt NT, Turner AJ, Hooper NM. Dual Mechanisms for Shedding of the Cellular Prion Protein. *J Biol Chem*. 2004;279(12):11170-11178. doi:10.1074/jbc.M312105200

49. Harris DA. Cellular biology of prion diseases. *Clin Microbiol Rev*. 1999;12(3):429-444. doi:10.1128/cmr.12.3.429

50. Shyng SL, Heuser JE, Harris DA. A glycolipid-anchored prion protein is endocytosed via clathrin-coated pits. *J Cell Biol*. 1994;125(6):1239-1250. doi:10.1083/jcb.125.6.1239

51. Shyng SL, Moulder KL, Lesko A, Harris DA. The N-terminal domain of a glycolipid-anchored prion protein is essential for its endocytosis via clathrin-coated pits. *J Biol Chem*. 1995;270(24):14793-14800. doi:10.1074/jbc.270.24.14793

52. Salzano G, Giachin G, Legname G. Structural Consequences of Copper Binding to the Prion Protein. *Cells*. 2019;8(8):770. doi:10.3390/cells8080770

53. Brown DR, Besinger A. Prion protein expression and superoxide dismutase activity. *Biochem J*. 1998;334(2):423-429. doi:10.1042/bj3340423

54. Haigh CL, Brown DR. Prion protein reduces both oxidative and non-oxidative copper toxicity. *J Neurochem*. 2006;98(3):677-689. doi:10.1111/j.1471-4159.2006.03906.x

55. Choi CJ, Anantharam V, Saetveit NJ, Houk RS, Kanthasamy A, Kanthasamy AG. Normal cellular prion protein protects against manganese-induced oxidative stress and apoptotic cell death. *Toxicol Sci*. 2007;98(2):495-509. doi:10.1093/toxsci/kfm099

56. Rachidi W, Chimienti F, Aouffen M, et al. Prion protein protects against zinc-mediated cytotoxicity by modifying intracellular exchangeable zinc and inducing metallothionein expression. *J Trace Elem Med Biol*. 2009;23(3):214-223. doi:10.1016/j.jtemb.2009.02.007

57.   Westaway D, Daude N, Wohlgemuth S, Harrison P. The PrP-Like Proteins Shadoo and Doppel. In: *Top Curr Chem*. ; 2011:225-256. doi:10.1007/128_2011_190

58.   Makrinou E, Collinge J, Antoniou M. Genomic characterization of the human prion protein (PrP) gene locus. *Mamm Genome*. 2002;13(12):696-703. doi:10.1007/s00335-002-3043-0

59.   Silverman GL, Qin K, Moore RC, et al. Doppel is an N-glycosylated, glycosylphosphatidylinositol-anchored protein: Expression in testis and ectopic production in the brains of Prnp(0/0) mice predisposed to purkinje cell loss. *J Biol Chem*. 2000;275(35):26834-26841. doi:10.1074/jbc.M003888200

60.   Mo H, Moore RC, Cohen FE, et al. Two different neurodegenerative diseases caused by proteins with similar structures. *Proc Natl Acad Sci U S A*. 2001;98(5):2352-2357. doi:10.1073/pnas.051627998

61.   Peoc'h K, Guérin C, Brandel JP, Launay JM, Laplanche JL. First report of polymorphisms in the prion-like protein gene (PRND): Implications for human prion diseases. *Neurosci Lett*. 2000;286(2):144-148. doi:10.1016/S0304-3940(00)01100-9

62.   Mead S, Beck J, Dickinson A, Fisher EMC, Collinge J. Examination of the human prion protein-like gene Doppel for genetic susceptibility to sporadic and variant Creutzfeldt - Jakob disease. *Neuroscience*. 2000;290:117-120.

63.   Premzl M, Sangiorgio L, Strumbo B, Marshall Graves JA, Simonic T, Gready JE. Shadoo, a new protein highly conserved from fish to mammals and with similarity to prion protein. *Gene*. 2003;314(1-2):89-102. doi:10.1016/S0378-1119(03)00707-8

64.   Watts JC, Drisaldi B, Ng V, et al. The CNS glycoprotein Shadoo has PrPC-like protective properties and displays reduced levels in prion infections. *EMBO J*. 2007;26(17):4038-4050. doi:10.1038/sj.emboj.7601830

65.   Daude N, Westaway D. Biological properties of the PrP-like Shadoo protein. *Front Biosci*. 2011;16(4):1505-1516. doi:10.2741/3801

66.   Young R, Le S, Tilly G, et al. Generation of Sprn -regulated reporter mice reveals gonadic spatial expression of the prion-like protein Shadoo in mice. *Biochem Biophys Res Commun*. 2011;412:752-756. doi:10.1016/j.bbrc.2011.08.049

67.   Daude N, Ng V, Watts JC, et al. Wild-type Shadoo proteins convert to amyloid-like forms under native conditions. *J Neurochem*. 2010;113(1):92-104. doi:10.1111/j.1471-4159.2010.06575.x

68.   Margit Miesbauer, Theresa Bamme, Constanze Riemer, Birgit Oidtmann, Konstanze F. Winklhofer, Michael Baier JT. Prion protein-related proteins from zebrafish are complex glycosylated and contain a glycosylphosphatidylinositol anchor. 2006;341:218-224. doi:10.1016/j.bbrc.2005.12.168

69.   Tóth E, Kulcsár PI, Fodor E, et al. The highly conserved , N-terminal (RXXX) 8 motif of mouse Shadoo mediates nuclear accumulation. *BBA - Mol Cell Res*. 2013;1833(5):1199-

1211. doi:10.1016/j.bbamcr.2013.01.020

70. Kang S, Mays CE, Daude N, Yang J, Kar S, Westaway D. Proteasomal Inhibition Redirects the PrP-Like Shadoo Protein to the Nucleus. *Mol Neurobiol*. 2019;56(11):7888-7904. doi:10.1007/s12035-019-1623-1

71. Pfeiffer N V., Dirndorfer D, Lang S, et al. Structural features within the nascent chain regulate alternative targeting of secretory proteins to mitochondria. *EMBO J*. 2013;32(7):1036-1051. doi:10.1038/emboj.2013.46

72. Premzl M, Gready JE, Jermiin LS, Simonic T, Marshall Graves JA. Evolution of vertebrate genes related to prion and shadoo proteins - Clues from comparative genomic analysis. *Mol Biol Evol*. 2004;21(12):2210-2231. doi:10.1093/molbev/msh245

73. Corley SM, Gready JE. Identification of the RGG Box Motif in Shadoo: RNA-Binding and Signaling Roles? *Bioinform Biol Insights*. 2008;2:383-400. doi:10.4137/bbi.s1075

74. Stahl N, Baldwin MA, Prusiner SB, Burlingame AL. Identification of Glycoinositol Phospholipid Linked and Truncated Forms of the Scrapie Prion Protein. *Biochemistry*. 1990;29(38):8879-8884. doi:10.1021/bi00490a001

75. Taylor DR, Parkin ET, Cocklin SL, et al. Role of ADAMs in the ectodomain shedding and conformational conversion of the prion protein. *J Biol Chem*. 2009;284(34):22590-22600. doi:10.1074/jbc.M109.032599

76. Pepe A, Avolio R, Matassa DS, et al. Regulation of sub-compartmental targeting and folding properties of the Prion-like protein Shadoo. *Sci Rep*. 2017;7(1):1-15. doi:10.1038/s41598-017-03969-2

77. Baumann F, Tolnay M, Brabeck C, et al. Lethal recessive myelin toxicity of prion protein lacking its central domain. *EMBO J*. 2007;26(2):538-547. doi:10.1038/sj.emboj.7601510

78. Lau A, Mays CE, Genovesi S, Westaway D. RGG repeats of PrP-like shadoo protein bind nucleic acids. *Biochemistry*. 2012;51(45):9029-9031. doi:10.1021/bi301395w

79. Lima LMTR, Cordeiro Y, Tinoco LW, et al. Structural insights into the interaction between prion protein and nucleic acid. *Biochemistry*. 2006;45(30):9180-9187. doi:10.1021/bi060532d

80. Gomes MPB, Millen TA, Ferreira PS, et al. Prion protein complexed to N2a cellular RNAs through its N-terminal domain forms aggregates and is toxic to murine neuroblastoma cells. *J Biol Chem*. 2008;283(28):19616-19625. doi:10.1074/jbc.M802102200

81. Passet B, Castille J, Makhzami S, et al. The Prion-like protein Shadoo is involved in mouse embryonic and mammary development and differentiation. *Sci Rep*. 2020;10(1):6765. doi:10.1038/s41598-020-63805-y

82. Young R, Passet B, Vilotte M, et al. The prion or the related Shadoo protein is required for early mouse embryogenesis. *FEBS Lett*. 2009;583(19):3296-3300. doi:10.1016/j.febslet.2009.09.027

83. Daude N, Westaway D. Shadoo/PrP (Sprn0/0/Prnp0/0) double knockout mice: More than zeroes. *Prion*. 2012;6(5):420-424. doi:10.4161/pri.21867

84. Daude N, Wohlgemuth S, Brown R, et al. Knockout of the prion protein (PrP)-like Sprn gene does not produce embryonic lethality in combination with PrPC-deficiency. *Proc Natl Acad Sci*. 2012;109(23):9035-9040. doi:10.1073/pnas.1202130109

85. Westaway D, Genovesi S, Daude N, et al. Down-regulation of shadoo in prion infections traces a pre-clinical event inversely related to PrP sc accumulation. *PLoS Pathog*. 2011;7(11):1-18. doi:10.1371/journal.ppat.1002391

86. Watts JC, Stöhr J, Bhardwaj S, et al. Protease-Resistant Prions Selectively Decrease Shadoo Protein. Mabbott NA, ed. *PLoS Pathog*. 2011;7(11):e1002382. doi:10.1371/journal.ppat.1002382

87. Beck JA, Campbell TA, Adamson G, et al. Association of a null allele of SPRN with variant Creutzfeldt-Jakob disease. *J Med Genet*. 2008;45(12):813-817. doi:10.1136/jmg.2008.061804

88. Li Q, Chevalier C, Henry C, Richard CA, Moudjou M, Vidic J. Shadoo binds lipid membranes and undergoes aggregation and fibrillization. *Biochem Biophys Res Commun*. 2013;438(3):519-525. doi:10.1016/j.bbrc.2013.07.104

89. Ciric D, Richard C-A, Moudjou M, et al. Interaction between Shadoo and PrP Affects the PrP-Folding Pathway. *J Virol*. 2015;89(12):6287-6293. doi:10.1128/jvi.03429-14

90. Watts JC, Huo H, Bai Y, et al. Correction: Interactome Analyses Identify Ties of PrPC and Its Mammalian Paralogs to Oligomannosidic N-Glycans and Endoplasmic Reticulum-Derived Chaperones. *PLoS Pathog*. 2009;5(10):e1000608. doi:10.1371/annotation/9eb11869-6acb-49b0-978e-abedc3cc545a

91. Jiayu W, Zhu H, Ming X, et al. Mapping the interaction site of prion protein and Sho. *Mol Biol Rep*. 2010;37(5):2295-2300. doi:10.1007/s11033-009-9722-0

92. Wang H, Wan J, Wang W, et al. Overexpression of Shadoo protein in transgenic mice does not impact the pathogenesis of scrapie. *Neurosci Lett*. 2011;496(1):1-4. doi:10.1016/j.neulet.2011.03.073

93. Miyazawa K, Manuelidis L. Agent-specific shadoo responses in transmissible encephalopathies. *J Neuroimmune Pharmacol*. 2010;5(1):155-163. doi:10.1007/s11481-010-9191-1

94. Sakthivelu V, Seidel RP, Winklhofer KF, Tatzelt J. Conserved stress-protective activity between prion protein and Shadoo. *J Biol Chem*. 2011;286(11):8901-8908. doi:10.1074/jbc.M110.185470

95. Moore RC, Lee IY, Silverman GL, et al. Ataxia in prion protein (PrP)-deficient mice is associated with upregulation of the novel PrP-like protein doppel. *J Mol Biol*. 1999;292(4):797-817. doi:10.1006/jmbi.1999.3108

96. Nyeste A, Bencsura P, Fodor E, Welker E. Expression of the Prion Protein Family Member Shadoo Causes Drug Hypersensitivity That Is Diminished by the Coexpression of the Wild Type Prion Protein *. *J Biol Chem*. 2016;291(9):4473-4486. doi:10.1074/jbc.M115.679035

97. Nyeste A, Stincardini C, Bencsura P, Cerovic M, Biasini E, Welker E. The prion protein family member Shadoo induces spontaneous ionic currents in cultured cells. *Sci Rep*. 2016;6(October):1-12. doi:10.1038/srep36441

98. Fabiani C, Antollini SS, Guido ME, Eckert GP, Stephan A. Alzheimer ' s Disease as a Membrane Disorder : Spatial Cross-Talk Among Beta-Amyloid Peptides , Nicotinic Acetylcholine Receptors and Lipid Rafts. 2019;13(July):1-28. doi:10.3389/fncel.2019.00309

99. Mohamed S, Badawy M, Okada XT, Kajimoto T, Hirase M. Extracellular α -synuclein drives sphingosine 1-phosphate receptor subtype 1 out of lipid rafts , leading to impaired inhibitory G-protein signaling. 2018;293:8208-8216. doi:10.1074/jbc.RA118.001986

100. Kubo S, Hatano T, Hattori N. Lipid rafts involvement in the pathogenesis of parkinson ' s disease. 2015:263-279.

101. Valencia A, Reeves PB, Sapp E, et al. Mutant huntingtin and glycogen synthase kinase 3-β accumulate in neuronal lipid rafts of a presymptomatic knock-in mouse model of Huntington's disease. *J Neurosci Res*. 2010;88(1):179-190. doi:10.1002/jnr.22184

102. Sanghera N, Pinheiro TJT. Binding of prion protein to lipid membranes and implications for prion conversion. *J Mol Biol*. 2002;315(5):1241-1256. doi:10.1006/jmbi.2001.5322

103. Mayor S, Riezman H. Sorting GPI-anchored proteins. *Nat Rev Mol Cell Biol*. 2004;5(2):110-120. doi:10.1038/nrm1309

104. Kim Y-C, Lee J, Lee D-W, Jeong B-H. Large-scale lipidomic profiling identifies novel potential biomarkers for prion diseases and highlights lipid raft-related pathways. *Vet Res*. 2021;52(1):105. doi:10.1186/s13567-021-00975-1

105. Simons K, Toomre D. Lipid rafts and signal transduction. *Nat Rev Mol Cell Biol*. 2000;1(October):31-39. doi:10.1038/35036052

106. Sezgin E, Levental I, Mayor S, Eggeling C. The mystery of membrane organization: composition, regulation and roles of lipid rafts. *Nat Rev Mol Cell Biol*. 2017;18(6):361-374. doi:10.1038/nrm.2017.16

107. Pike LJ. Rafts defined: a report on the Keystone symposium on lipid rafts and cell function. *J Lipid Res*. 2006;47(7):1597-1598. doi:10.1194/jlr.e600002-jlr200

108. Radeva G, Sharom FJ. Isolation and characterization of lipid rafts with different properties from RBL-2H3 (rat basophilic leukaemia) cells. *Biochem J*. 2004;380(1):219-230. doi:10.1042/bj20031348

109. Aguzzi A. Prion Toxicity: All Sail and No Anchor. *Science (80-)*. 2005;308(5727):1420-

1421. doi:10.1126/science.1114168

110. Leucht C, Simoneau S, Rey C, et al. The 37 kDa/67 kDa laminin receptor is required for PrPSc propagation in scrapie-infected neuronal cells. *EMBO Rep*. 2003;4(3):290-295. doi:10.1038/sj.embor.embor768

111. El-Sayed A, Harashima H. Endocytosis of gene delivery vectors: From clathrin-dependent to lipid raft-mediated endocytosis. *Mol Ther*. 2013;21(6):1118-1130. doi:10.1038/mt.2013.54

112. Taylor DR, Hooper NM. The prion protein and lipid rafts (Review). *Mol Membr Biol*. 2006;23(1):89-99. doi:10.1080/09687860500449994

113. Varma R, Mayor S. GPI-anchored proteins are organized in submicron domains at the cell surface. *Nature*. 1998;394(6695):798-801. doi:10.1038/29563

114. Campana V, Sarnataro D, Zurzolo C. The highways and byways of prion protein trafficking. 2005;15(2). doi:10.1016/j.tcb.2004.12.002

115. Taraboulos A. Cholesterol depletion and modification of COOH-terminal targeting sequence of the prion protein inhibit formation of the scrapie isoform [published erratum appears in J Cell Biol 1995 Jul;130(2):501]. *J Cell Biol*. 1995;129(1):121-132. doi:10.1083/jcb.129.1.121

116. Sarnataro D, Paladino S, Campana V, Grassi J, Nitsch L, Zurzolo C. PrPC is sorted to the basolateral membrane of epithelial cells independently of its association with rafts. *Traffic*. 2002;3(11):810-821. doi:10.1034/j.1600-0854.2002.31106.x

117. Baron GS. Conversion of raft associated prion protein to the protease-resistant state requires insertion of PrP-res (PrPSc) into contiguous membranes. *EMBO J*. 2002;21(5):1031-1040. doi:10.1093/emboj/21.5.1031

118. Pan KM, Baldwin M, Nguyen J, et al. Conversion of alpha-helices into beta-sheets features in the formation of the scrapie prion proteins. *Proc Natl Acad Sci U S A*. 1993;90(23):10962-10966.

119. Sarnataro D, Caputo A, Casanova P, et al. Lipid rafts and clathrin cooperate in the internalization of PrPC in epithelial FRT cells. *PLoS One*. 2009;4(6). doi:10.1371/journal.pone.0005829

120. Kang Y-S, Zhao X, Lovaas J, Eisenberg E, Greene LE. Clathrin-independent internalization of normal cellular prion protein in neuroblastoma cells is associated with the Arf6 pathway. *J Cell Sci*. 2009;122(22):4062-4069. doi:10.1242/jcs.046292

121. Peters PJ, Mironov A, Peretz D, et al. Trafficking of prion proteins through a caveolae-mediated endosomal pathway. *J Cell Biol*. 2003;162(4):703-717. doi:10.1083/jcb.200304140

122. Sarnataro D, Campana V, Paladino S, Stornaiuolo M, Nitsch L, Zurzolo C. PrPC association with lipid rafts in the early secretory pathway stabilizes its cellular

conformation. *Mol Biol Cell*. 2004;15(9):4031-4042. doi:10.1091/mbc.E03-05-0271

123. Morris RJ, Parkyn CJ, Jen A. Traffic of prion protein between different compartments on the neuronal surface, and the propagation of prion disease. *FEBS Lett*. 2006;580(23):5565-5571. doi:10.1016/j.febslet.2006.07.053

124. Taylor DR, Watt NT, Perera WSS, Hooper NM. Assigning functions to distinct regions of the N-terminus of the prion protein that are involved in its copper-stimulated, clathrin-dependent endocytosis. *J Cell Sci*. 2005;118(Pt 21):5141-5153. doi:10.1242/jcs.02627

125. Kaneko K, Vey M, Scott M, Pilkuhn S, Cohen FE, Prusiner SB. COOH-terminal sequence of the cellular prion protein directs subcellular trafficking and controls conversion into the scrapie isoform. *Proc Natl Acad Sci U S A*. 1997;94(6):2333-2338. doi:10.1073/pnas.94.6.2333

126. Abid K, Morales R, Soto C. Cellular factors implicated in prion replication. *FEBS Lett*. 2010;584(11):2409-2414. doi:10.1016/j.febslet.2010.04.040

127. Puig B, Altmeppen HC, Linsenmeier L, et al. GPI-anchor signal sequence influences PrP C sorting, shedding and signalling, and impacts on different pathomechanistic aspects of prion disease in mice. *PLoS Pathog*. 2019;15(1):1-30. doi:10.1371/journal.ppat.1007520

128. Brügger B, Graham C, Leibrecht I, et al. The Membrane Domains Occupied by Glycosylphosphatidylinositol-anchored Prion Protein and Thy-1 Differ in Lipid Composition. *J Biol Chem*. 2004;279(9):7530-7536. doi:10.1074/jbc.M310207200

129. Bate C, Nolan W, Williams A. Sialic acid on the glycosylphosphatidylinositol anchor regulates PrP-mediated cell signaling and prion formation. *J Biol Chem*. 2016;291(1):160-170. doi:10.1074/jbc.M115.672394

130. Bate C, Williams A. Neurodegeneration induced by clustering of sialylated glycosylphosphatidylinositols of prion proteins. *J Biol Chem*. 2012;287(11):7935-7944. doi:10.1074/jbc.M111.275743

131. Hetz C, Mollereau B. Disturbance of endoplasmic reticulum proteostasis in neurodegenerative diseases. *Nat Rev Neurosci*. 2014;15(4):233-249. doi:10.1038/nrn3689

132. Ogen-Shtern N, Ben David T, Lederkremer GZ. Protein aggregation and ER stress. *Brain Res*. 2016;1648:658-666. doi:10.1016/j.brainres.2016.03.044

133. Torres M, Matamala JM, Duran-Aniotz C, Cornejo VH, Foley A, Hetz C. ER stress signaling and neurodegeneration: At the intersection between Alzheimer's disease and Prion-related disorders. *Virus Res*. 2015;207:69-75. doi:10.1016/j.virusres.2014.12.018

134. Tatzelt J, Winklhofer KF. Folding and misfolding of the prion protein in the secretory pathway. *Amyloid*. 2004;11(3):162-172. doi:10.1080/1350-6120400000723

135. Sitia R, Braakman I. Quality control in the endoplasmic reticulum protein factory. *Nature*. 2003;426(6968):891-894. doi:10.1038/nature02262

136. Kanemoto S. Targeting the endoplasmic reticulum in prion disease treatment: breakthroughs and challenges. *Res Reports Biochem*. 2015:31. doi:10.2147/rrbc.s74357

137. Béranger F, Mangé A, Goud B, Lehmann S. Stimulation of PrPC retrograde transport toward the endoplasmic reticulum increases accumulation of PrPSc in prion-infected cells. *J Biol Chem*. 2002;277(41):38972-38977. doi:10.1074/jbc.M205110200

138. Ivanova L, Barmada S, Kummer T, Harris DA. Mutant Prion Proteins Are Partially Retained in the Endoplasmic Reticulum. *J Biol Chem*. 2001;276(45):42409-42421. doi:10.1074/jbc.M106928200

139. Campana V, Sarnataro D, Fasano C, Casanova P, Paladino S, Zurzolo C. Detergent-resistant membrane domains but not the proteasome are involved in the misfolding of a PrP mutant retained in the endoplasmic reticulum. 2006. doi:10.1242/jcs.02768

140. Drisaldi B, Stewart RS, Adles C, et al. Mutant PrP is delayed in its exit from the endoplasmic reticulum, but neither wild-type nor mutant PrP undergoes retrotranslocation prior to proteasomal degradation. *J Biol Chem*. 2003;278(24):21732-21743. doi:10.1074/jbc.M213247200

141. Hetz C, Soto C. Stressing Out the ER: A Role of the Unfolded Protein Response in Prion-Related Disorders. *Curr Mol Med*. 2006;6(1):37-43. doi:10.2174/156652406775574578

142. Welch WJ, Gambetti P. Chaperoning brain diseases. *Nature*. 1998;392(6671):23-24. doi:10.1038/32049

143. Jessop CE, Tavender TJ, Watkins RH, Chambers JE, Bulleid NJ. Substrate specificity of the oxidoreductase ERp57 is determined primarily by its interaction with calnexin and calreticulin. *J Biol Chem*. 2009;284(4):2194-2202. doi:10.1074/jbc.M808054200

144. Hetz C, Russelakis-Carneiro M, Maundrell K, Castilla J, Soto C. Caspase-12 and endoplasmic reticulum stress mediate neurotoxicity of pathological prion protein. *EMBO J*. 2003;22(20):5435-5445. doi:10.1093/emboj/cdg537

145. Torres M, Medinas DB, Matamala JM, et al. The protein-disulfide isomerase ERp57 regulates the steady-state levels of the prion protein. *J Biol Chem*. 2015;290(39):23631-23645. doi:10.1074/jbc.M114.635565

146. Kang SJ, Cresswell P. Calnexin, calreticulin, and ERp57 cooperate in disulfide bond formation in human CD1d heavy chain. *J Biol Chem*. 2002;277(47):44838-44844. doi:10.1074/jbc.M207831200

147. Williams DB. Beyond lectins: The calnexin/calreticulin chaperone system of the endoplasmic reticulum. *J Cell Sci*. 2006;119(4):615-623. doi:10.1242/jcs.02856

148. Thapa S, Abdulrahman B, Abdelaziz DH, Lu L, Aissa M Ben, Schatzl HM. Overexpression of quality control proteins reduces prion conversion in prion-infected cells. *J Biol Chem*. 2018;293(41):16069-16082. doi:10.1074/jbc.RA118.002754

149. Shiraishi N, Inai Y, Hirano Y, Ihara Y. Calreticulin inhibits prion protein PrP-(23-98)

aggregation in vitro. *Biosci Biotechnol Biochem*. 2011;75(8):1625-1627. doi:10.1271/bbb.110287

150. Schrag JD, Bergeron JJM, Li Y, et al. The structure of calnexin, an ER chaperone involved in quality control of protein folding. *Mol Cell*. 2001;8(3):633-644. doi:10.1016/S1097-2765(01)00318-5

151. Bedard K, Szabo E, Michalak M, Opas M. Cellular functions of endoplasmic reticulum chaperones calreticulin, calnexin, and ERp57. *Int Rev Cytol*. 2005;245:91-121. doi:10.1016/S0074-7696(05)45004-4

152. Guo XY, Liu YS, Gao XD, Kinoshita T, Fujita M. Calnexin mediates the maturation of GPI-anchors through ER retention. *J Biol Chem*. 2020;295(48):16393-16410. doi:10.1074/jbc.RA120.015577

153. Wang W, Chen R, Luo K, et al. Calnexin inhibits thermal aggregation and neurotoxicity of prion protein. *J Cell Biochem*. 2010;111(2):343-349. doi:10.1002/jcb.22698

154. Macdonald JL, Pike LJ. A simplified method for the preparation of detergent-free lipid rafts. *J Lipid Res*. 2005;46(5):1061-1067. doi:10.1194/jlr.D400041-JLR200

155. Persaud-Sawin DA, Lightcap S, Harry GJ. Isolation of rafts from mouse brain tissue by a detergent-free method. *J Lipid Res*. 2009;50(4):759-767. doi:10.1194/jlr.D800037-JLR200

156. Race RE, Fadness LH, Chesebro B. Characterization of scrapie infection in mouse neuroblastoma cells. *J Gen Virol*. 1987;68(5):1391-1399. doi:10.1099/0022-1317-68-5-1391

157. Tóth E, Welker E, Construction AP. Comparison of Anti-Shadoo Antibodies – Where is the endogenous Shadoo protein ? *Int J Biotechnol Bioeng*. 2012;6(11):259-261.

158. Zanusso G, Liu D, Ferrari S, et al. Prion protein expression in different species: Analysis with a panel of new mAbs. *Proc Natl Acad Sci U S A*. 1998;95(15):8812-8816. doi:10.1073/pnas.95.15.8812

159. Madore N, Smith KL, Graham CH, et al. Functionally different GPI proteins are organized in different domains on the neuronal surface. *EMBO J*. 1999;18(24):6917-6926. doi:10.1093/emboj/18.24.6917

160. Kokubo H, Helms JB, Ohno-Iwashita Y, Shimada Y, Horikoshi Y, Yamaguchi H. Ultrastructural localization of flotillin-1 to cholesterol-rich membrane microdomains, rafts, in rat brain tissue. *Brain Res*. 2003;965(1-2):83-90. doi:10.1016/S0006-8993(02)04140-9

161. Otto GP, Nichols BJ. The roles of flotillin microdomains - endocytosis and beyond. *J Cell Sci*. 2011;124(23):3933-3940. doi:10.1242/jcs.092015

162. Shogomori H, Futerman AH. Cholera Toxin Is Found in Detergent-insoluble Rafts / Domains at the Cell Surface of Hippocampal Neurons but Is Internalized via a Raft-independent Mechanism *. 2001;276(12):9182-9188. doi:10.1074/jbc.M009414200

163. Kaplan JH, Lutsenko S. Copper Transport in Mammalian Cells: Special Care for a Metal with Special Needs. *J Biol Chem*. 2009;284(38):25461-25465. doi:10.1074/jbc.R109.031286

164. Shimizu Y. Moving Ras in and out of lipid rafts. *Trends Immunol*. 2001;22(7):352. doi:10.1016/S1471-4906(01)01989-5

165. Cingaram PKR, Nyeste A, Dondapati DT, Fodor E, Welker E. Prion protein does not confer resistance to hippocampus-derived Zpl cells against the toxic effects of Cu2+, Mn2+, Zn2+ and Co2+ not supporting a general protective role for PrP in transition metal induced toxicity. *PLoS One*. 2015;10(10):1-20. doi:10.1371/journal.pone.0139219

166. Shmerling D, Hegyi I, Fischer M, et al. Expression of amino-terminally truncated PrP in the mouse leading to ataxia and specific cerebellar lesions. *Cell*. 1998;93:203-214. doi:10.1016/S0092-8674(00)81572-X

167. Levental I, Levental KR, Heberle FA. Lipid Rafts: Controversies Resolved, Mysteries Remain. *Trends Cell Biol*. 2020;30(5):341-353. doi:10.1016/j.tcb.2020.01.009

168. Kalappurakkal JM, Sil P, Mayor S. Toward a new picture of the living plasma membrane. *Protein Sci*. 2020;29(6):1355-1365. doi:10.1002/pro.3874

169. Schuck S, Honsho M, Ekroos K, Shevchenko A, Simons K. Resistance of cell membranes to different detergents. *Proc Natl Acad Sci U S A*. 2003;100(10):5795-5800. doi:10.1073/pnas.0631579100

170. Shogomori H, Brown DA. Use of detergents to study membrane rafts: The good, the bad, and the ugly. *Biol Chem*. 2003;384(9):1259-1263. doi:10.1515/BC.2003.139

171. Lichtenberg D, Goñi FM, Heerklotz H. Detergent-resistant membranes should not be identified with membrane rafts. *Trends Biochem Sci*. 2005;30(8):430-436. doi:10.1016/j.tibs.2005.06.004

172. Hancock JF. Lipid rafts: Contentious only from simplistic standpoints. *Nat Rev Mol Cell Biol*. 2006;7(6):456-462. doi:10.1038/nrm1925

173. Wang J, Yu RK. Association of glycolipids and growth factor receptors in lipid rafts. In: *Methods in Molecular Biology*. Vol 2187. ; 2021:131-145. doi:10.1007/978-1-0716-0814-2_8

174. Shah MB, Sehgal PB. Nondetergent isolation of rafts. *Methods Mol Biol*. 2007;398:21-28. doi:10.1007/978-1-59745-513-8_3

175. Sunyach C, Jen A, Deng J, et al. The mechanism of internalization of glycosylphosphatidylinositol-anchored prion protein. *EMBO J*. 2003;22(14):3591-3601. doi:10.1093/emboj/cdg344

176. Orberger G, Geyer R, Stirm S, Tauber R. Structure of the N-linked oligosaccharides of the human transferrin receptor. *Eur J Biochem*. 1992;205(1):257-267. doi:10.1111/j.1432-1033.1992.tb16776.x

177. Lucero HA, Robbins PW. Lipid rafts-protein association and the regulation of protein activity. *Arch Biochem Biophys*. 2004;426(2):208-224. doi:10.1016/j.abb.2004.03.020

178. Baumann O, Walz B. Endoplasmic reticulum of animal cells and its organization into structural and functional domains. *Int Rev Cytol*. 2001;205:149-214. doi:10.1016/S0074-7696(01)05004-5

179. Voeltz GK, Prinz WA. Sheets, ribbons and tubules - How organelles get their shape. *Nat Rev Mol Cell Biol*. 2007;8(3):258-264. doi:10.1038/nrm2119

180. Nixon-Abell J, Obara CJ, Weigel A V., et al. Increased spatiotemporal resolution reveals highly dynamic dense tubular matrices in the peripheral ER. *Science (80-)*. 2016;354(6311):aaf3928-aaf3928. doi:10.1126/science.aaf3928

181. Shibata Y, Shemesh T, Prinz WA, Palazzo AF, Kozlov MM, Rapoport TA. Mechanisms determining the morphology of the peripheral ER. *Cell*. 2010;143(5):774-788. doi:10.1016/j.cell.2010.11.007

182. Shibata Y, Voeltz GK, Rapoport TA. Rough Sheets and Smooth Tubules. *Cell*. 2006;126(3):435-439. doi:10.1016/j.cell.2006.07.019

DNA-plasmid maps and DNA-sequences of the coding regions of the protein constructs used in the studies.

1. Map of the plasmid DNA p_mPrP-EGFP-GPI(mPrP), used for generating the N2a/PrP-EGFP cells.

(A)
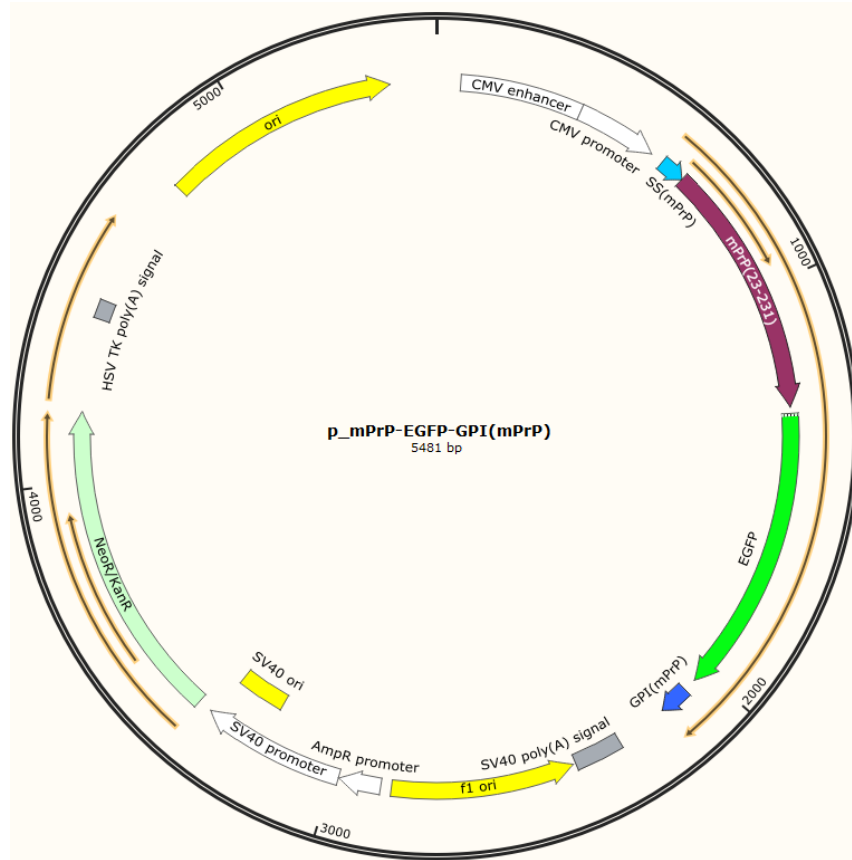
(B)
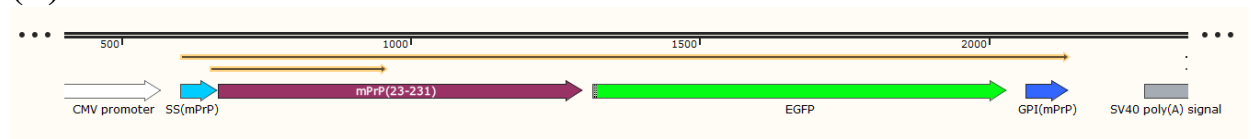
GCCAAGTACGCCCCCTATTGACGTCAATGACGGTAAATGGCCCGCCTGGCATTATGCCCAGTACATGA
CCTTATGGGACTTTCCTACTTGGCAGTACATCTACGTATTAGTCATCGCTATTACCATGGTGATGCGGTT
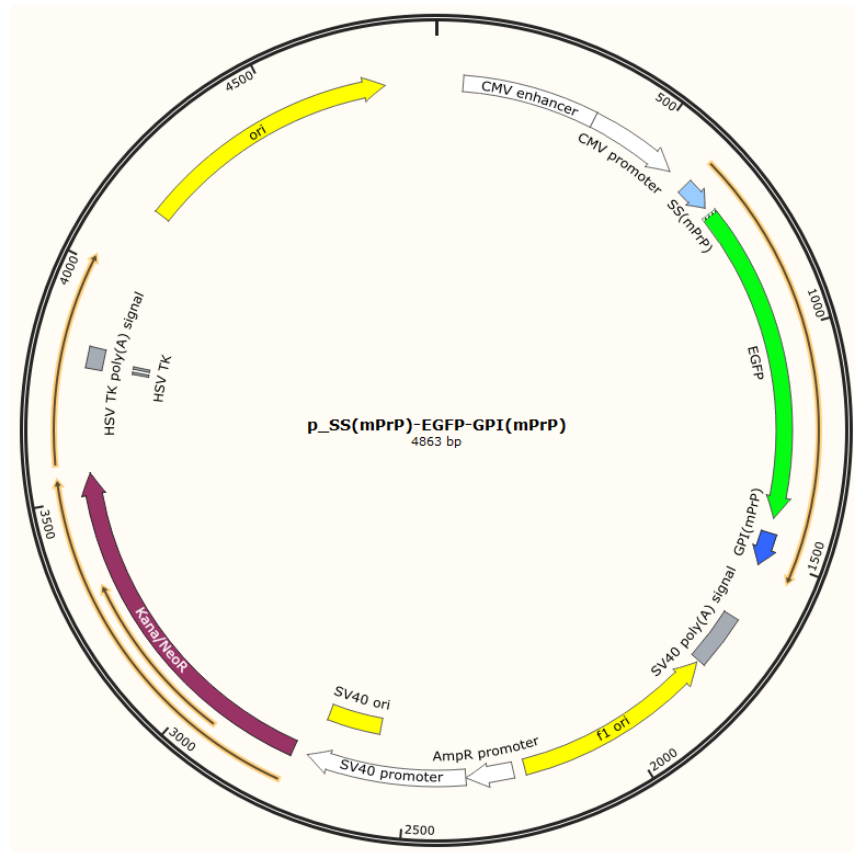TTGGCAGTACATCAATGGGCGTGGATAGCGGTTTGACTCACGGGGATTTCCAAGTCTCCACCCCATTGA

CGTCAATGGGAGTTTGTTTTGGCACCAAAATCAACGGGACTTTCCAAAATGTCGTAACAACTCCGCCCC
ATTGACGCAAATGGGCGGTAGGCGTGTACGGTGGGAGGTCTATATAAGCAGAGCTGGTTTAGTGAACC
GTCAGATCCGCTAGCCACCATGGCGAACCTTGGCTACTGGCTGCTGGCCCTCTTTGTGACTATGTGGAC
TGATGTCGGCCTCTGCAAAAAGCGGCCAAAGCCTGGAGGGTGGAACACCGGTGGAAGCCGGTATCCCG
GGCAGGGAAGCCCTGGAGGCAACCGTTACCCACCTCAGGGTGGCACCTGGGGGCAGCCCCACGGTGGT
GGCTGGGGACAACCCCATGGGGGCAGCTGGGGACAACCTCATGGTGGTAGTTGGGGTCAGCCCCATGG
CGGTGGATGGGGCCAAGGAGGGGGTACCCATAATCAGTGGAACAAGCCCAGCAAACCAAAAACCAAC
CTCAAGCATGTGGCAGGGGCTGCGGCAGCTGGGGCAGTAGTGGGGGGCCTTGGTGGCTACATGCTGGG
GAGCGCCATGAGCAGGCCCATGATCCATTTTGGCAACGACTGGGAGGACCGCTACTACCGTGAAAACA
TGTACCGCTACCCTAACCAAGTGTACTACAGGCCAGTGGATCAGTACAGCAACCAGAACAACTTCGTG
CACGACTGCGTCAATATCACCATCAAGCAGCACACGGTCACCACCACCACCAAGGGGGAGAACTTCAC
CGAGACCGATGTGAAGATGATGGAGCGCGTGGTGGAGCAGATGTGCGTCACCCAGTACCAGAAGGAG
TCCCAGGCCTATTACGACGGGAGAAGATCCAGCGGGCCCGGACCGGTCGCCACCATGGTGAGCAAGG
GCGAGGAGCTGTTCACCGGGGTGGTGCCCATCCTGGTCGAGCTGGACGGCGACGTAAACGGCCACAAG
TTCAGCGTGTCCGGCGAGGGCGAGGGCGATGCCACCTACGGCAAGCTGACCCTGAAGTTCATCTGCAC
CACCGGCAAGCTGCCCGTGCCCTGGCCCACCCTCGTGACCACCCTGACCTACGGCGTGCAGTGCTTCAG
CCGCTACCCCGACCACATGAAGCAGCACGACTTCTTCAAGTCCGCCATGCCCGAAGGCTACGTCCAGG
AGCGCACCATCTTCTTCAAGGACGACGGCAACTACAAGACCCGCGCCGAGGTGAAGTTCGAGGGCGAC
ACCCTGGTGAACCGCATCGAGCTGAAGGGCATCGACTTCAAGGAGGACGGCAACATCCTGGGGCACA
AGCTGGAGTACAACTACAACAGCCACAACGTCTATATCATGGCCGACAAGCAGAAGAACGGCATCAA
GGTGAACTTCAAGATCCGCCACAACATCGAGGACGGCAGCGTGCAGCTCGCCGACCACTACCAGCAGA
ACACCCCCATCGGCGACGGCCCCGTGCTGCTGCCCGACAACCACTACCTGAGCACCCAGTCCGCCCTG
AGCAAAGACCCCAACGAGAAGCGCGATCACATGGTCCTGCTGGAGTTCGTGACCGCCGCCGGGATCAC
TCTCGGCATGGACGAGCTGTACAAGTCCGGACTCAGATCTCGAGCTCAAGCTTCGAATTCTAGCAGCA
CCGTGCTTTTCTCCTCCCTCCTGTCATCCTCCTCATCTCCTTCCTCATCTTCCTGATCGTAGGCTAGCCC
ACCGGATCTAGATAACTGATCATAATCAGCCATACCACATTTGTAGAGGTTTTACTTGCTTTAAAAAAC
CTCCCACACCTCCCCCTGAACCTGAAACATAAAATGAATGCAATTGTTGTTGTTAACTTGTTTATTGCA
GCTTATAATGGTTACAAATAAAGCAATAGCATCACAAATTTCACAAATAAAGCATTTTTTTCACTGCAT
TCTAGTTGTGGTTTGTCCAAACTCATCAATGTATCTTAACGCGTAAATTGTAAGCGTTAATATTTTGTTA
AAATTCGCGTTAAATTTTTGTTAAATCAGCTCATTTTTTAACCAATAGGCCGAAATCGGCAAAATCCCT
TATAAATCAAAAGAATAGACCGAGATAGGGTTGAGTGTTGTTCCAGT

▮ : SS(mPrP), ▮ : mPrP(23-231); ▮ : EGFP; ▮ : GPI(mPrP)-signal peptide

Figure A1. Map of the plasmid DNA **p_mPrP-EGFP-GPI(mPrP)**, used for generating the N2a/PrP-EGFP cells. The plasmid is constructed to express the mouse prion protein (mPrP) in fusion with EGFP at its C-terminus, upstream of its GPI-signal peptide. (A) Circular map of the plasmid, indicating the major features along the DNA sequence, with the top three open reading frames marked (thin orange arrows). (B) Horizontal map of the sequence region harbouring the fusion protein's coding sequence, with the major features indicated. The sequence of the plasmid-DNA segment comprising the coding region of the constructed fusion-protein is given below the map. The color-coded features encode for the protein-segments as indicated and as follows: the secretion signal of mPrP, SS(mPrP) (cyan); mature mPrP protein, mPrP(23-231) (pink); EGFP (green); sequence of the GPI-anchor signal peptide of mPrP, GPI(mPrP-signal peptide (blue).

2. Map of the plasmid DNA p_SS(mPrP)-EGFP-GPI(mPrP), used for generation of the N2a/EGFP cells.

(A)

(B)
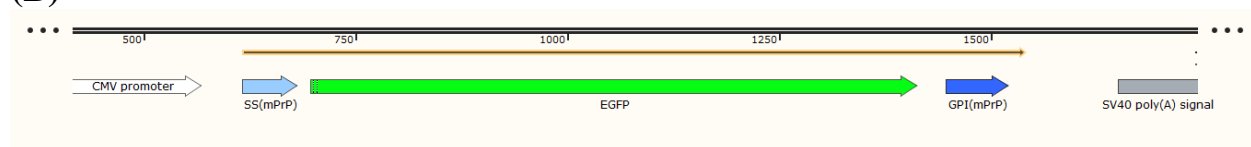
AGTCTCCACCCCATTGACGTCAATGGGAGTTTGTTTTGGCACCAAAATCAACGGGAC
TTTCCAAAATGTCGTAACAACTCCGCCCCATTGACGCAAATGGGCGGTAGGCGTGTA
CGGTGGGAGGTCTATATAAGCAGAGCTGGTTTAGTGAACCGTCAGATCCGCTAGCGC
TACCGGTATCAGTCATCATGGCGAACCTTGGCTACTGGCTGCTGGCCCTCTTTGTGAC
TATGTGGACTGATGTAGGCCTCTGCTTACCGGTCGCCACCATGGTGAGCAAGGGCGA
GGAGCTGTTCACCGGGGTGGTGCCCATCCTGGTCGAGCTGGACGGCGACGTAAACG
GCCACAAGTTCAGCGTGTCCGGCGAGGGCGAGGGCGATGCCACCTACGGCAAGCTG
ACCCTGAAGTTCATCTGCACCACCGGCAAGCTGCCCGTGCCCTGGCCCACCCTCGTG
ACCACCCTGACCTACGGCGTGCAGTGCTTCAGCCGCTACCCCGACCACATGAAGCAG
CACGACTTCTTCAAGTCCGCCATGCCCGAAGGCTACGTCCAGGAGCGCACCATCTTC
TTCAAGGACGACGGCAACTACAAGACCCGCGCCGAGGTGAAGTTCGAGGGCGACAC

CCTGGTGAACCGCATCGAGCTGAAGGGCATCGACTTCAAGGAGGACGGCAACATCC
TGGGGCACAAGCTGGAGTACAACTACAACAGCCACAACGTCTATATCATGGCCGAC
AAGCAGAAGAACGGCATCAAGGTGAACTTCAAGATCCGCCACAACATCGAGGACGG
CAGCGTGCAGCTCGCCGACCACTACCAGCAGAACACCCCCATCGGCGACGGCCCCGT
GCTGCTGCCCGACAACCACTACCTGAGCACCCAGTCCGCCCTGAGCAAAGACCCCAA
CGAGAAGCGCGATCACATGGTCCTGCTGGAGTTCGTGACCGCCGCCGGGATCACTCT
CGGCATGGACGAGCTGTACAAGTCCGGACTCAGATCTCGAGCTCAAGCTTCGAATTC
TAGCAGCACCGTGCTTTTCTCCTCCCCTCCTGTCATCCTCCTCATCTCCTTCCTCATCT
TCCTGATCGTGGGTGGATCCACCGGATCTAGATAACTGATCATAATCAGCCATACCA
CATTTGTAGAGGTTTTACTTGCTTTAAAAAACCTCCCACACCTCCCCCTGAACCTGAA
ACATAAAATGAATGCAATTGTTGTTGTTAACTTGTTTATTGCAGCTTATAATGGTTAC
AAATAAAGCAATAGCATCACAAATTTCACAAATAA

: SS(mPrP);   : EGFP;   : GPI(mPrP)-signal peptide

Figure A2. Map of the plasmid DNA **p_SS(mPrP)-EGFP-GPI(mPrP)**, used for generation of the N2a/EGFP cells. The plasmid is constructed to express the control fusion protein composed of EGFP in fusion with the ER signal peptide of mPrP at its N-terminus and with the GPI-signal peptide of mPrP at its C-terminus. (A) Circular map of the plasmid, indicating the major features along the DNA sequence, with the top three open reading frames marked (thin orange arrows). (B) Horizontal map of the region harbouring the fusion protein's coding sequence, with the major features indicated. The sequence of the plasmid-DNA segment comprising the coding region of the constructed fusion-protein is given below the map. The color-coded features encode for the protein-segments as indicated and as follows: the secretion signal of mPrP, SS(mPrP) (cyan); EGFP (green); the sequence of the GPI-anchor signal peptide of mPrP, GPI(mPrP)-signal peptide (blue).

3. Map of the plasmid DNA p_mSho-EYFP-FLAG-GPI(mSho), used for generating the N2a/Sho-EYFP-FLAG cells.

(A)
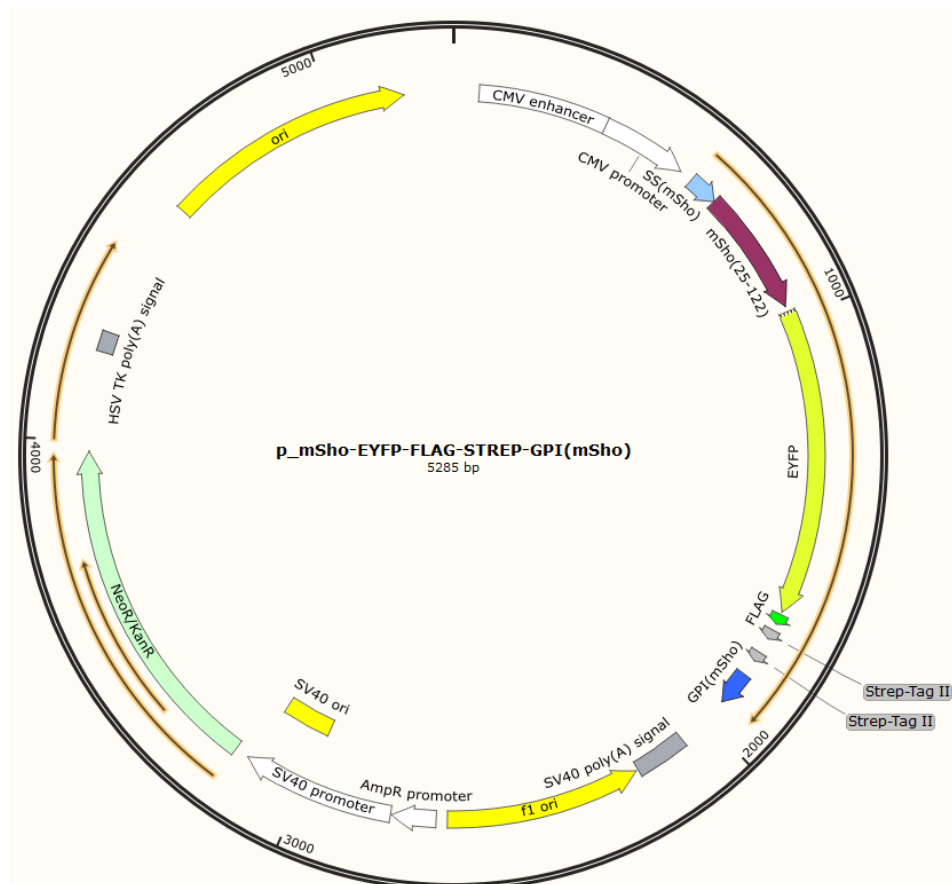
(B)
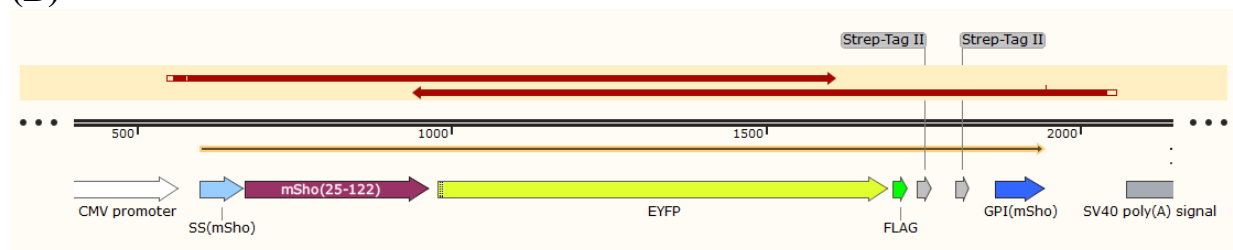
TAGCAGAGCTGGTTTAGTGACCGTCAGATCCGCTAGCCACCATGAACTGGACTGCTGCCACGTGCTGG
GCTCTGCTGCTGGCCGCCGCCTTCCTCTGTGACAGCTGTTCCGCCAAGGGCGGCCGCGGAGGCGCTCGA
GGCAGTGCCCGGGGGGTGCGCGGAGGTGCACGCGGGGCATCAAGAGTACGCGTAAGGCCGGCGCCCC
GCTACGGCTCCTCTCTGCGCGTGGCGGCTGCAGGGGCAGCAGCAGGGGCTGCAGCGGGTGTGGCTGCG
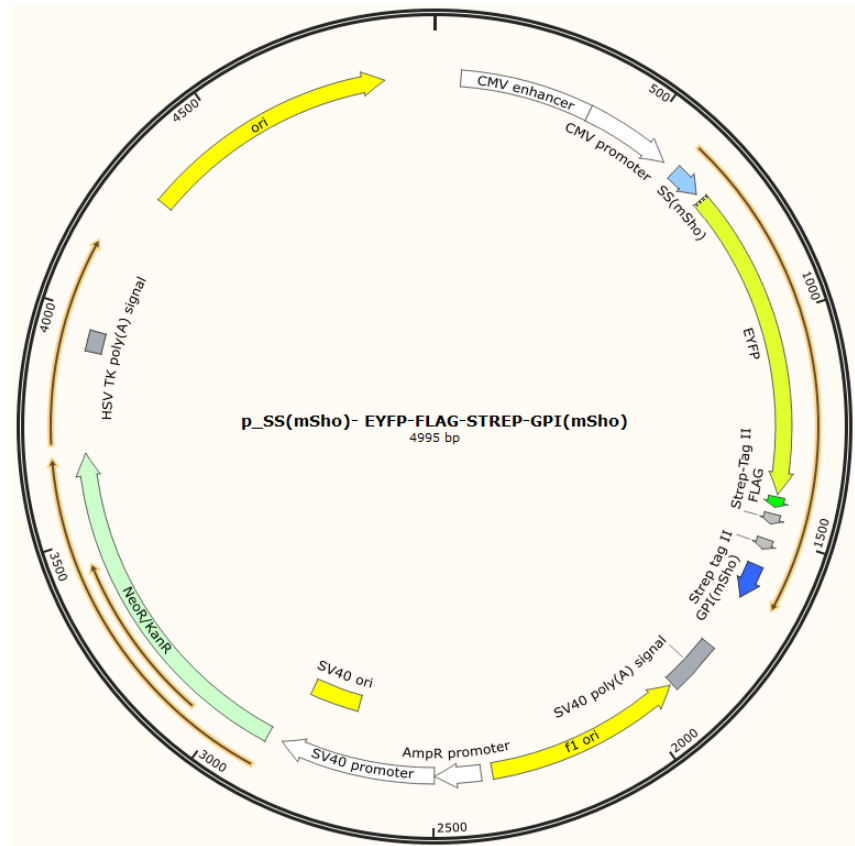GGCCTTGCTACCGGCTCTGGCTGGAGGAGGACCTCAGGGCCTGGAGAGCTAGGCCTGGAGGACGATGA

GAATGGGGCAATGGGAGGCAACGGAACCGACCGAGGAGTCTACAGCTACTGGGCCTGGACTTCCTTAC
CGGTCGCCCATATGGTGAGCAAGGGCGAGGAGCTGTTCACCGGGGTGGTGCCCATCCTGGTCGAGCTG
GACGGCGACGTAAACGGCCACAAGTTCAGCGTGTCCGGCGAGGGCGAGGGCGATGCCACCTACGGCA
AGCTGACCCTGAAGTTCATCTGCACCACCGGCAAGCTGCCCGTGCCCTGGCCCACCCTCGTGACCACCT
TCGGCTACGGCCTGCAGTGCTTCGCCCGCTACCCCGACCACATGAAGCAGCACGACTTCTTCAAGTCCG
CCATGCCCGAAGGCTACGTCCAGGAGCGCACCATCTTCTTCAAGGACGACGGCAACTACAAGACCCGC
GCCGAGGTGAAGTTCGAGGGCGACACCCTGGTGAACCGCATCGAGCTGAAGGGCATCGACTTCAAGG
AGGACGGCAACATCCTGGGGCACAAGCTGGAGTACAACTACAACAGCCACAACGTCTATATCATGGCC
GACAAGCAGAAGAACGGCATCAAGGTGAACTTCAAGATCCGCCACAACATCGAGGACGGCAGCGTGC
AGCTCGCCGACCACTACCAGCAGAACACCCCCATCGGCGACGGCCCCGTGCTGCTGCCCGACAACCAC
TACCTGAGCTACCAGTCCGCCCTGAGCAAAGACCCCAACGAGAAGCGCGATCACATGGTCCTTAAGGA
GTTCGTGACCGCCGCCGGGATCACTCTCGGCATGGACGAGCTGTACAAGATGCAGGATTATAAAGATG
ATGATGATAAAGGGTCGGCCGCCAGCTGGAGCCACCCTCAGTTCGAGAAGGGAGGAGGAAGCGGCGG
AGGCAGCGGAGGAGGAAGCTGGAGCCACCCGCAGTTCGAGAAAGGAGCTAGATCAAGATCTCGAGCT
CAAGCTTCGAATTCTGGCTCAGGGTCCGTGCACAGCCCACGTATTTGTCTGCTTCTGGGCGGCACCCTT
GGTGCCCTAGAACTGCTTCGGCCTTAGGGATCCACCGGATCTAGATAACTGATCATAATCAGCCATACC
ACATTTGTAGAGGTTTTACTTGCTTTAAAAAACCTCCCACACCTCCCCCTGAACCNAAACATAAAANNN
NNNNT

□ : SS(mSho) ■ : mSho(25-122); □ : EYFP; ■ : FLAG-tag; □ : Strep-tag II; ■ : GPI(mSho)-signal peptide

Figure A3. Map of the plasmid DNA **p_mSho-EYFP-FLAG-GPI(mSho)**, used for generating the N2a/Sho-EYFP-FLAG cells. The plasmid encodes for the expression of mouse Shadoo (mSho) protein in fusion with EYFP-, FLAG- and Strep-tag II tags at its C-terminal, upstream of its GPI-signal peptide sequence. (A) Circular map of the plasmid, indicating the major features along the DNA sequence, with the top three open reading frames (thin orange arrows). (B) Horizontal map of the region of Sanger-sequenced region (indicated by the top, red-coloured forward and reverse arrows) comprising the coding region of the fusion protein constructed. The translated region is indicated by thin orange arrow, below which the major features are indicated on the map. The resulting sequence from Sanger-sequencing is shown below the map, with the specific features highlighted by colors, as indicated, encoding for as follows: secretion signal of mSho, SS(mSho) (cyan); mature mShadoo protein, mSho(25-122) (pink); EYFP (yellow); FLAG-tag (green); two Strep-tag II tags (grey) and the sequence of GPI-anchor signal peptide of mSho, GPI(mSho)-signal peptide (blue).

4. Map of the plasmid DNA p_SS(mSho)-EYFP-FLAG-GPI(mSho), used for generating the N2a/EYFP-FLAG cells.

(A)

(B)
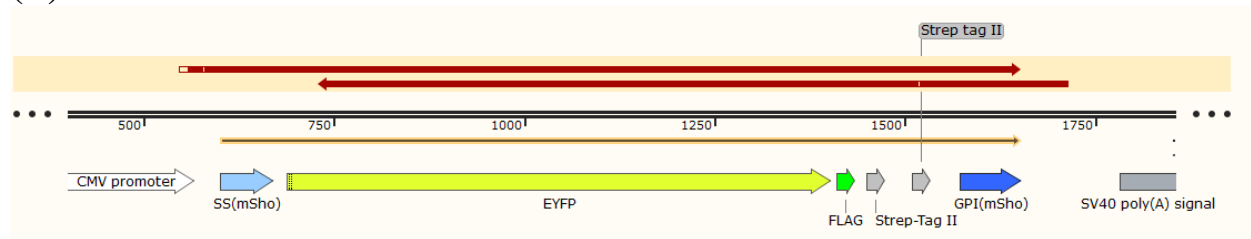
TNNNTGNNNNYNNTAGCAGAGCTGGTTTAGTGACCGTCAGATCCGCTAGCCACC<mark>ATGAACTGGACTGC</mark>
<mark>TGCCACGTGCTGGGCTCTGCTGCTGGCCGCCGCCTTCCTCTGTGACAGCTGTAGCGCC</mark>TTACCGGTCGC
CCAT<mark>ATGGTGAGCAAGGGCGAGGAGCTGTTCACCGGGGTGGTGCCCATCCTGGTCGAGCTGGACGGCG</mark>
<mark>ACGTAAACGGCCACAAGTTCAGCGTGTCCGGCGAGGGCGAGGGCGATGCCACCTACGGCAAGCTGAC</mark>
<mark>CCTGAAGTTCATCTGCACCACCGGCAAGCTGCCCGTGCCCTGGCCCACCCTCGTGACCACCTTCGGCTA</mark>
<mark>CGGCCTGCAGTGCTTCGCCCGCTACCCCGACCACATGAAGCAGCACGACTTCTTCAAGTCCGCCATGCC</mark>
<mark>CGAAGGCTACGTCCAGGAGCGCACCATCTTCTTCAAGGACGACGGCAACTACAAGACCCGCGCCGAGG</mark>
<mark>TGAAGTTCGAGGGCGACACCCTGGTGAACCGCATCGAGCTGAAGGGCATCGACTTCAAGGAGGACGG</mark>
<mark>CAACATCCTGGGGCACAAGCTGGAGTACAACTACAACAGCCACAACGTCTATATCATGGCCGACAAGC</mark>
<mark>AGAAGAACGGCATCAAGGTGAACTTCAAGATCCGCCACAACATCGAGGACGGCAGCGTGCAGCTCGC</mark>
<mark>CGACCACTACCAGCAGAACACCCCCATCGGCGACGGCCCCGTGCTGCTGCCCGACAACCACTACCTGA</mark>

GCTACCAGTCCGCCCTGAGCAAAGACCCCAACGAGAAGCGCGATCACATGGTCCTTAAGGAGTTCGTG
ACCGCCGCCGGGATCACTCTCGGCATGGACGAGCTGTACAAGATGCAGGATTATAAAGATGATGATGA
TAAAGGGTCGGCCGCCAGCTGGAGCCACCCTCAGTTCGAGAAGGGAGGAGGAAGCGGCGGAGGCAGC
GGAGGAGGAAGCTGGAGCCACTCGCAGTTCGAGAAAGGAGCTAGATCAAGATCTCGAGCTCAAGCTT
CGAATTCTGGCTCAGGGTCCGTGCACAGCCCACGTATTTGTCTGCTTCTGGGCGGCACCCTTGGTGCCC
TAGAACTGCTTCGGCCTTAG

▭ : SS(mSho); ▭ : EYFP; ▭ : FLAG-tag; ▭ : Strep-tag II; ▭ : GPI(mSho)-signal
peptide

Figure A4. Map of the plasmid DNA **p_SS(mSho)-EYFP-FLAG-GPI(mSho)**, used for generating the N2a/EYFP-FLAG cells. The plasmid is constructed to express the control protein EYFP with the ER signal sequence of mSho and in-fusion with a FLAG- and two Strep-tag II tags followed by the GPI-signal peptide of mSho, respectively, at its C-terminus. (A) Circular map of the plasmid, indicating the major features along the DNA sequence, with the top three open reading frames marked (thin orange arrows). (B) Horizontal map of sequences region containing the Sanger-sequenced segments (indicated by the top, red-coloured forward and reverse arrows) comprising the coding region of the fusion protein constructed. The translated region is indicated by thin orange arrow, below which the major features are indicated. The resulting sequence from Sanger-sequencing is shown below the map, with the specific features highlighted by colors, as indicated on the figure, encoding for as follows: secretion signal of mSho, SS(mSho) (cyan); EYFP (yellow); FLAG-tag (green); two Strep-tag II tags (gray) and the sequence of the signal peptide of GPI-anchor of mSho, GPI(mSho)-signal peptide (blue). Note: according to the sequencing, the second Strep-Tag II contains a point mutation (dark grey).